AN ABSTRACT OF THE THESIS OF

De-qian Wang for the degree of

Master of Science in Agricultural Engineering

Presented on January 13, 1987

Title: Improved Prediction of Heat Leakage for Fish Hold Wall Sections

Abstract approved: _____
Dr. Edward R. Kolbe

Controlling storage quality of fish in vessels at sea is one of the important links in fisheries production. Steel vessels with refrigeration systems are common to the West Coast. The cooling capacity of the refrigeration system depends greatly upon the heat leakage from the areas surrounding the fish hold. In this project, heat leakage through fish hold wall sections was investigated both numerically and experimentally. The objective was to provide useful information on design of fish hold wall sections and especially on the effects of insulation thickness and steel frame dimensions and spacing.

Two predicting models, which use finite element and finite difference methods, respectively, were developed. The comparison of these two models indicates that the finite difference model is more feasible to this project. In order to verify calculated results, eight representative fish hold wall sections for a 14 m (45 ft) boat were tested

using the "guarded hot box" technique. Good agreement was obtained between calculated results and tested results.

Using the finite difference model, 24 design curves were developed to predict thermal resistance of the fish hold panels with different frames representative of vessel size 14-32 m (45-105 ft). The results show that insulation thickness is critical. The best configuration results from an insulation thickness being at least 25 mm (1 in) greater than the frame depth.

The effects of inside liner materials, frame spacing, frame and steel skin thickness, and fasteners were also investigated in this research. Material used as an inside liner is only important when insulation thickness is less than or equal to the frame depth; the effects of frame spacing is less important than that of insulation thickness; frame and steel skin thickness does not significantly influence insulation effectiveness, and 5% heat leakage added to allow for the effect of fasteners is applicable in practice.

Further research is needed to predict heat leakage through different parts of the hold boundary. An optimization procedure, which balances the cost, insulation effectiveness, frame strength and hold volume, will be neccessary in order to set up a standard design of the fish hold wall.

Improved Prediction of Heat Leakage for Fish Hold Wall Sections

by

De-qian Wang

A THESIS

submitted to

Oregon State University

in partial fullfillment of

the requirements for the

degree of

Master of Science

Completed January 13, 1987

Commencement June 1987

APPROVED:

Redacted for Privacy

Associate Professor of Agricultural Engineering

in Charge of Major

Redacted for Privacy

Head of Department of Agricultural Engineering

Redacted for Privacy

Dean of Graduate School

Date of Thesis Presented January 13, 1987

Typed by: The Author

ACKNOWLEGEMENTS

I would like to express my gratitude to the OSU Sea Grant Program which funded the research for this project.

I would also like to express my deep appreciation to my major advisor, Dr. Edward R. Kolbe, for his excellent guidance and encouragement. Without his faith and understanding, none of this would have been possible.

I would like to thank my committe members, Dr. Marshall J. English, Dr. Alan H. Robinson and Dr. Eldon D. Olsen for their time, consideration and assistance.

Special thanks to Alan Rea for his assistance in transporting the panels to Minnesota, for his proofreading this thesis and for his friendship over the last three years. Also, I would like to thank Robert Schnekenburger for his assistance in constructing the panels. I would also like to take this opportunity to express my appreciation to all faculty, staff and graduate students in the Agricultural Engineering Department for their support and friendship.

I express my heartfelt appreciation to my wife Yan and my son Nye for their loves and sacrifices. Finally, to my parents:

Such a tiny blade of grass
Can you ever repay the sunshine of spring?

TABLE OF CONTENTS

LIST OF FIGURES

LIST OF TABLES

Improved Prediction of Heat Leakage for Fish Hold Wall Sections

CHAPTER I. INTRODUCTION AND LITERATURE REVIEW

I.1. Introduction

In modern fisheries, controlling storage quality of fish in vessels at sea is a very important link in the production chain. Fish begin to spoil as soon as they are caught. The rate of spoilage is dependant on the preservation practices on board the fishing vessel. The most common methods used to maintain a low fish and hold temperature are by using adequate ice; chilled sea water with the addition of ice; and mechanically refrigerated sea water. In any case, the cooling capacity greatly depends upon the heat leakage from areas surrounding the hold. Predicting heat leakage into the fish hold involves many factors, such as external weather, air and sea water temperature, solar radiation, construction and insulation of fish hold wall enclosure, etc. Even though there are many uncertainties involved, the heat leakage can be evaluated under certain circumstances if one has knowledge of thermal performance of fish hold wall sections.

In the Pacific Northwest, steel vessels are common. In this project we will concentrate our attention on steel vessels in the range of 14-32 m (45-105 ft). Typical

construction information for vessels of this size was provided by American Bureau of Shipping (1), Hanson (15) and personal communications (7, 12, 20, and 36). According to these sources, there are a few difficulties involved in predicting heat leakage through steel hold wall sections. First, there is a great amount of structural variations in the wall enclosures. The boundary of the fish hold usually is thermally insulated to help reduce hold temperature, but the insulation thickness differs from one application to another. For example, it may be different if the insulation is installed during the course of construction or as an addition to an existing vessel. Some vessels have no insulation at all, because the builders or designers wish to cut down the cost, or they simply do not have knowledge of the value of insulation. Another difficulty in predicting fish hold heat leakage involves the important role played by the inside liner of the hold. Sheet steel, plywood and fiberglass are common as inside liner in steel vessels found in the Pacific Northwest. Finally, the steel frames in an insulated wall also cause difficulty in predicting the heat leakage. Those steel frames act as "thermal bridges" and increase heat flow significantly, whatever the wall enclosure structure being used. This is particularly true if the insulation thickness is inadequate. In West Coast steel vessels both angle iron and flat bar are commonly used as frames. Obviously, at

least a two-dimensional heat transfer analysis has to be carried out because of those frames. The size of the frames depends upon the vessel size. Representative frame structures for different size of vessels are given in Table I-1.

In general, this project is intended to provide useful information to improve prediction of heat leakage through steel vessel fish hold wall sections. The specific objectives were:

1. To develop computer models to predict heat flow through fish hold wall sections, using both finite element and finite difference methods.
2. To experimentally evaluate the thermal performance of various representative panels of 14 m (45 ft) steel vessel by using "Guarded Hot Box" technique.
3. To verify the numerical models by comparing with test results, then selecting the best model for further application.
4. To obtain design curves by applying the selected model to predict the thermal performance of those configerations not being measured.
5. To interpret and report results for industry specialists.

Table I-1: Frame Structures for Different Size of Steel Vessels

Vessel Size	Angle iron	Flat bar*
14 m (45 ft)	63.5x38.1x6.4 mm (2.5x1.5x1/4 in)	101.6x7.9 mm (4x5/16 in)
20 m (65 ft)	76.2x50.8x6.4 mm (3x2x1/4 in)	127.0x7.9 mm (5x5/16 in)
26 m (85 ft)	88.9x63.5x6.4 mm (3.5x2.5x1/4 in)	152.4x7.9 mm (6x5/16 in)
32 m (105 ft)	101.6x76.2x7.9 mm (4x3x5/16 in)	152.4x12.7 mm (6x1/2 in)

* Determination of flat bar dimensions depends upon the consideration of the frame strength. That is, the section modulus of the wall constructed with flat bar should be equivalent to that of the wall constructed with angle iron. Based on this consideration, the center of gravity and neutral axis of angle iron section were first calculated. Then, the section modulus was determined by SM=I/C, where I is cross section moment of inertia and C is the maximum distance of the neutral axis to the edge of the cross section. The section modulus of flat bar was calculated in the same way, with calculations repeated until a value equivalent to that of the angle iron is obtained. The dimensions of the flat bar was determined by selecting the standard size nearest to that matching the equivalent section modulus calculated (20).

I.2. Literature Review

Merritt et al. (27) have recently worked on a report concerning the insulation of fish holds and sizing of ice-keeping mechanical refrigeration systems. However, their efforts were concentrated on the wooden boats typical of those found on the Atlantic coast of Canada. In their investigation, they carried out the heat transfer analysis to calculate heat transmission rate into the wooden fish hold by assuming that parallel or series/parallel flow paths are applicable to the thermal resistance of wall sections. This is known as "Zone Method" (6). However, their calculations were not experimentally verified. As they indicated, the "Zone Method" might be accurate for the case of wooden hold wall sections, but it could break down for the case of steel vessels. Therefore, they recommended that a more detailed analysis should be made for those steel vessels, i.e., that a finite difference analysis and verifying experiments should be conducted.

MacCallum (24, 25 and 26), examined fish hold design practice and provided some theoretical predictions of ice use and heat leakage through the hold. However, his analysis was limited to the 35 meter (115 foot) wooden trawlers and no measurements were made to verify his predictions. In addition, the information he provided is thirty years out of date.

SNAME (The Society of Naval Architects and Marine

Engineers) (31) presented a method for determining required insulation for sea going steel vessels by considering the economy of installation, construction and maintenance for different temperature levels. However, they did not include insulation analysis for cases with insulation thickness greater than 76 mm (3 in). Heavy insulation layers are common in West Coast steel vessels. In addition, they cited some tests of panels having 101.6x76.2x6.35 mm (4x3x0.25 in) frames conducted by "Pennsylvania State College", but adequate description of the procedure was lacking. Through contact with Pennsylvania State University, we were unable to learn about any of the procedures they used because the tests were done twenty-three years ago. It is also noted that the construction materials which they had considered are outdated.

Munton and Stott (28) gave an outline of the fundamental design principles of refrigerated vessels at sea. In particular, some short cuts to estimate the performance of insulation were offered. One of methods offered is an empirical equation developed by Joelson (18). This equation represents an experimentally derived relationship for thermal resistance of an insulated steel wall section. However, the equation is limited to the specific case in which the depth of insulation exceeds the depth of the angle iron frames.

Finally, SABROE (29), a Danish refrigeration company, included with some of their advertising literature, curves indicating the thermal resistance of steel walls both fully and partially insulated. The information appears to be the theoretical prediction. However, all conditions are not given and contact with the company failed to determine the source of the information.

As indicated in the previous section, because of the complexities of steel frames and composition typically found in the steel vessel hold wall, simple analytical techniques based on series and parallel combinations of one-dimensional heat flow paths, may be inadequate. Therefore, numerical methods appear to be the most promising. A literature search indicated that there is mach published information on simulating heat transfer problems using numerical methods. However, to date none of them have dealt with the thermal performance of constructions typical of fish hold wall sections. Some investigators have used numerical analysis to simulate composite building wall sections. A similar procedure can be applied to fish hold wall sections.

It is found that the most common method to analysis heat transfer through composite buliding wall sections are the finite element and the finite difference methods. Wilson et al. (37) surveyed the development of finite element methods in linear heat transfer analysis and

presented the techniques that permit the practical analysis of large and complex three-dimensional heat conduction problems. They also presented some sample solutions to deal with the case in which the thermal conductivity of the slab material is a linear function of temperature. Both steady-state and transient heat transfer were considered. It appears that the finite element method is a powerful tool to solve similar problems, such as the case of steel hold wall sections in which the thermal conductivity of the material is a function of position instead of temperature.

The finite element method and its application in engineering is also detailed by Segerlind (30). He gave a step by step procedure on how to use three-node trianglar elements to solve two-dimensional heat conduction problems. He also gave a sample computer program to calculate the temperture distribution in two-dimensional bodies subject to either prescribed boundary temperatures or surface convections. It was found that this sample computer program is easy to modify to use for our fish hold wall section problems.

The other possible method for simulating the heat transfer performance of fish hold wall sections is to use the finite difference method. This was suggested by Merritt et al. (27) as indicated earlier.

Kuehn and Maldonado (19) used an explicit finite difference computer program to simulate thermal performance

of composite building envelopes. Even though this computer program is basically for engineering education purposes, it gives a good example of how to solve this kind of problem numerically.

A summary of numerical methods for solving transient and steady-state heat conduction problems given by Trent and Welty (33) was found to be very useful for our purpose. In their summary, both implicit and explicit finite difference schemes were reviewed and both steady-state and transient temperature distributions were considered. In particular, they presented a procedure to use node centered mesh to set up the heat transfer system, to calculate internode conductances, and to handle boundary conditions. They also introduced the contact resistance, R_c, into the calculation when two kinds of materials are in contact. All of these methods appear to be applicable to this project.

In order to verify the numerical solutions, experimental data is needed. A literature search indicates that most field measurements, especially those for transient heat transfer or life-cycle tests, use copper constantan thermocouples or heat-flux sensors. This is true whether the test is done on a fishing vessel or on the house site (18,20). However, in the case of steady-state heat transfer problems for building wall panels, much experimental work has been conducted using the "Guarded Hot

Box" technique (4). ASTM (American Society for Testing and Materials) has set up a standard test method for using this technique. According to their specifications, this method covers the measurement of the steady-state thermal transfer properties of panels. It is suitable for building construction assemblies, building panels, and other nonhomogeneous sections in similar temperature ranges. Therefore, the test of thermal performance of fish hold wall sections should be adequate. The details of this technique will be presented in Chapter III.

CHAPTER II. NUMERICAL MODELING

II.1 Introduction

There are various structural designs of fish hold wall section found in practice. A representative one is shown in Figure II-1. The dimensions of the section in the figure are for the case of a 14 m (45 ft) fishing boat. (1, 7, 12, 16, 20 and 36) Two types of frames, angle iron and flat bar, are common on West Coast steel vessels. Flat bar is initially considered in developing a numerical model, because it makes the structure simpler to analysis. Angle iron will be considered in Chapter IV for further applications. Steel skin, defined as the warm surface for convenience, is the outside skin of the vessel and usually contacts sea water and atmosphere. Plywood sheet (or sheet steel in later chapters), defined as the cold surface, is the inside liner of the fish hold wall and usually contacts the refrigerated storage air, fish or ice. Insulating urethane foam is generally sprayed between two surfaces. However, a variation of foam thickness occurs in practice.

In considering heat flow through the fish hold wall section, the following assumptions are made:

a. Convection boundaries occur on the warm and cold surfaces.

b. Adiabatic boundaries occur on the other two surfaces because of symmetry of structure.

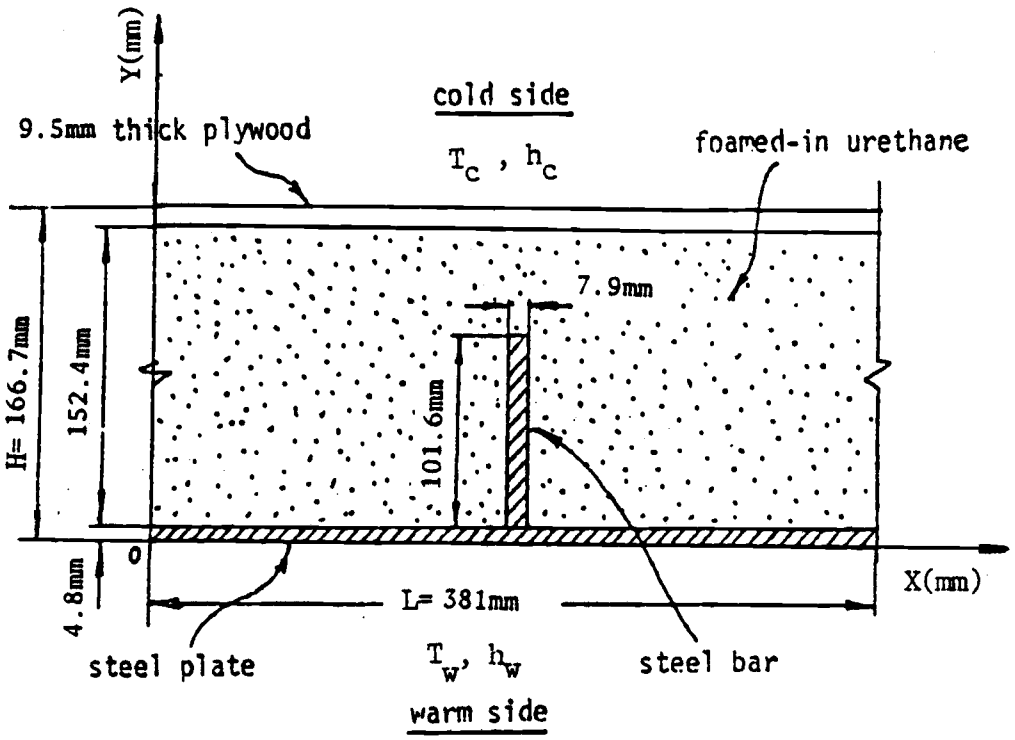

Fig.II-1

REPRESENTATIVE FISH HOLD WALL SECTION

(not to scale)

c. Thermal conductivitiy is uniform for each material, but will vary with different materials.

d. The system is a two-dimensional in the (x,y) coordinates.

e. Steady-state conditions will prevail.

f. There is no internal heat generation.

II.2 Partial Differentail Equation and Boundary Conditions

An energy equation for a steady-state two-dimensional heat conduction problem is

$$\frac{\partial}{\partial x}[k(x,y)\frac{\partial T}{\partial x}]+\frac{\partial}{\partial y}[k(x,y)\frac{\partial T}{\partial y}]=0 \qquad \text{(II-1)}$$

where

k(x,y)=thermal conductivity (W/mK) which is a function of (x,y) coordinates,

T=temperature in °C.

To solve this equation, specific boundary conditions are required. As assumed, convective and adiabatic boundaries are encountered. For the convective boundaries in steady-state, heat transfer to or from the surface by conduction equals that leaving or entering the surface by convection. This condition can be written mathematically for the cold surface as

$$h_c(T\big|_{y=H}-T_c)=-k(x,y)\frac{\partial T}{\partial y}\Big|_{y=H} \qquad \text{(II-2)}$$

and for the warm surface as

$$h_w(T_w - T\big|_{y=0}) = -k(x,y)\frac{\partial T}{\partial y}\Big|_{y=0} \qquad \text{(II-3)}$$

where

h_c=convective coefficient for the cold side surface, in W/m^2K.

h_w=convective coefficient for the warm side surface, in W/m^2K.

T_c=temperature on the cold side surface, in °C.

T_w=temperature on the warm side surface, in °C.

H=total thickness of the panel, in m.

The left and right vertical surfaces are adiabatic boundaries. Mathematically, this condition is stated as

$$-k(x,y)\frac{\partial T}{\partial X}\Big|_{x=0} = 0 \qquad \text{(II-4)}$$

for the case of the left vertical surface, and

$$-k(x,y)\frac{\partial T}{\partial X}\Big|_{x=L} = 0 \qquad \text{(II-5)}$$

for the case of the right vertical surface.

where

L=frame spacing of the panel, in m.

II.3 Finite Element Method

The finite element method is a powerful numerical procedure to solve mathematical problems in engineering. Its advantages are:

1. The material properties in adjacent elements do not have to be the same.
2. Irregularly shaped boundaries can be approximated easily.
3. The size of the elements can be varied.
4. Mixed boundary conditions can easily be handled.(30)

In the case of such boundary-value differential equations as II-1, Galerkin's approach (30) leads to

$$\int_A [\frac{\partial}{\partial x}(k_x \frac{\partial T}{\partial x}) + \frac{\partial}{\partial y}(k_y \frac{\partial T}{\partial y})] [W]^T dA = 0 \qquad \text{(II-6)}$$

where

$[W]^T$=transform vector of weight function.

k_x=thermal conductivity which is a function of x coordinate, in W/mK.

k_y=thermal conductivity which is a function of y coordinate, in W/mK.

A=area of the element, in m^2.

Using the method of integration by parts, the two integrals can be expressed as

$$\int_A \frac{\partial}{\partial x}(k_x \frac{\partial T}{\partial x}) [W]^T dA$$

$$= -\int_A k_x \frac{\partial T}{\partial x} \frac{\partial [W]^T}{\partial x} dA + \int_S k_x \frac{\partial T}{\partial x} \eta_x [W]^T dS \qquad \text{(II-7)}$$

and

$$\int_A \frac{\partial}{\partial y}(k_y \frac{\partial T}{\partial y}) [W]^T dA$$

$$= -\int_A k_y \frac{\partial T}{\partial y} \frac{\partial [W]^T}{\partial y} dA + \int_S k_y \frac{\partial T}{\partial y} \eta_y [W]^T dS \qquad \text{(II-8)}$$

where

S=integral along the boundary

η_x=x component of the unit vector normal to the surface.

η_y=y component of the unit vector normal to the surface.

By substituting Equation II-7 and II-8 into II-6, we obtain

$$-\int_A (k_x \frac{\partial T}{\partial x} \frac{\partial [W]^T}{\partial x} + k_y \frac{\partial T}{\partial y} \frac{\partial [W]^T}{\partial y}) dA + \int_S (k_x \frac{\partial T}{\partial x} \eta_x + k_y \frac{\partial T}{\partial y} \eta_y) [W]^T dS = 0 \quad \text{(II-9)}$$

The surface integral relates to the boundary condition. In vector form, it may be written as

$$k_x \frac{\partial T}{\partial x} \eta_x + k_y \frac{\partial T}{\partial y} \eta_y = q_n \quad \text{(II-10)}$$

where

q_n=heat flux normal to the surface, in W. If the heat is in, q_n is defined to be positive, otherwise, it is negtive.

Thus, from Equation II-9 and II-10, we obtain

$$\int_A (k_x \frac{\partial T}{\partial x} \frac{\partial [W]^T}{\partial x} + k_y \frac{\partial T}{\partial y} \frac{\partial [W]^T}{\partial y}) dA = \int_S q_n [W]^T dS \quad \text{(II-11)}$$

Next we define the approximate temperature by

$$T=[W]\{T\}=[W_i \; W_j \; W_k]\begin{Bmatrix} T_i \\ T_j \\ T_k \end{Bmatrix} \qquad \text{(II-12)}$$

where

T =solution vector of the approximated temperature, in °C.

W_i=weight at node i.

W_j=weight at node j.

W_k=weight at node k.

T_i=temperature at node i, in °C.

T_j=temperature at node j, in °C.

T_k=temperature at node k, in °C.

Thus,

$$\frac{\partial T}{\partial x}=\frac{\partial [W]}{\partial x}\{T\}, \quad \frac{\partial T}{\partial y}=\frac{\partial [W]}{\partial y}\{T\}. \qquad \text{(II-13)}$$

Rearranging the terms, Equation II-11 becomes

$$\{T\}\int_A [k_x \frac{\partial [W]^T}{\partial x}\frac{\partial [W]}{\partial x}+k_y \frac{\partial [W]^T}{\partial y}\frac{\partial [W]}{\partial y}]\, dA=\int_S q_n [W]^T dS \qquad \text{(II-14)}$$

The left integral in Equation II-14 yields the element coefficient matrix $[K^e]$ and the right integral contributes to both $[K^e]$ and $\{F^e\}$. $\{F^e\}$ is an element force vector. Thus, Equation II-14 can be written in matrix notation as

$$[K^e]\{T\}=\{F^e\} \qquad \text{(II-15)}$$

The three-node triangular element, shown in Figure II-2,

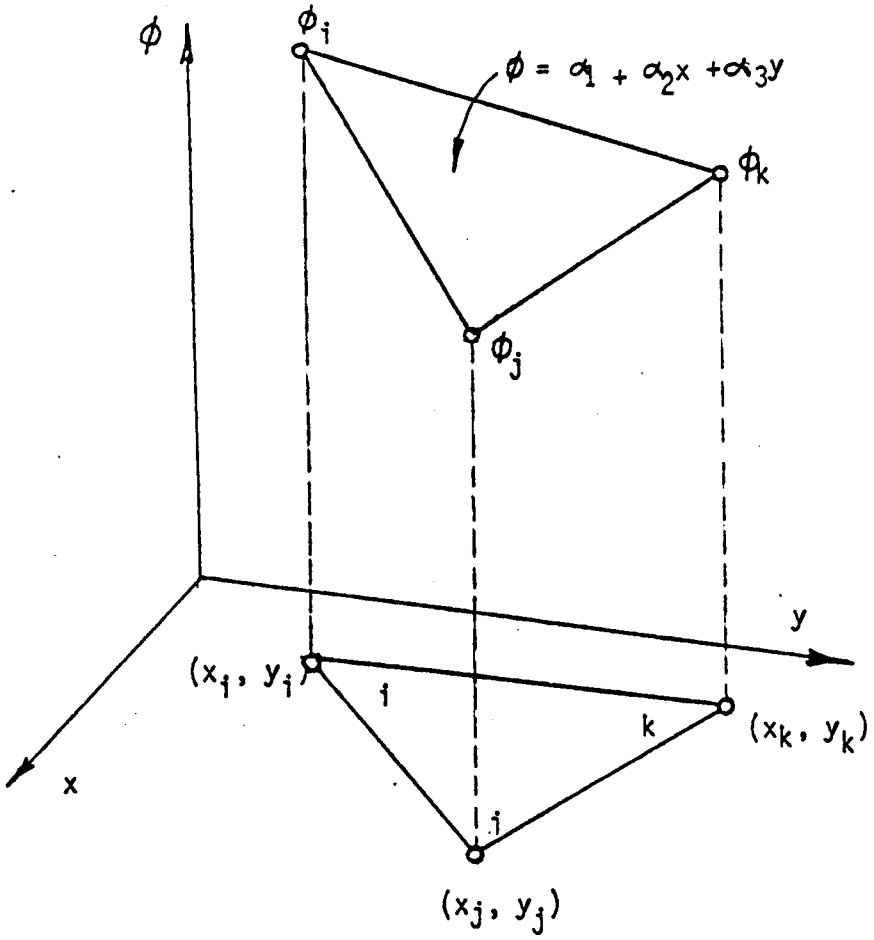

Fig. II-2

TWO-DIMENSIONAL SIMPLEX ELEMENT (30)

has been used extensively for the solution of two-dimensional heat conduction problems. The labeling here always proceeds counterclockwise from node i, which is arbitrarily specified. The general interpolating polynomial for T over an element is

$$T=\alpha_1+\alpha_2 x+\alpha_3 y \qquad \text{(II-16)}$$

with the nodal conditions

$T=T_i$ at $x=X_i$, $y=Y_i$

$T=T_j$ at $x=X_j$, $y=Y_j$

and

$T=T_k$ at $x=X_k$, $y=Y_k$

where

$\alpha_1, \alpha_2, \alpha_3$=coefficients for each node in an element;

X_i, X_j, X_k=x coordinates for nodes i,j, and k;

Y_i, Y_j, Y_k=y coordinates for nodes i,j, and k.

Substitution of these into Equation II-16 produces the system of equations

$$T_i=\alpha_1+\alpha_2 X_i+\alpha_3 Y_i$$

$$T_j=\alpha_1+\alpha_2 X_j+\alpha_3 Y_j$$

$$T_k=\alpha_1+\alpha_2 X_k+\alpha_3 Y_k$$

which can be simutaneously solved to yield

$$\alpha_1=\frac{1}{2A}(X_jY_k-X_kY_j)T_i+(X_kY_i-X_iY_k)T_j+(X_iY_j-X_jY_i)T_k$$

$$\alpha_2 = \frac{1}{2A}(Y_j - Y_k)T_i + (Y_k - Y_i)T_j + (Y_i - Y_j)T_k \qquad \text{(II-17)}$$

$$\alpha_3 = \frac{1}{2A}(X_k - X_j)T_i + (X_i - X_k)T_j + (X_j - X_i)T_k$$

where

$$2A = \begin{vmatrix} 1 & X_i & Y_i \\ 1 & X_j & Y_j \\ 1 & X_k & Y_k \end{vmatrix} \qquad \text{(II-18)}$$

Substitution of the equations of II-17 into Equation II-16 and rearrangement of the terms produce an equation which has three weight functions, one for each node,

$$T = W_i T_i + W_j T_j + W_k T_k \qquad \text{(II-19)}$$

The weight functions are respectively defined as

$$W_i = \frac{1}{2A}(a_i + b_i x + c_i y)$$

where

$$a_i = X_j Y_k - X_k Y_j$$

$$b_i = Y_j - Y_k$$

$$c_i = X_k - X_j$$

$$W_j = \frac{1}{2A}(a_j + b_j x + c_j y)$$

where

$$a_j = X_k Y_i - Y_k X_i$$

$$b_j = Y_k - Y_i$$

$$c_j = X_i - X_k$$

and

$$W_k = \frac{1}{2A}(a_k + b_k x + c_k y)$$

where

$$a_k = X_i Y_j - X_j Y_i$$

$$b_k = Y_i - Y_j$$

$$c_k = X_j - X_i$$

Thus, the temperature over an element may be expressed in matrix form which is identical to the Equation II-12.

We can now proceed with the evaluation of the element conduction matrix. For instance, one of the entries, K_{ij}, can be calculated as follows:

Since

$$\frac{\partial W_i}{\partial x} = \frac{b_i}{2A}; \qquad \frac{\partial W_i}{\partial y} = \frac{c_i}{2A};$$

$$\frac{\partial W_j}{\partial x} = \frac{b_j}{2A}; \qquad \frac{\partial W_j}{\partial y} = \frac{b_j}{2A}.$$

Then, K_{ij} from Equation II-14 is

$$K_{ij} = \int_A \left(k_x \frac{\partial W_i}{\partial x}\frac{\partial W_j}{\partial x} + k_y \frac{\partial W_i}{\partial y}\frac{\partial W_j}{\partial y}\right) dA$$

$$= \int_A k_x \left(\frac{b_i}{2A}\right)\left(\frac{b_j}{2A}\right) + k_y \left(\frac{c_i}{2A}\right)\left(\frac{c_j}{2A}\right) dA \qquad \text{(II-20)}$$

$$= \frac{k_x}{4A} b_i b_j + \frac{k_y}{4A} c_i c_j$$

Thus,

$$[K^e]=\frac{k_x}{4A}\begin{bmatrix} b_ib_i & b_ib_j & b_ib_k \\ b_jb_i & b_jb_j & b_jb_k \\ b_kb_i & b_kb_j & b_kb_k \end{bmatrix} + \frac{k_y}{4A}\begin{bmatrix} c_ic_i & c_ic_j & c_ic_k \\ c_jc_i & c_jc_j & c_jc_k \\ c_kc_i & c_kc_j & c_kc_k \end{bmatrix} \quad \text{(II-21)}$$

This is the conduction matrix for an internal triangular element. No convection is involved.

For an external element which has one side involved with convection, a little more effort must be taken. The term on the right-hand side of Equation II-14 represents a convective heat transfer effect. Heat flux, q_n, may be rewritten as

$$q_n=k(x,y)\frac{\partial T}{\partial n}$$

$$=h(T_s-T_\infty)$$

along the boundary, where n is the outward vector normal to the surface as Figure II-3 shows. We wish to evaluate

$$\int_S q_n[W]^T dS=\int_S h(T_s-T_\infty)[W]^T dS \quad \text{(II-22)}$$

along the boundary. Where

h=surface convection coefficient, in W/m^2K.

T_s=temperature on the surface, in °C. For convection occurring at ij side of the element,

$T_s=W_iT_i+W_jT_j+0T_k$.

T_∞=air temperature near the surface, in °C.

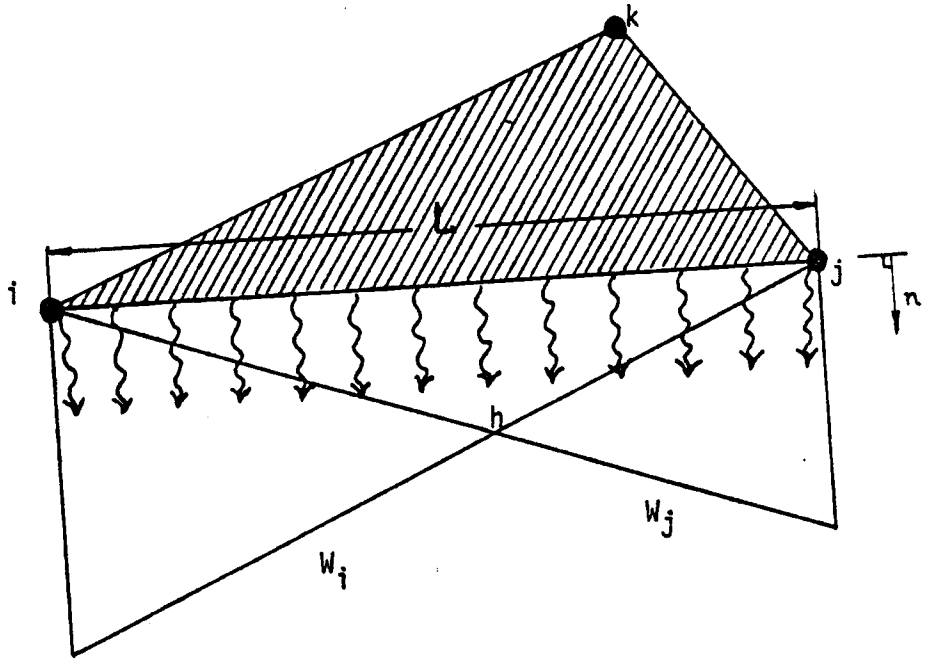

Fig. II-3

AN ELEMENT WITH CONVECTION BOUNDARY

Therefore, the flux term becomes

$$h(T_s-T_\infty)=h\begin{bmatrix}W_i & W_j & 0\end{bmatrix}\begin{Bmatrix}T_i\\T_j\\T_k\end{Bmatrix}-hT_\infty \qquad \text{(II-23)}$$

By substituting Equation II-23 into II-22, the right-hand side becomes

$$\int_S h(T_s-T_\infty)[W]^T dS$$

$$=h\int_S [W]^T[W]\{T\}dS-\int_S [W]^T hT_\infty dS \qquad \text{(II-24)}$$

Where the weight function integration of the first term at the right-hand side contributes to $[K^e]$ by following:

$$h\int_S [W]^T[W]dS=h\int_S \begin{bmatrix}W_iW_i & W_iW_j & W_iW_k\\ W_jW_i & W_jW_j & W_jW_k\\ W_kW_i & W_kW_j & W_kW_k\end{bmatrix} dS \qquad \text{(II-25)}$$

By considering that W_k is zero for the element shown in Figure II-3, the integral reduces to

$$h\int_S [W]^T[W]dS=h\int_S \begin{bmatrix}W_iW_i & W_iW_j & 0\\ W_jW_i & W_jW_j & 0\\ 0 & 0 & 0\end{bmatrix} dS \qquad \text{(II-26)}$$

The evaluation of the product terms in Equation II-26 can be carried out by employing area coordinates and related integral formula (30) and gives

$$h\int_S [W]^T[W]dS=\begin{bmatrix} \frac{hL}{3} & \frac{hL}{6} & 0 \\ \frac{hL}{6} & \frac{hL}{3} & 0 \\ 0 & 0 & 0 \end{bmatrix} \qquad \text{(II-27)}$$

The $[K^e]$ for an element with one side of ij in convection can now be written as

$$[K^e]=\frac{k_x}{4A}\begin{bmatrix} b_ib_i & b_ib_j & b_ib_k \\ b_jb_i & b_jb_j & b_jb_k \\ b_kb_i & b_kb_j & b_kb_k \end{bmatrix}+\frac{k_y}{4A}\begin{bmatrix} c_ic_i & c_ic_j & c_ic_k \\ c_{jci} & c_jc_j & c_jck \\ c_kc_i & c_kc_j & c_kc_k \end{bmatrix}$$

$$+\frac{hL}{6}\begin{bmatrix} 2 & 1 & 0 \\ 1 & 2 & 0 \\ 0 & 0 & 0 \end{bmatrix} \qquad \text{(II-28)}$$

As we indicated previously, the second integral of the right-hand side of Equation II-24 contributes to vector {F}. Since there is no internal heat generation in this domain, {F} for the element shown in Figure II-3 can be presented as

$$\{F\}=\int_S [W]^T hT_\infty dS$$

$$=hT_\infty\int_S [W]^T dS$$

$$=\frac{hT_\infty}{2}\begin{Bmatrix} 1 \\ 1 \\ 0 \end{Bmatrix} \qquad \text{(II-29)}$$

The results of Equation II-27 through II-29 depend on which side of the element is subjected to convection.

Similar procedures can be carried out for the other two sides of the element. If the convection occurs from two sides of an element, then the surface integral becomes a sum of the integral for each side. In addition, the integral of Equation II-14 for the whole domain can be obtained by a summation of elemental integrals and can be written in matrix form as

$$[K]\{T\}=\{F\}. \qquad \text{(II-30)}$$

[K] is generally referred to as the global conduction matrix and the column vector {F} is global force vector.

The computer program for the finite element method is shown in Appendix 1. This program is a modification of an existing code (30) for a two-dimensional field with constant material properties. The field domain is discretized with linear triangular elements. The modified program accounts for variable thermal properties by assigning different values to each element.

Program GRID, shown in Appendix 1, automatically generates the element data. The principle of GRID is to subdivide a domain in regions, locate the nodal points within a region and then subdivide the region in elements. For the representative wall section shown in Figure II-1, the nodes and elements of the subdivided domain are shown in Figure II-4. The grid system shown here was only for the purpose of developing the program. A non-symmetric

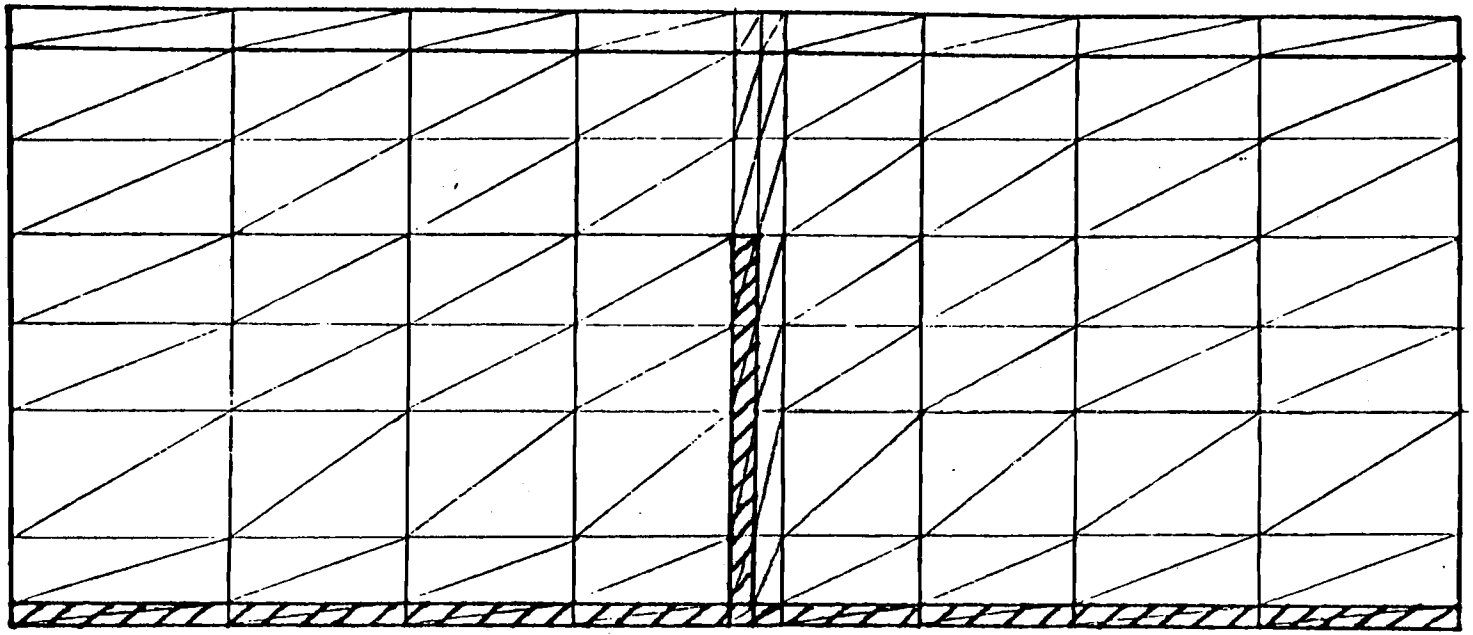

Fig. II-4

SUBDIVIDED NODES AND ELEMENTS FOR THE
REPRESENTATIVE FISH HOLD WALL SECTION

grid was used in the central area because it took less computer time and memory. A finer and more symmetrical grid should have been used had we decided to use the finite element program. (However, the finite difference method was later found to be more feasible, and further study on the finite element program was then no longer necessary.)

The program HT calculates the temperature distribution in two-dimensional bodies subject to either prescribed boundary temperature or surface convection. First, the program reads inputs which are generated by GRID. Then, the global stiffness matrix and global force vector are assembled. Subroutine BDYVAL reads the specified values of {F} and {T} and modifies [K], using the procedure of deletion of rows and columns. The subroutine DCMPBD decomposes the band matrix [K] into an upper triangular matrix using the Gaussian elimination procedure (30). The subroutine SLVBD is used with DCMPBD to obtain the solution using a backward substitution method (30).

So far, formulation of finite element model has been completed. Next step is to analyse the same problem using finite difference method.

II.4 Finite Difference Method

There are two different approaches for the formulation of a heat conduction problem with the finite difference method. One is called "differencing technique", the other is called "heat balance method". Since the heat balance

method gives greater flexibility and better physicalinsight (34), it is a better choice to solve our problem.

Figure II-5 shows node ij surrounded by its four immediate neighboring nodes. These neighboring nodes are designated as 1, 2, 3 and 4, as well as subscripts such as (i+1,j), (i-1,j), (i,j+1) and (i,j-1). The quantities designated δ_{1i}, δ_{i1} and etc, are the half-distances between two neighboring nodes and may have different values. The system of subscripting is apparent from the figure.

The heat flux at the boundary of node i may now be expressed as

$$q_{(i-1,j)-(i,j)} = \frac{1}{R_{1i} + R_{i1}} (T_{i-1,j} - T_{i,j})$$

$$= K^1_{i,j} (T_{i-1,j} - T_{i,j})$$

$$q_{(i+1,j)-(i,j)} = \frac{1}{R_{2i} + R_{i2}} (T_{i+1,j} - T_{i,j})$$

$$= K^2_{i,j} (T_{i+1.j} - T_{i,j})$$

$$q_{(i,j-1)-(i,j)} = \frac{1}{R_{3j} + R_{j3}} (T_{i,j-1} - T_{i,j})$$

$$= K^3_{i,j} (T_{i,j-1} - T_{i,j})$$

$$q_{(i,j+1)-(i,j)} = \frac{1}{R_{4j} + R_{j4}} (T_{i,j+1} - T_{i,j})$$

$$= K^4_{i,j} (T_{i,j+1} - T_{i,j}) \qquad \text{(II-31)}$$

where

q=heat flux, in Watts.

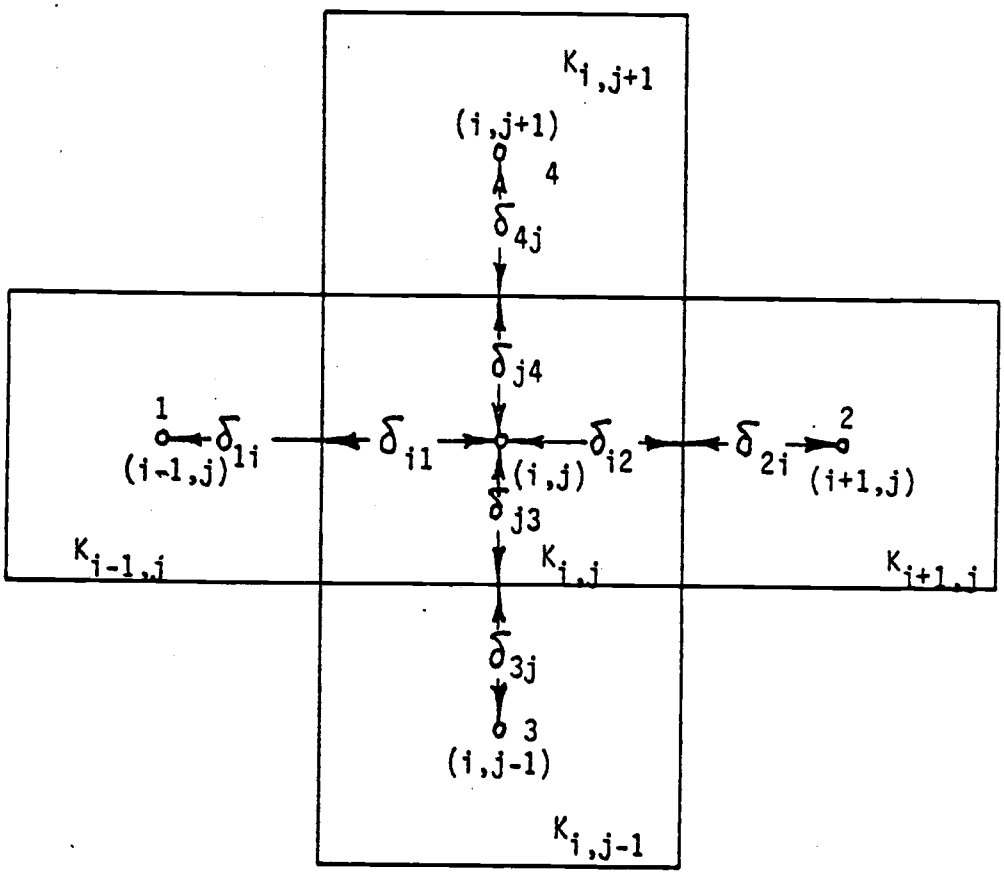

Fig. II-5

NODE IJ AND ITS IMMEDIATE NEIGHBORS (33)

R_{1i}=thermal resistance of δ_{1i} thick material, in K/W. (Same definitions respond to other subscripts.)

$T_{i,j}$=temperature at node ij, in °C.

$K^k_{i,j}$=conductance between node ij and its four neighbors, in W/K. (k=1, 2, 3, 4.)

For the case of steady-state two-dimensional heat flow with no internal heat generation term, the heat balance equation may be expressed as

$$K^1_{i,j}(T_{i-1,j}-T_{i,j})+K^2_{i,j}(T_{i+1,j}-T_{i,j}) +K^3_{i,j}(T_{i,j-1}-T_{i,j})+K^4_{i,j}(T_{i,j+1}-T_{i,j})=0 \quad \text{(II-32)}$$

If we define

$$B=K^1_{i,j}+K^2_{i,j}+K^3_{i,j}+K^4_{i,j}$$

and

$$C^1_{i,j}=K^1_{i,j}/B$$

$$C^2_{i,j}=K^2_{i,j}/B$$

$$C^3_{i,j}=K^3_{i,j}/B$$

$$C^4_{i,j}=K^4_{i,j}/B$$

The implicit form of Equation II-33 may be written as

$$T_{i,j}=C^1_{i,j}T_{i-1,j}+C^2_{i,j}T_{i+1,j}$$
$$+C^3_{i,j}T_{i,j-1}+C^4_{i,j}T_{i,j+1} \qquad \text{(II-33)}$$

Using the Gauss-Seidel iteration method (9), we can express the equation as

$$T^p_{i,j}=T^{p-1}_{i,j}+w(T^*_{i,j}-T^{p-1}_{i,j}) \qquad \text{(II-34)}$$

In this equation, $T^*_{i,j}$ is the $T_{i,j}$ in Equation II-33, superscript p is the number of iteration steps, and w is an overrelaxation coefficient which makes iteration converge more rapidly (9).

The development thus far has indicated the general equation for a conducting medium. The calculation of $K_{i,j}$ quantities varies with different conditions. For the internode surface with two different materials, as shown in Figure II-6, $K_{i,j}$ can be obtained from

$$K^k_{i,j}=\frac{1}{\frac{\delta_{i2}}{k_i A_{i2}}+\frac{\delta_{2i}}{k_2 A_{i2}}+R_c}$$

where

k_i=thermal conductivity at node i, in W/mK.

A_{i2}=cross section area between nodes i and 2, in m^2.

R_c=contact resistance between the different materials, in K/W.

For the surface node involved with convection, as shown in Figure II-7, $K^k_{i,j}$ may be calculated from

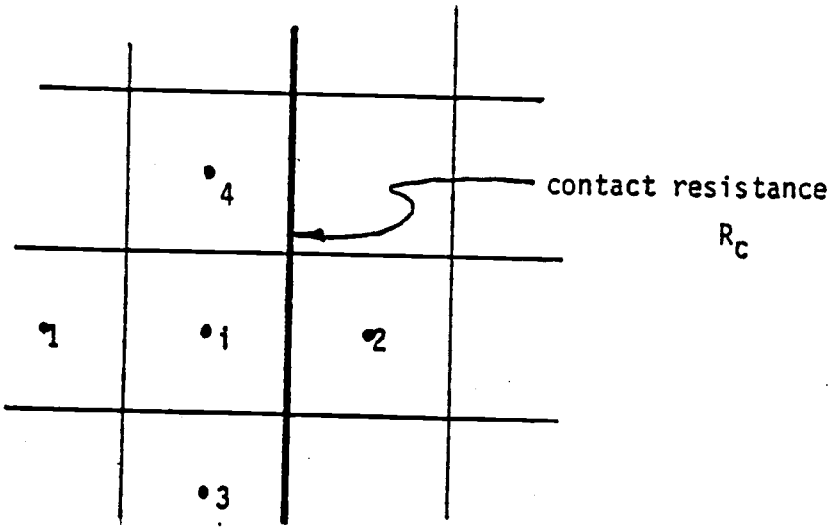

$$K_{i2} = \frac{1}{\frac{\delta_{i2}}{K_i A_{i2}} + \frac{\delta_{2i}}{K_2 A_{i2}} + R_c}$$

Fig. II-6

INTERNAL CONTACT RESISTANCE FOR MATERIALS
HAVING TWO DIFFERENT THERMAL CONDUCTIVITY VALUES (33)

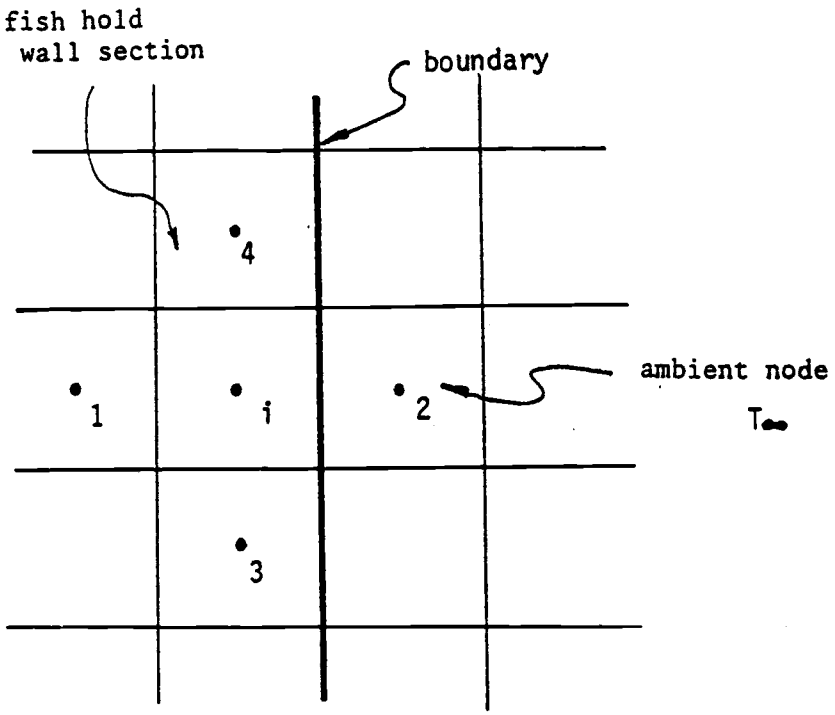

$$k_{i2} = \frac{1}{\frac{\delta_{i2}}{K_i A_{i2}} + \frac{1}{h_i A_{i2}}}$$

Fig. II-7

CONVECTION AT SURFACE (33)

$$K_{i,j} = \frac{1}{\frac{\delta_{i2}}{k_i A_{i2}} + \frac{1}{h_i A_{i2}}}$$

where

h_i=surface convective coefficient at node i, in W/m^2K.

For an adiabatic surface, we can designate $T_{i,j} = T_{i+1,j}$ instead of calculating $K^k_{i,j}$.

We now consider a computer program, named FD, for determining the temperature distribution in a steady-state two-dimensional system. The grid describing the two-dimensional region for the representative wall section appears in Figure II-8. The program listing appears in Appendix 2. (The program listed is for the case of flat bar frames. A slightly modified mesh system is needed for angle iron frames. Detailed information related to the mesh system of both angle iron and flat bar is availabe in the Department of Agricultural Engineering, Oregon State University.) The node size and various thermal properties can be varied by modifying statements at the begining of the program. Values of $K_{i,j}$ are then calculated for different conditions, as for an internode surface, convective surface, and so on. Solution is obtained by the Gauss-Seidel iteration (9). Desired accuracy is controlled by a criterion of convergence as well as a heat balance check. The criterion of convergence is established for the maximum difference between two successive values of $T_{i,j}$

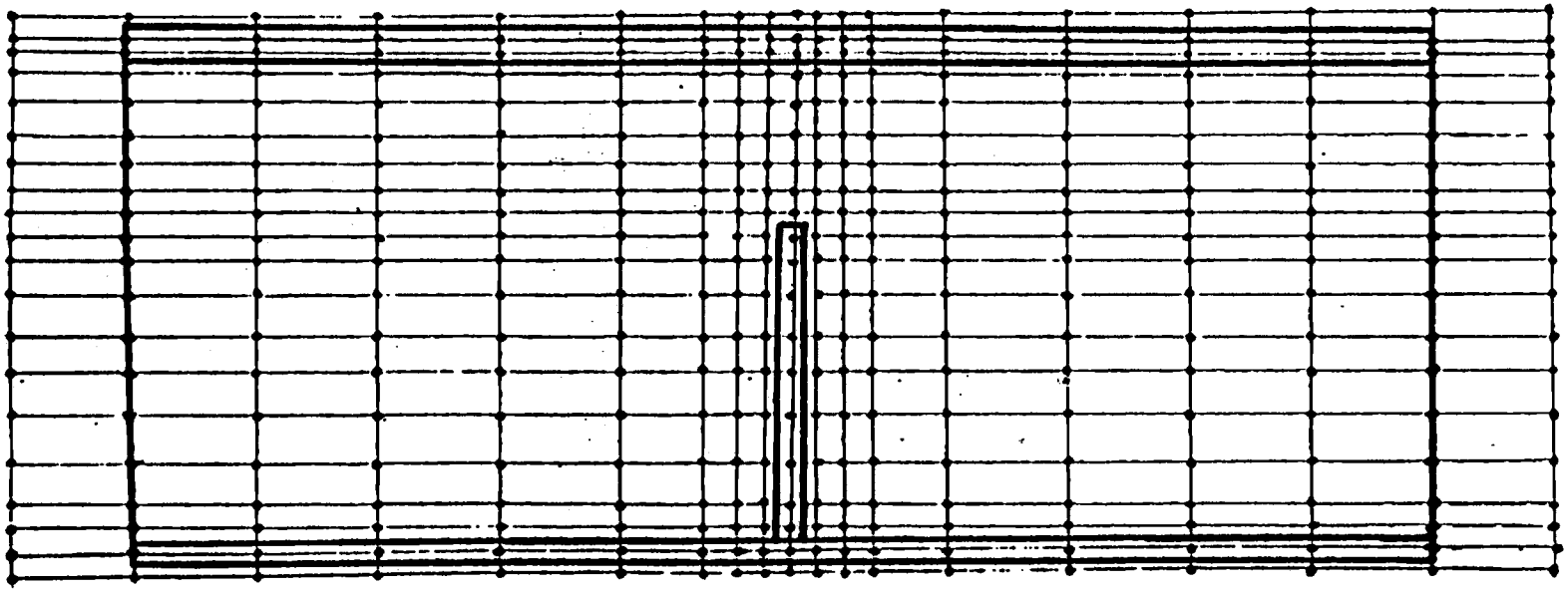

Fig. II-8

TWO-DIMENSIONAL GRID FOR APPLYING FINITE DIFFERENCE METHOD

for all nodes in the domain, i.e.,

$$\text{Max.}\frac{\sum_{i=1}^{m}\sum_{j=1}^{n}\left|T_{i,j}^{p}-T_{i,j}^{p-1}\right|}{m\,n}<\varepsilon$$

where

m=number of nodes in x direction.

n=number of nodes in y direction.

ε=criterion for convergence.

The heat balance is checked by calculating and comparing heat fluxes through the cold and warm surface. That is, the difference of heat inflowing and outflowing should approach zero for this problem.

Figure II-9 shows how the optimum value of an overrelaxation coefficient to be chosen. Generally, the range of choice is $1<W<2$ (9). The curve shows that the overrelaxation coefficient of 1.6 decreases iteration steps to 5 from 175. Stability need cause no concern in this case since the implicit scheme has been used.

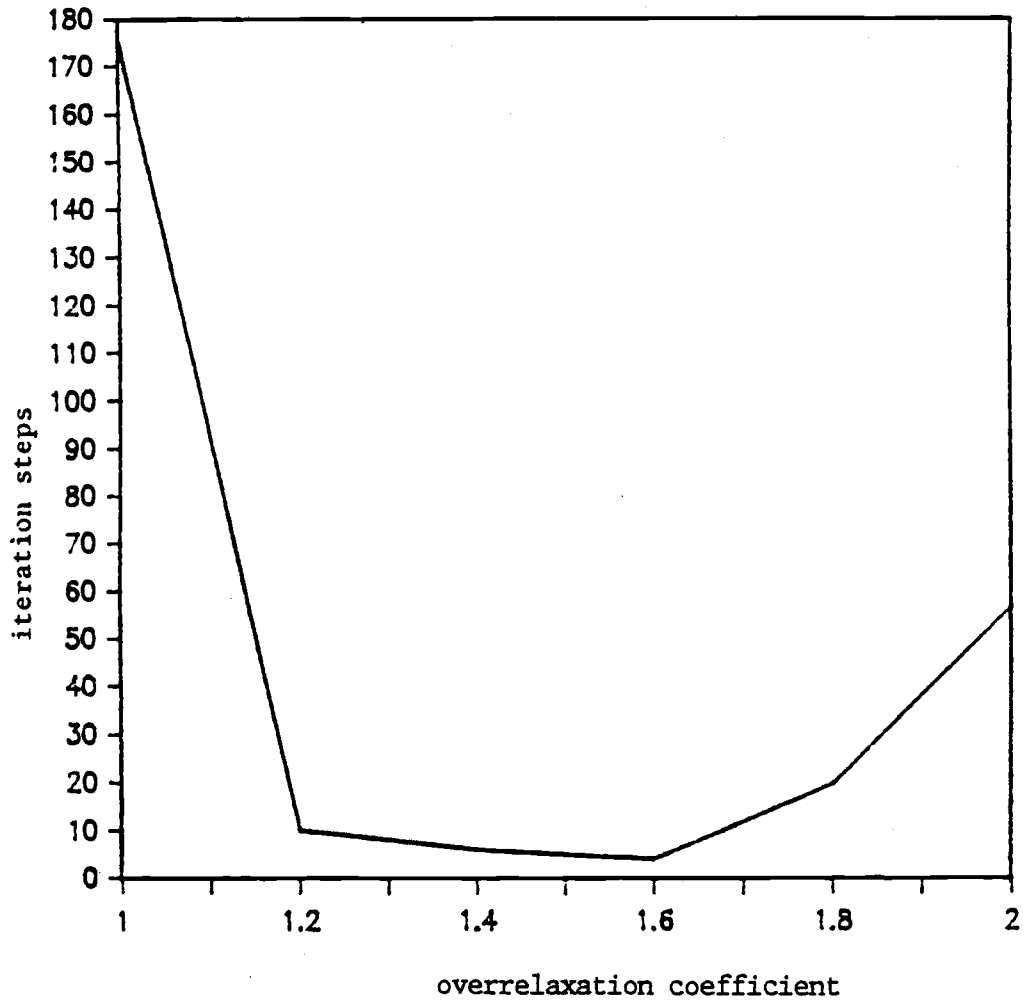

Fig. II-9

OVERRELAXATION COEFFICIENT vs ITERATION STEPS

CHAPTER III. EXPERIMENTAL INVESTIGATION AND RESULTS

III.1 Introduction

In Chapter II, the energy equation for steady-state, two-dimensional heat conduction was introduced. Two computer programs were developed to simulate the two-dimensional temperature profiles in wall sections, using finite difference and finite element methods, respectively. The purpose of the experimental investigation was to verify the results obtained from these computer models.

The experiments consisted of a straightforward determination of the two-dimensional temperature field with a "guarded hot box" (4) technique. Particular attention was given to heat flux, q in W/m^2, thermal transmittance, U in W/m^2K, panel conductance, C in W/m^2K, and panel resistance, R=1/C. In addition, thermal conductivities and densities of insulation material were also measured using "guarded hot plate" equipment (5). In Chapter IV, the measurements will be compared with results predicted by the computer programs.

Two test assemblies, each of which could be modified for different insulation thicknesses and cold surface liners, were designed, then constructed in the Agricultural Engineering Department shop at Oregon State University,

with assistance from Robert Schneckenberger. They were then insulated by a commercial firm, and tested by Dynatherm Engineering, a specialized laboratory in Lino Lakes, Minnesota.

In the discussion that follows, Section III.2 describes the "guarded hot box" technique and the experimental setup. Section III.3 introduces the design and construction of test assemblies. Section III.4 lists the experimental procedures. Finally, test results are reported in Section III.5.

III.2 Guarded Hot Box

The "guarded hot box" technique involves the measurement of steady-state thermal transfer properties of panels. This method is especially suitable for evaluation of thermal performance of building construction assemblies and other applications of nonhomogeneous specimens at similar temperature ranges (4). Therefore, it can be used for our purpose.

To determine the thermal transmittance, U, and the thermal resistance, R, of any specimen, it is necessary to know the area, A, the heat flux, q, and the temperature differences. All of these must be determined under steady-state conditions. The hot box is an arrangement for establishing and maintaining a desired steady temperature difference across a test panel for the period of time necessary to ensure constant heat flux and steady

temperature, and for an additional period adequate to measure these quantities to the desired accuracy (4). The area and temperatures can be measured directly. To determine q, a metering box is placed with its open side against the warm surface of the test panel as shown in Figure III-1. If a zero temperature difference across the wall of the metering box is maintained, then the net interchange between the metering box and the surrounding space is zero. Thus, the heat input into the metering box is a measure of the heat flux through a known area of the panel. The portion of the test panel outside the meter area and in contact with by the air of the guard space, constitutes a guard area to minimize lateral heat flow in the test panel near the metering area. Figure III-1 also shows a schematic arrangement of the test panel and of various major elements of the apparatus. Figure III-2 shows a possible arrangement of equipment during the test. A fan provides an even, gentle movement of air over the metering area of the panel. The air movement, heat source, and temperature should be well controlled and measured. The test panel is usually set in ambient air long enough to come to practical equilibrium. When a test panel is installed, its edges are insulated to minimize heat loss or gain. A test usually runs at least 8 hours after steady-state is achieved. Steady-state here means to impose and maintain the test conditions until constant temperatures

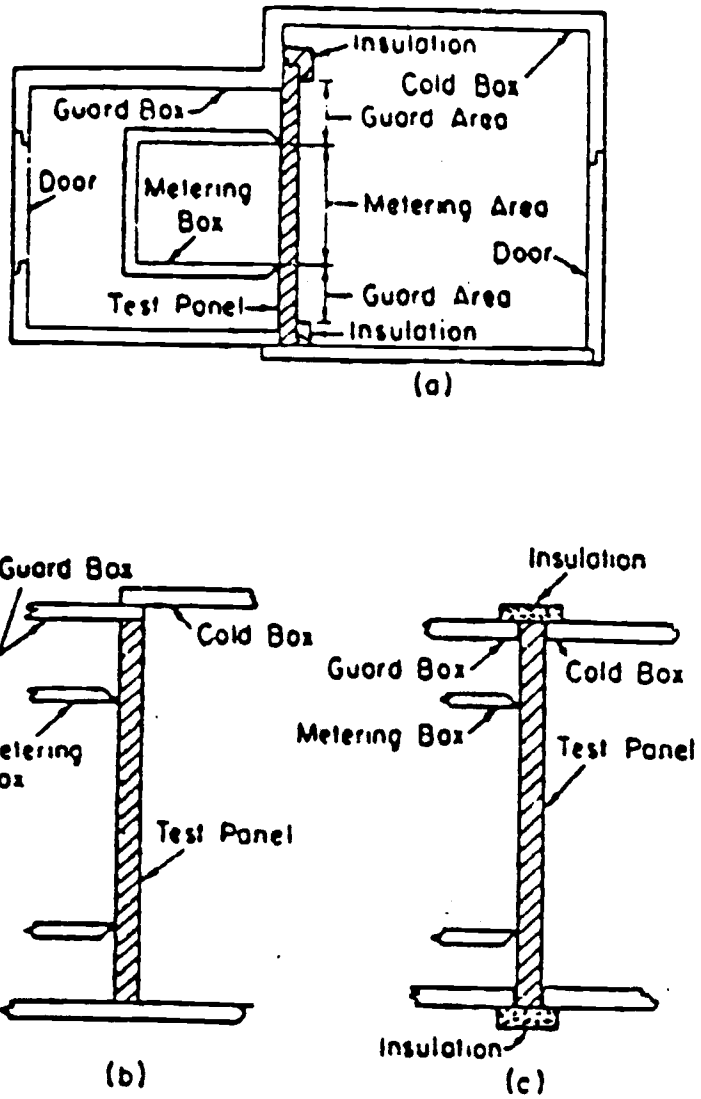

Fig. III-1

GENERAL ARRANGEMENTS OF TEST BOX, GUARD BOX, TEST PANEL, AND COLD BOX. (4)

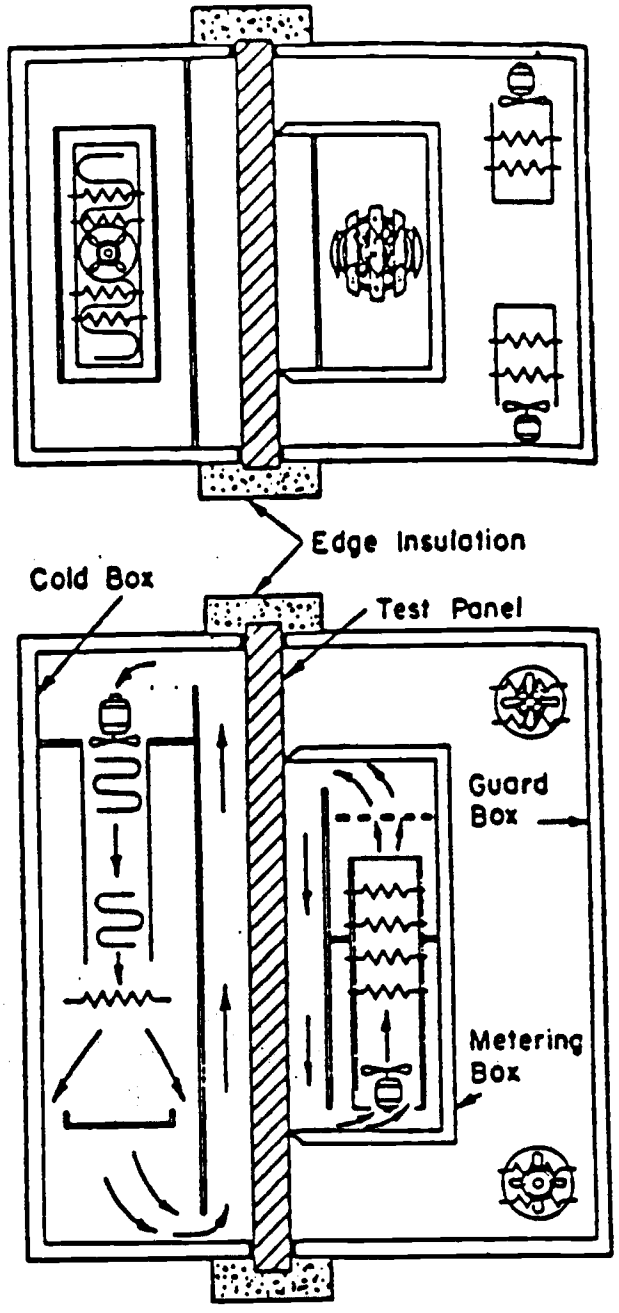

Fig. III-2

ARRANGEMENT OF EQUIPMENT DURING THE TEST (4)

and heat flow readings are attained. After each test, the final test results can be calculated by means of several equations given by ASTM (4). These equations are listed in Appendix 3.

The guarded hot box equipment in the Dynatherm Engineering laboratory is shown in Figure III-3. It can accept test panels up to 1.83x2.13 m (7.17x6.0 ft) in size and has a 1.22x1.52 m (4x5 ft) metering box. The thickness of the tested panel can be up to 406.4 mm (16 in). Still air can be maintained on the warm side, and the exterior (cold side) velocity can be adjusted from 0.2 to 6.7 m/sec. Cold side temperatures are adjustable from about -18 °C (-0.4 °F) to 49 °C (120 °F) and warm side temperatures are adjustable from about 29 °C (84 °F) to 74 °C (165 °F). The range of tested thermal resistance, "R" values are from less than 0.2 to over 7.0 m^2K/W.

III.3 Assemblies Preparation

According to ABS (1) and the investigation done by Dr. Edward Kolbe (20) at Oregon State University, two types of frames, angle iron and flat bar, are common to the West Coast steel vessels. Fish holds and tanks are usually insulated by foamed-in-place urethane of different thicknesses, but some vessels are not insulated at all. Plywood sheet, sheet steel and glass reinforced plastic (fiberglass) are used as the liner of inside walls for many fish holds. (This is the cold surface during the test.)

Fig. III-3 "GUARDED HOT BOX" EQUIPMENT IN DYNATHERM ENGINEERING LABORATORY

For the consideration of various fish hold wall constructions, eight representative panels, as shown in Figure III-4, were obtained by modifying the two test assemblies. The "assembly" here means the one originally constructed at the shop, while the "panel" means the specimen which is reconstructed from the assembly during the test. The insulation thickness and other dimensions are also shown in the figure. Obviously, Panel 4 is the worst case because there is no insulation and a steel sheet was used as the cold surface liner. Panel 6 is the best, with the deepest insulation.

One of test assemblies, called Assembly 1, having angle iron frames, is shown in Figure III-5. The angle iron frames are sized and spaced as in a 14 m (45 ft) fishing boat. A 4.76 mm (3/16 in) steel plate, which simulates the outside vessel skin (warm surface during the test), has a sawcut around a 1.22x1.52 m (4x5 ft) area to match the central metered area of the metering box. This cut essentially prevents lateral heat flow. The overall assembly is about 1.78 m (7.2 ft) wide and 2.13 m (6 ft) high. Five 63.5x38.1x6.4 mm (2.5x1.5x1/4 in) angle irons were symmetrically welded to the center line of the steel skin. 25.4 mm (1 in) welds were staggered on alternate sides at 306 mm (1 ft) intervals as specified by ABS (1). The angle irons were oriented with the 38.1 mm (1.5 in) flange facing the colder exterior side, providing

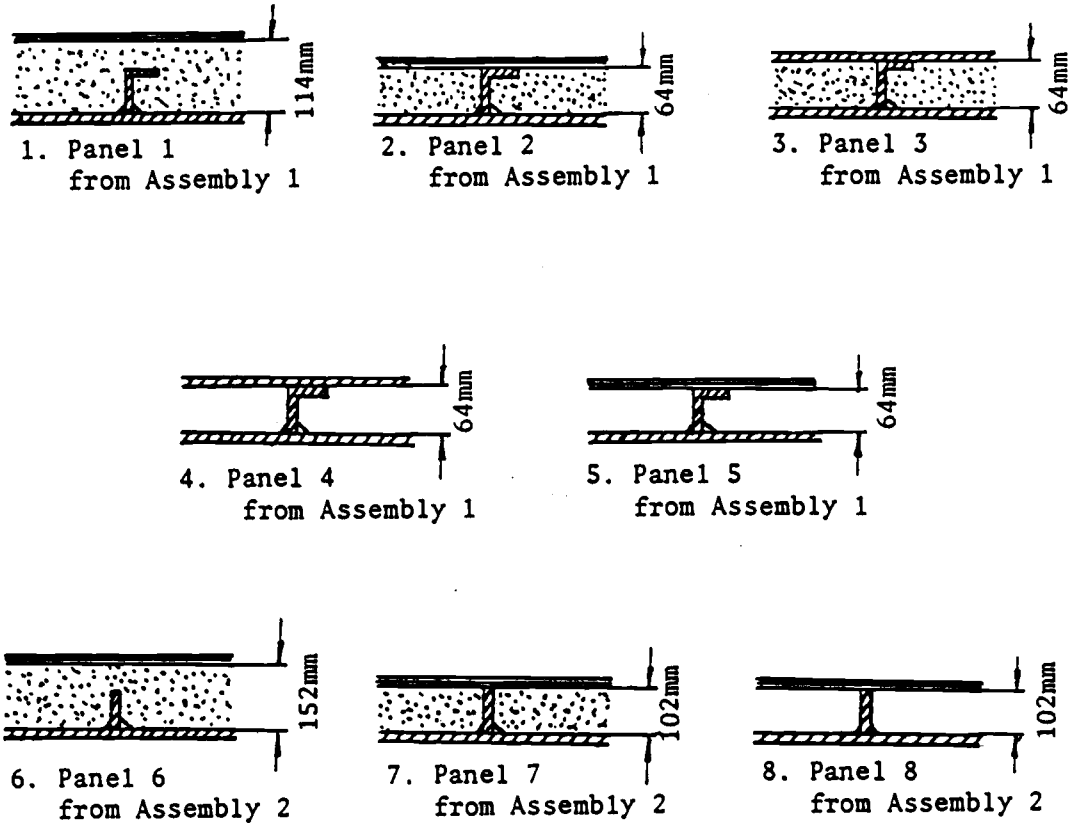

Dimensions: Angle iron frames: 63.5x38.1x6.4mm ($2\frac{1}{2}$x$1\frac{1}{2}$x$\frac{1}{4}$ in.)

Flat bar frames: 101.6x7.9mm (4x$\frac{5}{16}$ in.)

Plywood thickness: 9.5 mm ($\frac{3}{8}$ in.)

Steel liner (cold side) thickness: 2.9 mm (11 gauge)

Steel skin (warm side) thickness: 4.8 mm ($\frac{3}{16}$ in.)

Fig. III-4

EIGHT REPRESENTATIVE TEST PANELS
(not to scale)

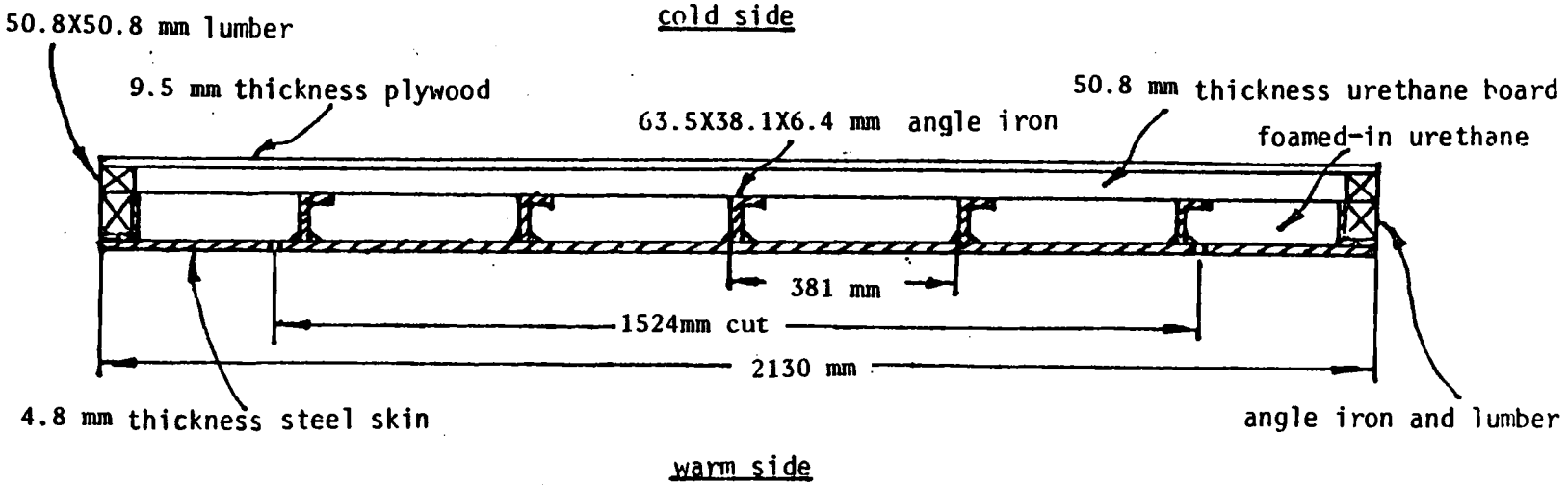

Fig. III-5

ASSEMBLY 1 WITH ANGLE IRON FRAMES

a 63.5 mm (2.5 in) frame depth. The space between the top ofthe angle irons and the steel skin was filled with foamed-in-place urethane measured to be 47 kg/m^3 in density. In order to obtain a flat surface, the foam was then shaved. Four 50.8 X 63.5 mm (2 X 2.5 in) wood strips were then installed around the perimeter of the assembly, with up-right wood strips placed at the left and right edges of the central metered area. The space within the wood strips was then filled with unfaced urethane board with a measured density of 34 kg/m^3, as shown in Figure III-6. A 9.5 mm (3/8 in) marine plywood sheet was then fastened to the cold face of the assembly. Eleven internal thermocouples were installed during the construction. The thermocouples used were copper-constantan and were placed at the locations shown in Figure III-7.a. Thermocouples 7 and 8 were used to determine effects of weld on the heat flow.

A second test assembly, called Assembly 2 (Figure III-8), is also 1.78 m (7.2 ft) wide and 2.13 m (6 ft)high. The main difference with Assembly 1 is that flat bars are used as frames instead of angle irons. The interior (warm surface) is of 4.8 mm (3/16 in) thick steel plate with a sawcut through the steel plate at the perimeter of the central 1.22x1.52 m (4x5 ft) metered area. Five flat bars were welded to the steel plate in the same manner as Assembly 1. The flat bars are 7.9 mm (5/16 in) thick and

Fig. III-6 ASSEMBLY 1 DURING THE CONSTRUCTION

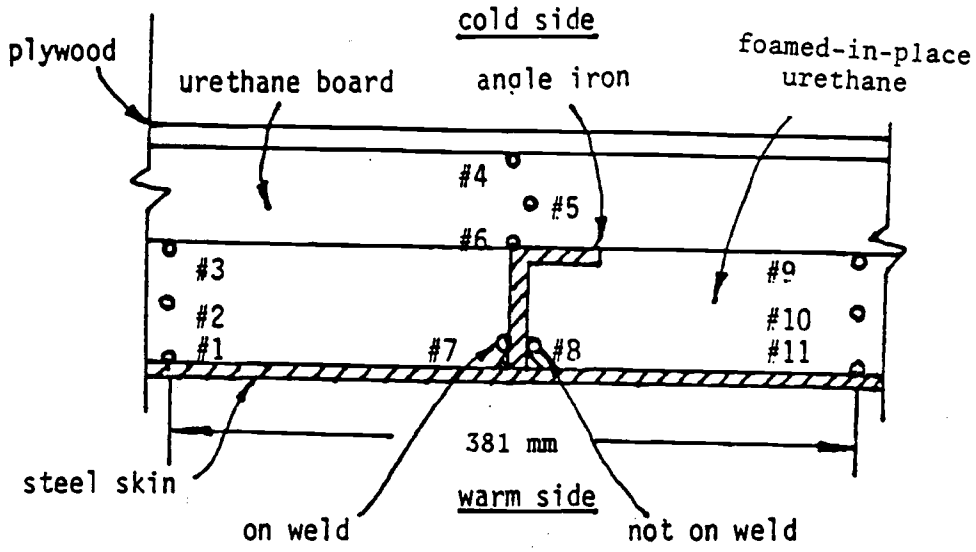

a. Thermocouple Locations in Assembly 1

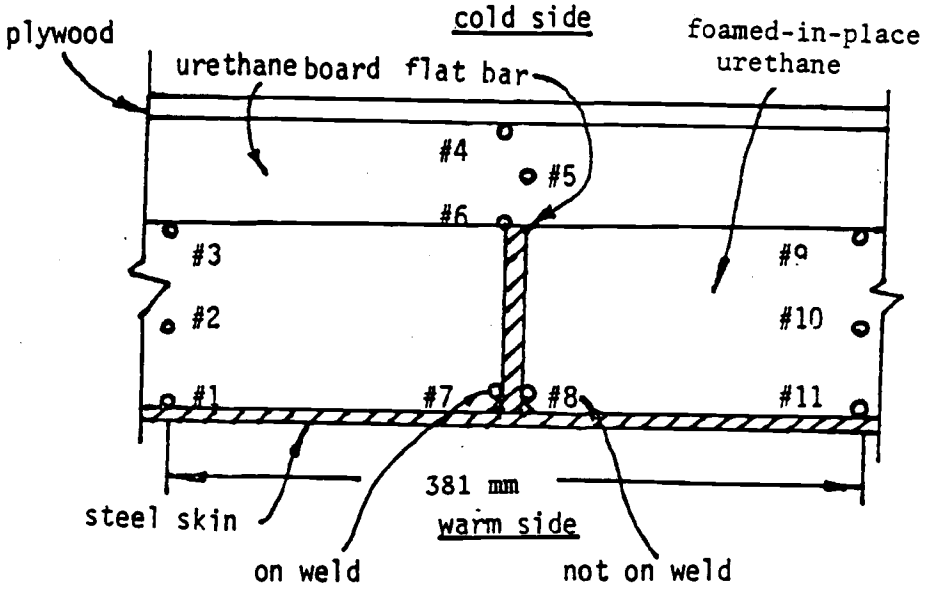

b. Thermocouple Locations in Assembly 2

Fig. III-7
INTERNAL THERMOCOUPLE LOCATIONS
(not to scale)

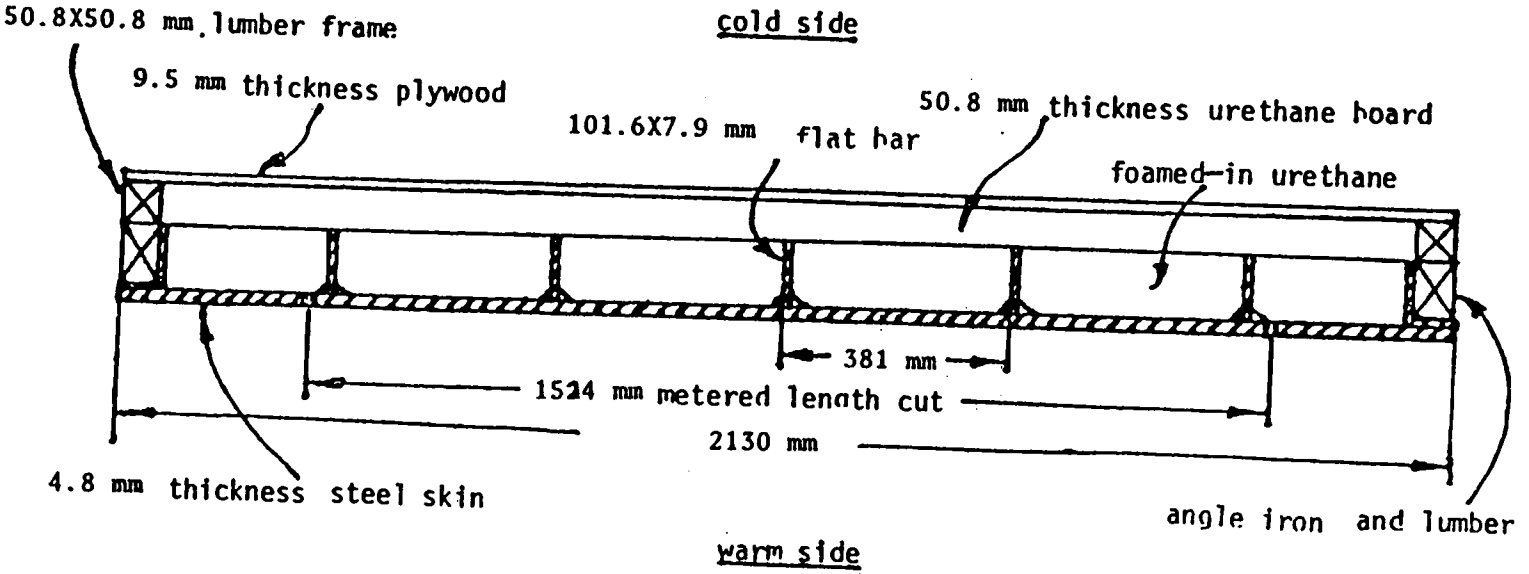

Fig. III-8

Assembly 2 with falt Bar Frames

101.6 mm (4 in) deep. Nominal 50.8x50.8 mm (2x2 in) wood strips were installed at the perimeter of the test assembly with two upright strips installed at the left and right edges of the metered portion. Nominal 50.8 mm (2 in) thick unfaced urethane board insulation was inserted into the recessed area provided by installation of the wood stripping. The exterior (cold surface) was lined with 9.5 mm (3/8 in) marine plywood. Eight 25.4x25.4x6.4 mm (1x1x1/4 in) angle irons uniformly distributed corresponding to the metering area, were welded to the flat bar frames to secure the plywood liner. Eleven internal thermocouples were installed as shown in Figure III-7.b.

The Dynatherm Engineering laboratory conducted a series of eight tests on the two assemblies over a 22 day period, commencing June 24, 1985.

III.4 Experimental Procedures

Eight tests for eight representative panels shown in Figure III-4 were run at Dynatherm Engineering Laboratory. The panels were set up vertically as shown in Figure III-9. Each test panel was instrumented on two surfaces with 30 gage copper-constantan thermocouples at the locations shown in Figure III-10. Four thermocouples, indicated by "weld checking" in the figure, were located at both the cold and warm surfaces. Two of them were fixed on the top of staggered welds while the other two were not. The internal thermocouples, as shown in Figure III-7, were

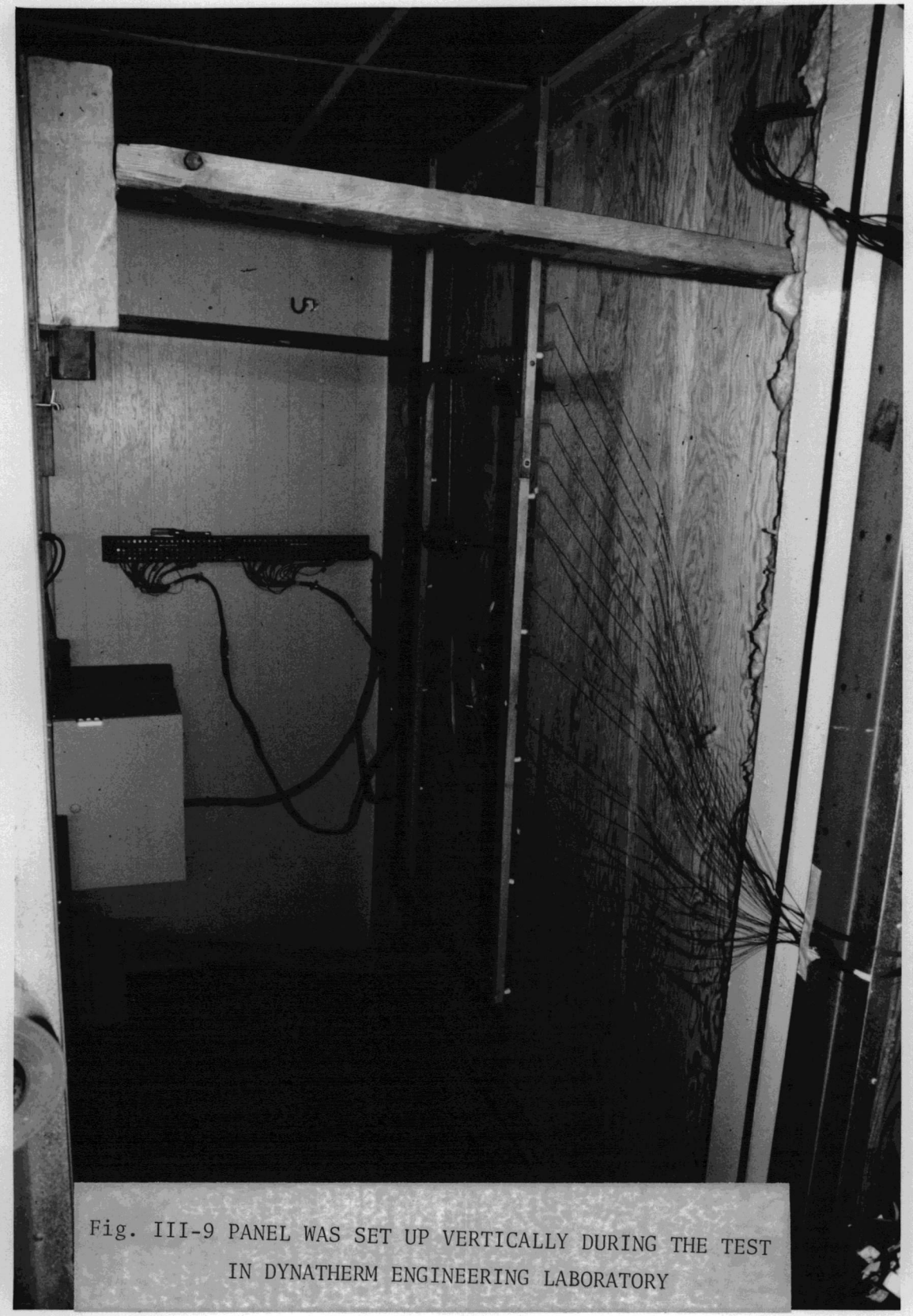

Fig. III-9 PANEL WAS SET UP VERTICALLY DURING THE TEST IN DYNATHERM ENGINEERING LABORATORY

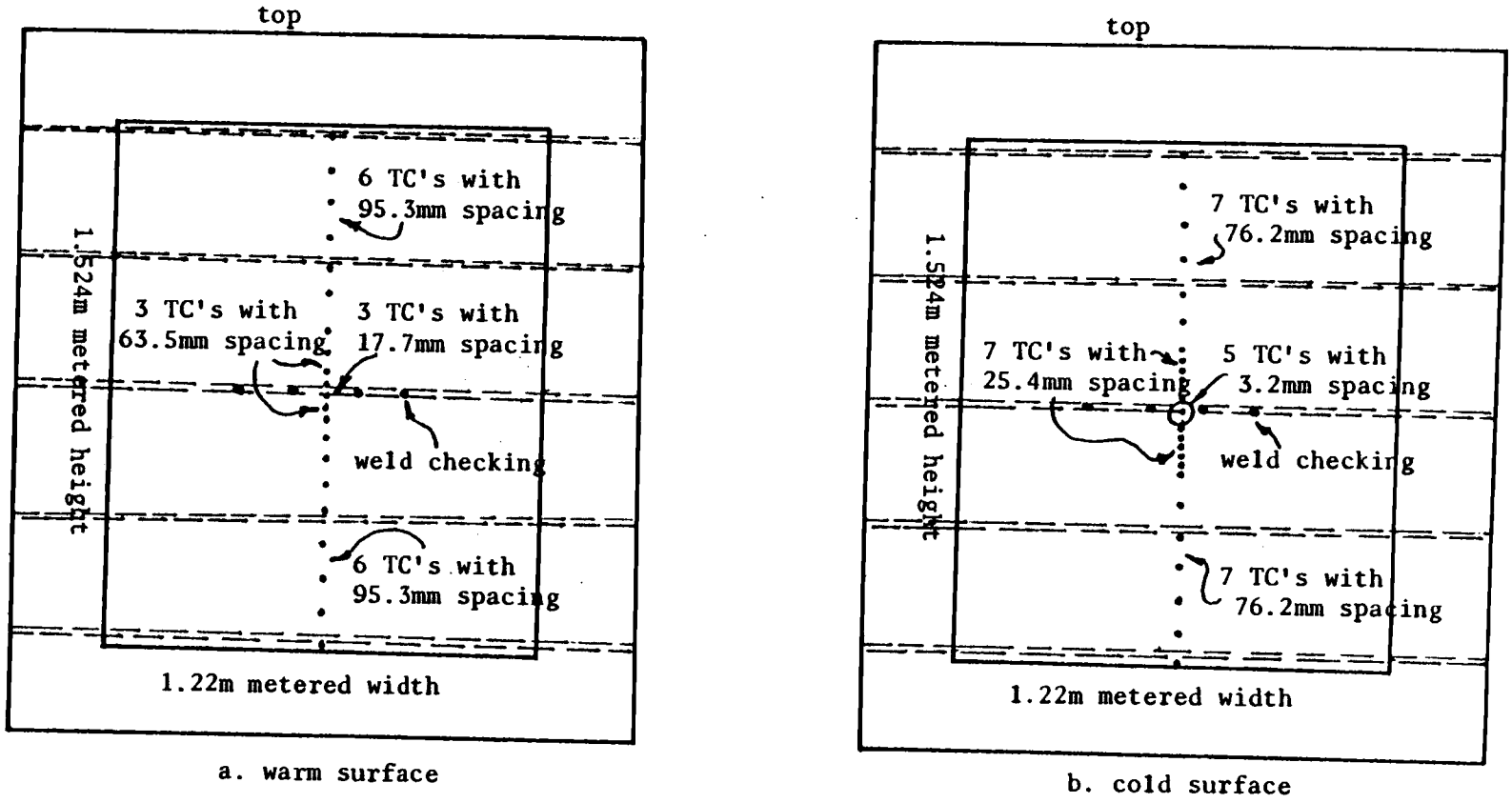

Fig. III-10

EXTERNAL THERMOCOUPLE LOCATIONS

connected to the laboratory monitoring equipment. Each panel was then individually installed in the guarded hot box and allowed to equilibrate under selected steady warm and cold air temperatures until steady-state condition was reached. Test data were then taken. Due to the mass of the steel plate in the panels, a two day period was required to reach the equilibrium condition. The required panel modifications were made after each test, and the same procedure followed in subsequent tests.

Since the assemblies were tested in a vertical position, the heat flow direction was horizontal. Very slow moving airflow was used on both sides according to the requirement of ASTM (4). Air velocities were measured by a "hot-wire" anemometer near the surface. The velocity on the cold side was about 0.4 m/sec for all tests. Varying air velocities were used on the warm side, about 0.1 m/sec for the high "R" panel tests, and about 0.3 m/sec for the low "R" panel tests. The reason to use higher air velocities for low "R" panels is to increase Biot number so that conduction can control the process. The Biot number here is generally referred to as Biot=hL/k (35), where h is heat transfer coefficient, L is half panel thickness, and k is thermal conductivity. Airflow was parallel to both sides for all tests. The testing sequence was as follows:

Test 1: Panel 1 was the same as Assembly 1 originally

constructed (refer to Figure III-4.1 and III-5). In order to simulate the fishing boat at sea, the steel skin was the hot side (metering box side) at an air temperature of 15.6 °C (60 °F), and the plywood was the cold side at an air temperature of -15.6 °C (4 °F).

Test 2: Panel 2 was made from Assembly 1. The cold side plywood was first removed. Then, wood stripping and outer urethane board insulation was removed, and the plywood reinstalled. The configuration of Panel 2 is shown in Figure III-4.2. Plywood was secured to the perimeter wood frame with screws, and secured to steel angles using 38.1 mm (1.5 in) #12 self-tapping screws. Within the metered area, three screws were evenly spaced for each frame giving a separation distance of about 0.3 m (1 ft).

Test 3: Panel 3 was made from Assembly 1 after Test 2. Plywood was removed from the panel cold side. Then, an 11-gauge (2.9 mm thick) steel sheet was secured over the cold side of the panel. The configuration of Panel 3 is shown in Figure III-4.3. The steel sheet was secured to the wood perimeter using wood screws and secured to the steel angles using 38.1 mm (1.5 in) self-tapping screws. Within the metered area, three screws were evenly spaced to secure the steel sheet to each frame with the same spacing as Test 2.

Test 4: Panel 4 was made from Assembly 1 after Test 3. The steel sheet was removed. Then, the foamed-in-

place urethane insulation was removed, leaving only the empty cavities. The steel sheet was then reinstalled on the cold side using the same fastener locations and quantities. The configuration of Panel 4 is shown in Figure III-4.4. This is obviously the worst case of insulation effectiveness.

Test 5: Panel 5 was made from Assembly 1 after Test 4. The steel sheet was removed from the cold side and the plywood reinstalled using the same fastener locations and quantities. The configuration of Panel 5 is shown in Figure III-4.5.

Test 6: Panel 6 was Assembly 2 as originally constructed (refer to Figure III-8 and III-4.6). It had a plywood liner, foamed-in-place urethane and a layer of 50.8 mm (2 in) board insulation, as well as flat bar frames.

Test 7: Panel 7 was made from Assembly 2 after Test 6. The plywood was removed from the cold side. The wood stripping and board urethane insulation was then removed. The plywood was reinstalled on the flat bars at 8 locations of angle iron taps giving a screw spacing of about 0.3 m (1 ft) and with wood screws in the perimeter. The configuration of Panel 7 is shown in Figure III-4.7.

Test 8: Panel 8 was made from Assembly 2 after Test 7. The plywood was removed, all insulation materials were removed leaving only the empty cavities. The plywood was then reinstalled and the panel was tested as shown in

Figure III-4.8.

In order to verify computer models, the thermal conductivities and densities of insulation materials were measured using "guarded hot plate" equipment in accordance with ASTM C 177-76 (5). The "guarded hot plate" equipment is similar to the "guarded hot box" except for the use of plates instead of a box. Measurement of heat supply and temperature difference allows calculation of thermal conductivity from

$$k = \frac{Q \times D}{A(T_1 - T_2)}$$

where

Q=time rate of heat flow, in W.

D=thickness of specimen along a path normal to isothermal surface, in m.

A=area measured on a selected isothermal surface, in m^2.

T_1=temperature of warm surface of specimens, in °C.

T_2=temperature of cold surface of specimens, in °C.

The density of specimens can be calculated as

$$\rho = \frac{M_2}{V}$$

where

ρ=density of the dry material as tested, in Kg/m^3.

M_2=mass of material after conditioning.

V=volume occupied by material in specimens during test, in m^3. (5)

Three insulation material samples were taken from

Assembly 2 for testing. One was removed from the urethane board and had dimensions 609.6x609.6 mm (24x24 in) by 50.8 mm (2 in) thick. The other two were removed from foamed-in-place urethane and had dimensions 304.8x304.8 mm (12x12 in) by 38.1 mm (1.5 in) thick. Dynatherm Engineering Laboratory conducted the tests according to ASTM C 177 (5) after completing those "guarded hot box" experiments. During the "guarded hot plate" test, the temperatures of the warm and cold side were 18.3 °C (65 °F) and -9.4 °C (15 °F), respectively.

III.5 Experimental Results

A typical result of Panel 1 is reported in the following pages. Temperature measurement results are shown in Figure III-11 through Figure III-13. The results for the rest of the panels are attached in Appendix 4. The other test results, such as heat flux q, area weighted average surface temperatures T_w and T_c, panel resistance R, etc, are listed in Tables III-1, III-2 and III-3. Table III-1 shows the results of Panel 1 thru Panel 5 on Assembly 1. Table III-2 shows the results of Panel 6 thru Panel 8 on Assembly 2. Table III-3 shows the results of thermal conductivity testing. Some of these results, such as temperatures, were obtained directly from the test; the others were obtained from equations given in ASTM C 236-80 (4) and summarized in Appendix 3.

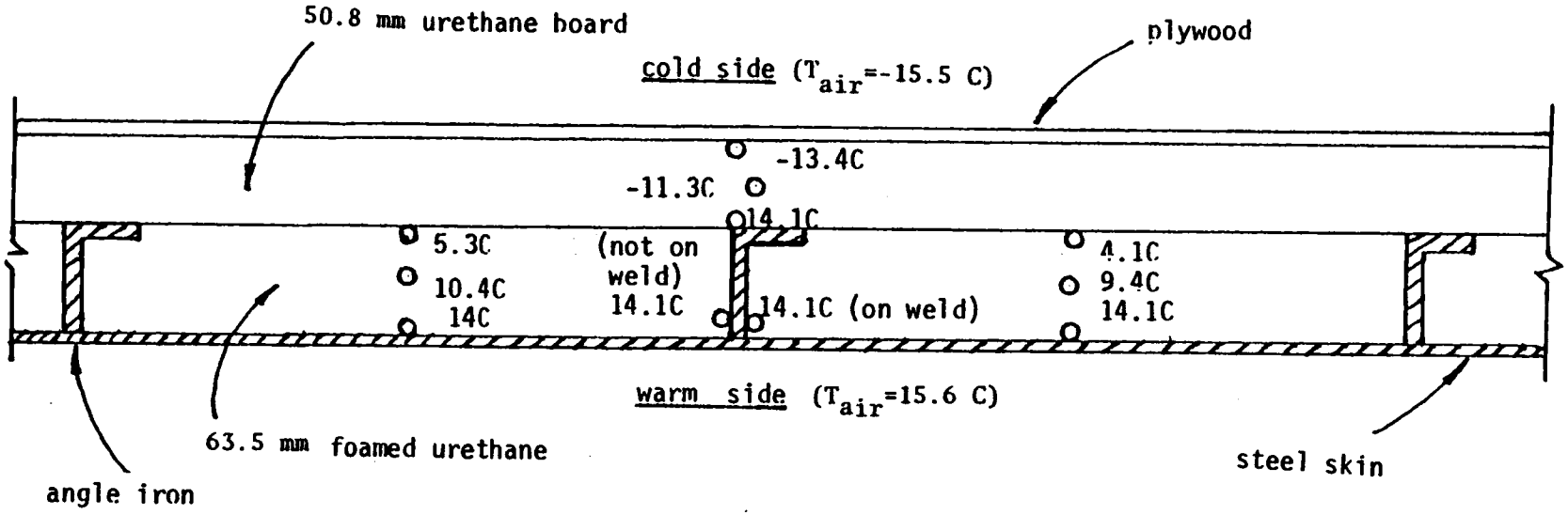

Fig. III-11
INTERNAL TEMPERATURES AND THERMOCOUPLE LOCATIONS
Panel 1 Tested as Submitted

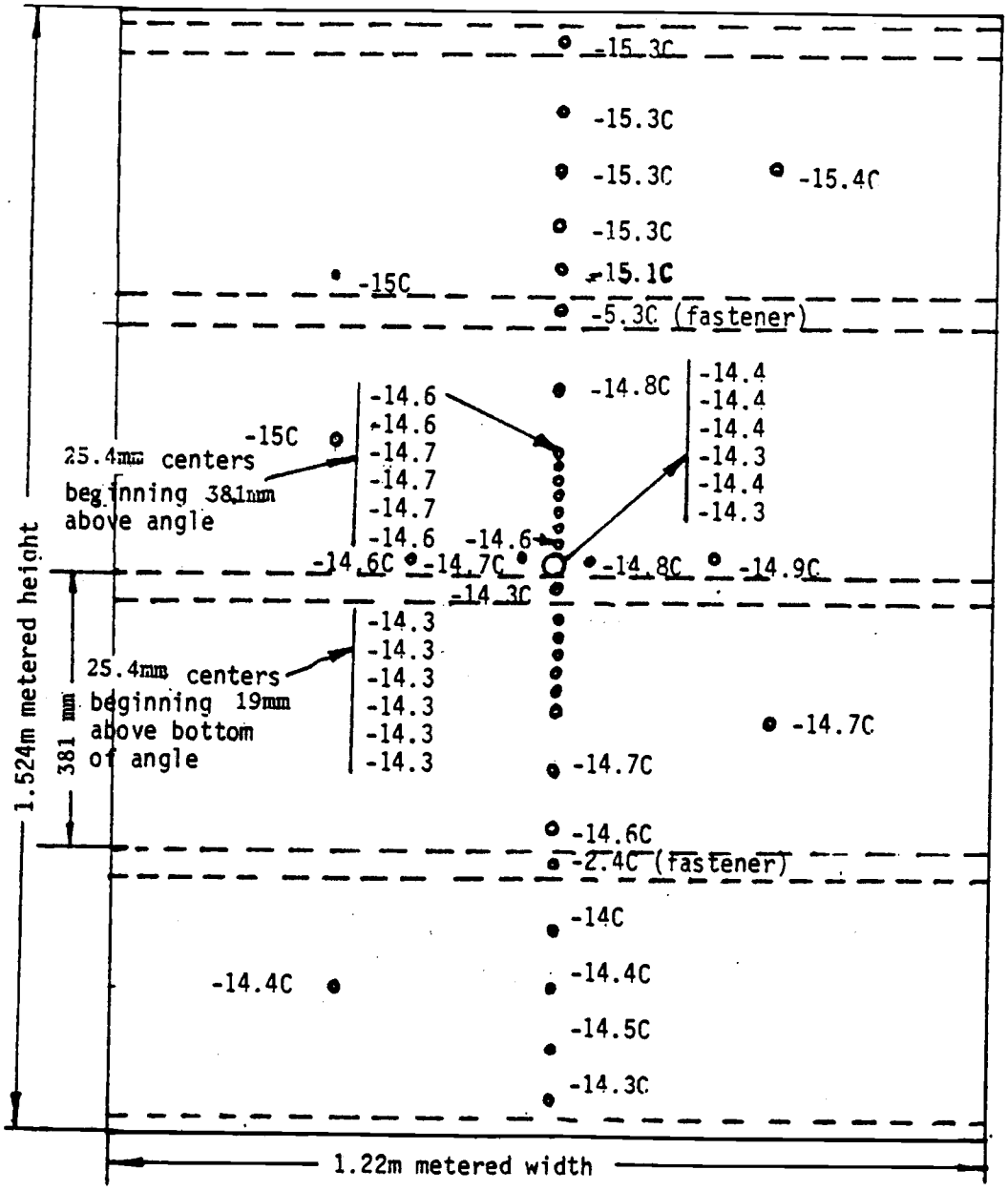

Fig. III-12
COLD SURFACE TEMPERATURES AND THERMOCOUPLE LOCATIONS
Panel 1 Tested as Submitted

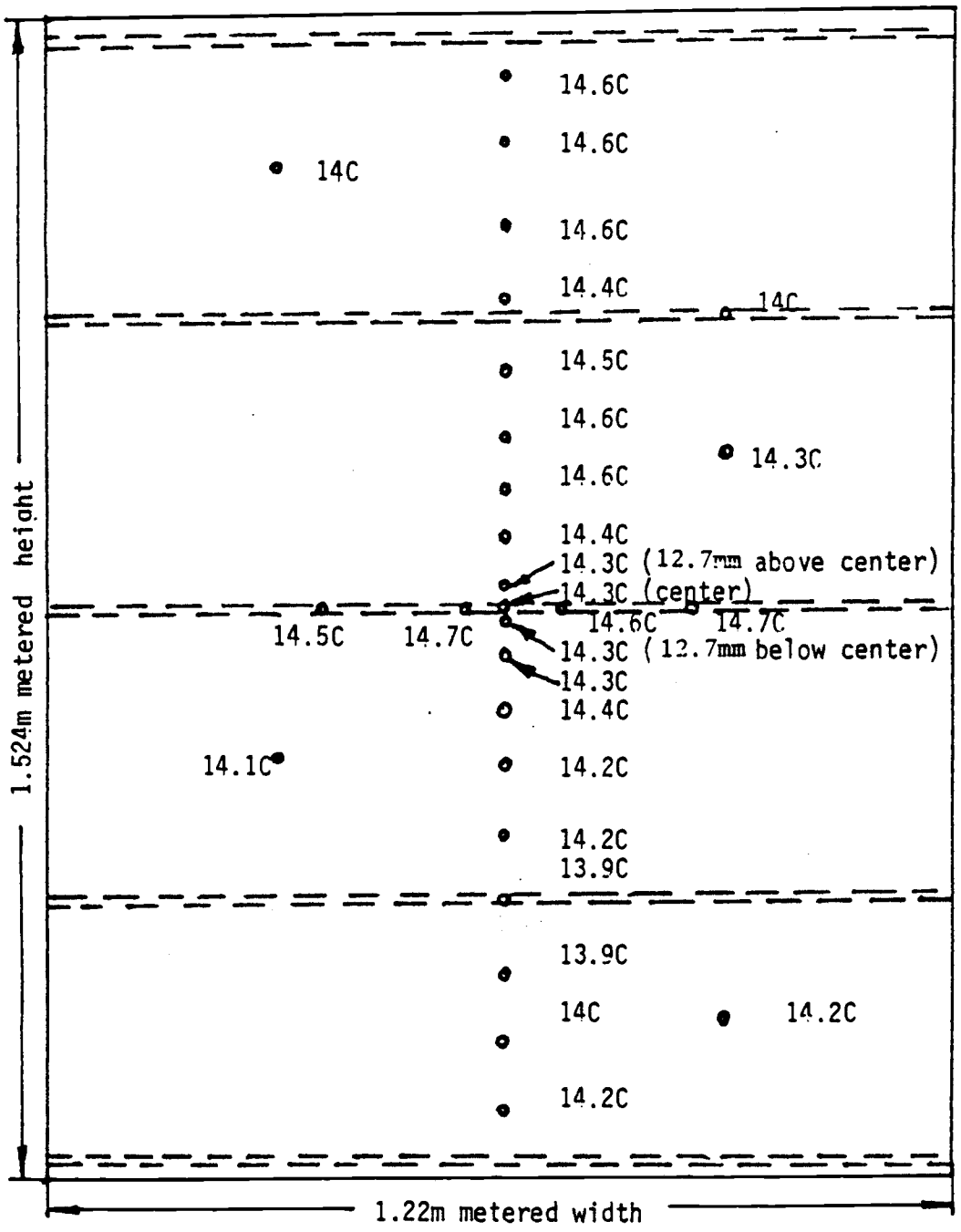

Fig. III-13
WARM SURFACE TEMPERATURES AND THERMOCOUPLE LOCATIONS
Panel 1 Tested as Submitted

Table III-1: Test Results for Assembly 1

ITEM	Panel1	Panel2	Panel3	Panel4	Panel5
Heat flow rate, (W/m^2)	6.55	23.37	53.09	77.98	56.00
Warm air temperature (°C)	15.6	15.6	15.8	15.7	15.7
Cold air temperature (°C)	-15.5	-15.3	-18.2	-18.0	-15.9
Thermal transmittance[a] U, (W/m^2K)	0.21	0.76	1.56	2.31	1.78
Area weighted average warm surface temperature, (°C)	14.3	11.4	8.7	5.7	8.0
Area weighted average cold surface temperature, (°C)	-14.7	-13.3	-11.5	-8.2	-9.3
Mean temperature (°C)	-0.2	-1.0	-1.4	-1.3	-0.6
Warm surface convection coeff. (W/m^2K)	5.17	5.62	7.38	7.78	7.33
Cold surface convection coeff. (W/m^2K)	7.84	11.70	7.95	7.95	8.46
Panel conductance[b] C, (W/m^2K)	0.23	0.94	2.63	5.64	3.24
Panel resistance R=1/C, (m^2K/W)	4.42	1.06	0.38	0.18	0.31

a Thermal transmittance U is overall value including surface convection effect, defined as

$$U = \frac{1}{\frac{1}{h_1} + \frac{L_1}{k_1} + \cdots + \frac{1}{h_2}}$$

where h is convection coefficient, L is material thickness and k is thermal conductivity.

b Panel conductance C does not consider the surface convection and is defined as

$$C = \frac{1}{\frac{L_1}{k_1} + \frac{L_2}{k_2} + \cdots}$$

Table III-2: Test Results for Assembly 2

ITEM	Panel 6	Panel 7	Panel 8
Heat flow rate (W/m^2)	5.95	15.45	54.01
Warm air temperature (°C)	15.4	15.5	15.6
Cold air temperature (°C)	-16.4	-16.3	-15.3
Thermal transmittance[a] U, (W/m^2K)	0.19	0.49	1.73
Area weight average warm surface temperature(°C)	14.4	12.7	8.3
Area weighted average cold surface temperature(°C)	-15.5	-14.7	-9.3
Mean temperature (°C)	-0.6	-1.0	-0.5
Warm surface convection coeff. (W/m^2K)	5.62	5.56	7.38
Cold surface convection coeff. (W/m^2K)	6.30	9.26	8.91
Panel conductance, C,[b] (W/m^2K)	0.20	0.56	3.08
Panel resistance, R=1/C, (m^2K/W)	5.03	1.77	0.32

a As same as Table 1.
b As same as Table 1.

Table III-3: Guarded Hot Plate Test Results

ITEM	BOARD URETHANE	FOAMED-IN-PLACE URETHANE
Sample size(mm)	609.6X609.6	304.8X304.8
Density(Kg/m^3)	33.80	46.94
Thickness(mm)	49.56	38.00
Mean temperature(°C)	4.4	4.4
Thermal conductivity (W/mK)	0.02	0.016

CHAPTER IV. COMPARISON AND APPLICATION

Two questions arise from previous sections. First, which computer program, HT (finite element) or FD (finite difference), is more appropriate? Second, does the computer model agree with experimental results? This chapter will first address these two questions. Then, further application of the finite difference method will be presented.

IV.1. Comparing Calculated Temperature Distribution with Test Results

As described in Chapter II, analysis of the flat bar case, which has been represented by Panel 6 (refer to Figure II-1), was first considered because of its simple structure. In order to compare the two computer programs, thermal performance of Panel 6 was selected as a typical case and analysed using both HT and FD. Figure IV-1 gives the resulting temperature distributions along the center line of the cold surface perpendicular to the frame. The distribution is also compared with the test results. Figure IV-2 gives the temperature distribution on the warm surface. If we define a driving force, ΔT=(air temperature)-(area weighted average surface temperature), then the comparison can be carried out by contrasting the numerical result of ΔT with the test result as shown in

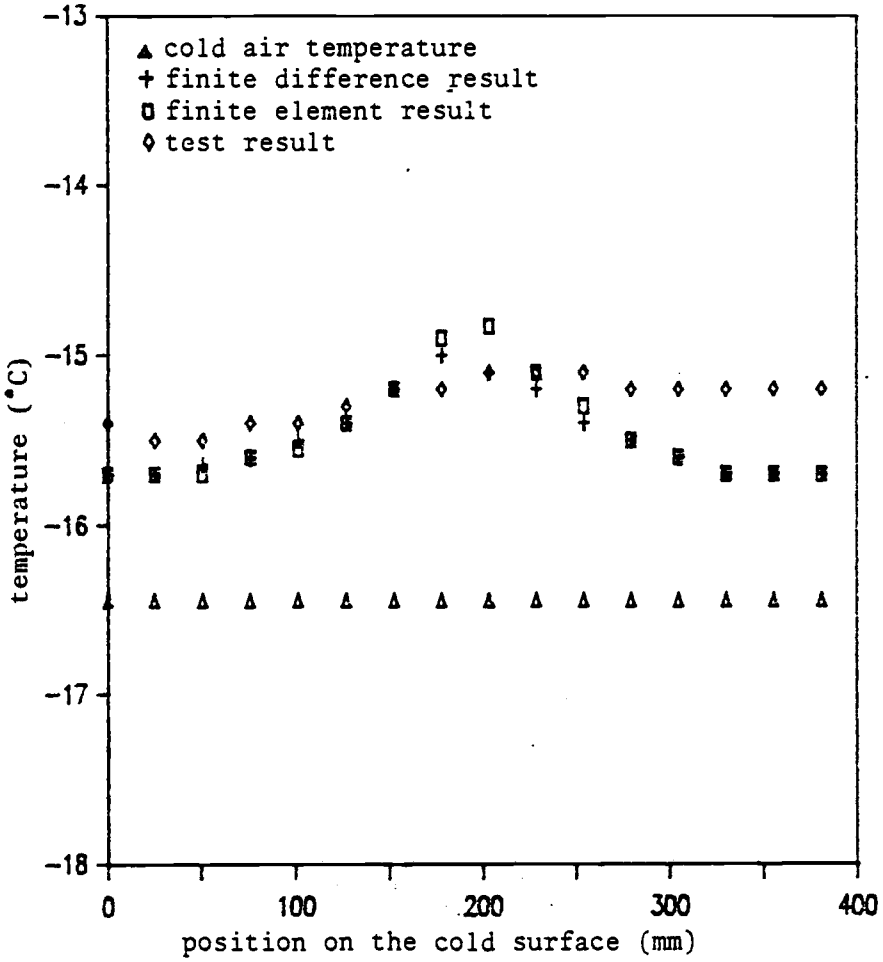

Fig. IV-1

TEMPERATURE DISTRIBUTIONS ALONG THE CENTER LINE OF THE COLD SURFACE FOR PANEL 6

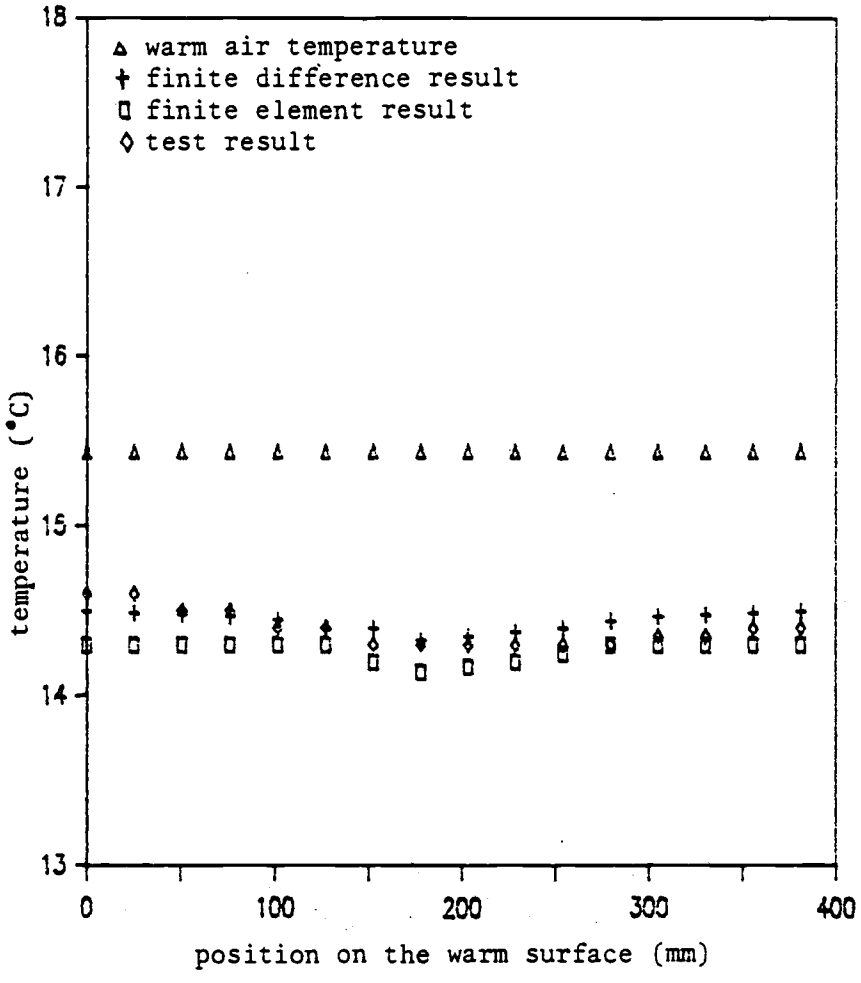

Fig. IV-2
TEMPERATURE DISTRIBUTIONS ALONG THE CENTER LINE OF THE WARM SURFACE FOR PANEL 6

these two figures. Good agreement shows that both models are applicable. However, considering the rectangular geometry of this problem, the finite difference model, FD, is more feasible by comparing with the finite element model, such as

a. Its results are as good as those of finite element model.
b. It is easier to program.
c. It takes less computer time and memory and it is more convenient to use on a personal computer.
d. It is easier to modify for other configurations.

IV.2. Comparing Calculated Panel Resistances with Test Results

For simulating the "guarded hot box" test, the computer program FD was then modified to calculate heat flux, average warm and cold surface temperatures, thermal transmittance, panel conductance and panel resistance. These calculations are carried out as shown at the end of the program (Appendix 2). Some calculations were based on the equations from ASTM C 236-80, reproduced from reference 4 in Appendix 3.

The finite difference treatment of the angle iron case (refer to Figure III-7,a) is the same as that of the flat bar case previously described. A finer grid was used near the angle iron frame, similar to that used in Figure II-9 for the flat bar frame. Although assumption b in Section

II.1 of Chapter II does not strictly apply, (because of the asymmetry of the angle iron,) we can still take it as a reasonable assumption, since the width of insulation between frame members is so much greater than the insulation thickness.

The panel resistances calculated using the program FD were further compared with the test results for the eight representative wall sections. The following factors have been considered in the calculations.

Panel resistance

The literature search indicated that both thermal transmittance U and thermal resistance R are commonly used for evaluating thermal performance of composite panels. By the definition of ASTM for the "guarded hot box" technique, thermal transmittance of a panel is the overall heat transfer coefficient, $U=q/A(T_c-T_h)$, (Refer to Appendix 3,) which depends on surface film coefficient. However, thermal resistance of the panel is defined as $R=A(T_1-T_2)/q$. This is not the overall resistance; its use makes the problem simpler because the convective effect has been eliminated. This is justified since the convective resistance will be different in each particular application. Therefore, the panel resistance is used in this project. If the convective coefficients and ambient temperatures on both sides of the panel are known, program FD can be used to calculate the panel transmittance, U. Otherwise, these

values can be chosen arbitrarily and they will not influence the calculation of panel resistance.

Thermal properties of insulation material

Closed cell insulations are extensively used in West Coast steel vessels. Foamed-in-place urethane is most common and this project has concentrated on this material. Since thermal conductivity is the most important property to be considered for this steady-state problem, the test results of urethane foam conductivities (Table III-3) were used in the calculations. Other frequently used data are the conductivities of mild steel and plywood. They were selected as:

conductivity of mild steel: k=42.9 W/mK. (35)

conductivity of plywood: k=0.1155 W/mK. (6)

SNAME (31) reported that the thermal conductivity of plywood (Douglas, Fir, Pressure treated) is 0.1124 W/mK. We use higher value of k=0.1155 W/mK here because there are no voids in marine plywood.

Contact resistance

Contact resistance, R_c, must be introduced where two different materials interface with each other. In the case of steel fish hold wall sections considered in this project, there are four kinds of contact: metal-to-metal, metal-to-plywood, metal-to- urethane-foam, and plywood-to-urethane-foam. The contact resistance can be neglected where the urethane foam is contacting other materials,

since cellular air spaces are formed at the interface when the urethane foam is sprayed on. However, where there are metal-to-plywood contacts, the situation is greatly changed and contact resistance can no longer be neglected. In order to estimate the range of R_c value in this project, we can analyse as follows. From a microscopic viewpoint, the roughness of the contacting surfaces, and some foam cells or dirt left from the shaving process form tiny cellular air spaces between the two contact surfaces. These tiny air spaces have very low thermal conductivity, therefore it is reasonable to assume that the tiny air spaces function like the urethane foam and a contact resistance exists between the face of the frame and inside liner. Figure IV-3 shows the effect of contact resistance on the panel resistance in Panel 2 and Panel 3. The relationship appears to be almost linear. For metal-to-plywood contacts (Curve 1), R_c=5.17 K/W matched the tested panel resistance of Panel 2 and it was therefore chosen to be used in subsequent calculations. For metal-to-metal contacts, although there are many tiny air spaces between two metal surfaces, many tight contacts still exist due to the pressure provided by fasteners. We can assume that the contact resistance is not significant in this case because these tight contacts act as many "bridges" to transfer heat through the interface. Since Curve 2 shows that R_c=0 matched tested panel resistance of Panel 3, this assumption

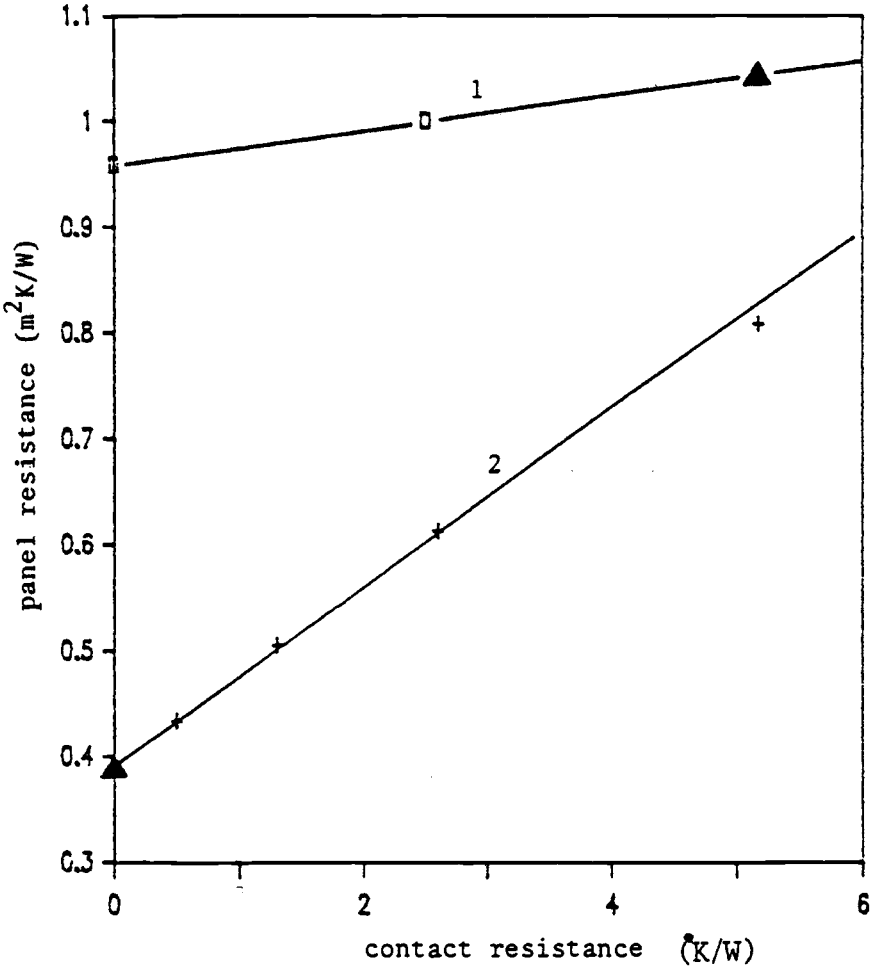

Fig. IV-3

THE EFFECT OF CONTACT RESISTANCE

1. metal-to-plywood contact for Panel 2.
2. metal-to-metal contact for Panel 3.

▲ chosen values which matched the test results.

appears to be valid. The same assumption can also be extended to the case of the frames being welded to the steel skin, i.e., the welds have provided a good thermal contact between the frame and steel skin. Thus, R_c=0 was used in the subsequent calculations when metal-to-metal contacts encountered.

Thermal conductance of air space

As shown in Figure III-4, there is no insulation at all for Panels 4, 5, and 8. In order to simulate thermal performance for such wall sections, the thermal conductance of the air space must be considered. Here, the conductance means the total conductance from one bounding surface to the other, and includes the combined effect of radiation and convection. ASHRAE (6) gives the thermal resistance values for sealed air spaces of uniform width and having moderately smooth, plane, parallel surfaces. These values have been used for our purpose with appropriate interpolation and extrapolation. For example, considering Panel 4 as shown in Figure III-4. 4, we can conclude that the direction of heat flow is horizontal, mean temperature is close to 10 °C (50 °F), the temperature difference is close to 16.7 °C (30 °F), and the effective emittance is approximately 0.28 (according to Table 3 of Chapter 23 in ASHRAE Handbook). With this information, we can determine that the thermal resistance of the 63.5 mm (2.5 in) air space is 0.3 m^2K/W (1.7 ft^2-F-hr/Btu) by interpolation.

Finally, we obtain the air space conductance of 0.21 W/m^2K from the equation K=L/RA, where L is the width of the air space, R is the air space resistance, and A is a unit area.

Based on the above considerations, resistance values for eight representative panels are shown in Table IV-1. This table also shows error terms based on the numerical results compared with the test results. The comparisons indicate that program FD is appropriate for predicting the panel resistance. Therefore, we are now ready to calculate the thermal resistance for the configurations which have not been measured.

IV.3. Application

As introduced in Chapter I, we selected four sizes of steel vessels, namely 14, 20, 26 and 32 m (45, 65, 85, and 105 ft), to be representatives of Pacific Northwest vessels. For each size of vessel, both angle iron and flat bar are commonly used in the frames. The wide range of variations in frame spacing, frame dimension, insulation thickness, plywood or steel sheet liners and skin thicknesses, creates a great variety of possible panel configurations. To provide basic design information, 24 design curves have been developed for different sizes of steel angle and flat bar frames. There are three curves for each size of frame. They describe:

1. Panel resistance vs insulation thickness with the use of two different liners;

Table IV-1. Comparison of Panel Resistance for Eight Representative Test Panels

Number of the test panel	Panel resistance (m^2K/W)		Error compared with the test result
	Numerical result	Test result	
1	4.74	4.42	+7.2%
2	1.15	1.06	+8.5%
3	0.42	0.38	+9.5%
4	0.19	0.18	+5.6%
5	0.32	0.31	+3.2%
6	5.31	5.03	+5.6%
7	1.85	1.77	+4.5%
8	0.33	0.32	+3.1%

2. Panel resistance vs frame spacing with a plywood liner. Included are different insulating conditions, such as air space (no insulation at all) and insulation thickness equal to, and greater than the frame depth;
3. Same as 2, but with steel sheet liner being considered.

To obtain these curves, each data point was calculated by running program FD once. Some of the parameters are identical. They are:

Mild steel conductivity: k_1=42.9 W/mK

Plywood conductivity: k_2=0.1155 W/mK

Urethane foam conductivity: k_3=0.023 W/mK

Contact resistance: R_c=5.17 K/W (metal-to-plywood)

R_c=0 K/W (metal-to-metal)

Convergence criteria: EPS=0.001

The urethane foam conductivity here is the "aged value", which is a term commonly used for this type of cellular insulation material. For example, the foamed-in-place urethane has an apparent thermal conductivity of 0.016 W/mK (0.11 Btu/hr-ft^2-F/in) when it is initially produced. However, this value increases with time as air and moisture diffuse into the cells, and the fluorocarbon gas diffuses out. The "aged value" is determined when the diffusion has stopped after a period of time. According to the ASHRAE

Handbook, the aged conductivity of urethane foam is 0.023 W/mK (0.16 Btu-in/hr-ft^2-F) (6).

The resulting design curves are shown in Figures IV-4 through IV-27. Included in each figure are the size of angle iron or flat bar, frame spacing, and the thicknesses of the liner and of the steel skin. In order to simplify the problem, two assumptions have been made in developing these curves. One is that a linear relationship exists between panel resistance and insulation thickness if the insulation thickness is less than the frame depth. The error produced by this assumption was investigated. Figure IV-28 shows the high and low band of the linear regression for angle iron frame with insulation thickness less than frame depth. The relative error due to this assumption is about 6.7% with 90% confidence. In the calculation, the existance of an air space between the urethane insulation and inside liner was assumed. The determination of the thermal conductance of the air space is carried out as previously described. Another assumption is that a linear relationship exists between the panel resistance and frame spacing. Figure IV-29 shows the high and low band for this assumption. The relative error is about 11.4% with 90% confidence. This error caused some of the curves, such as Curves 3 on both Figure IV-5 and IV-6, to look flat while a positive slope would be expected. In fact, These curves do have a very little positive slope. For example, Curve

3 of Figure IV-5 shows that the panel resistance is 0.3090 m^2K/W when the frame spacing is 381 mm, and is 0.3123 m^2K/W at a frame spacing of 508 mm.

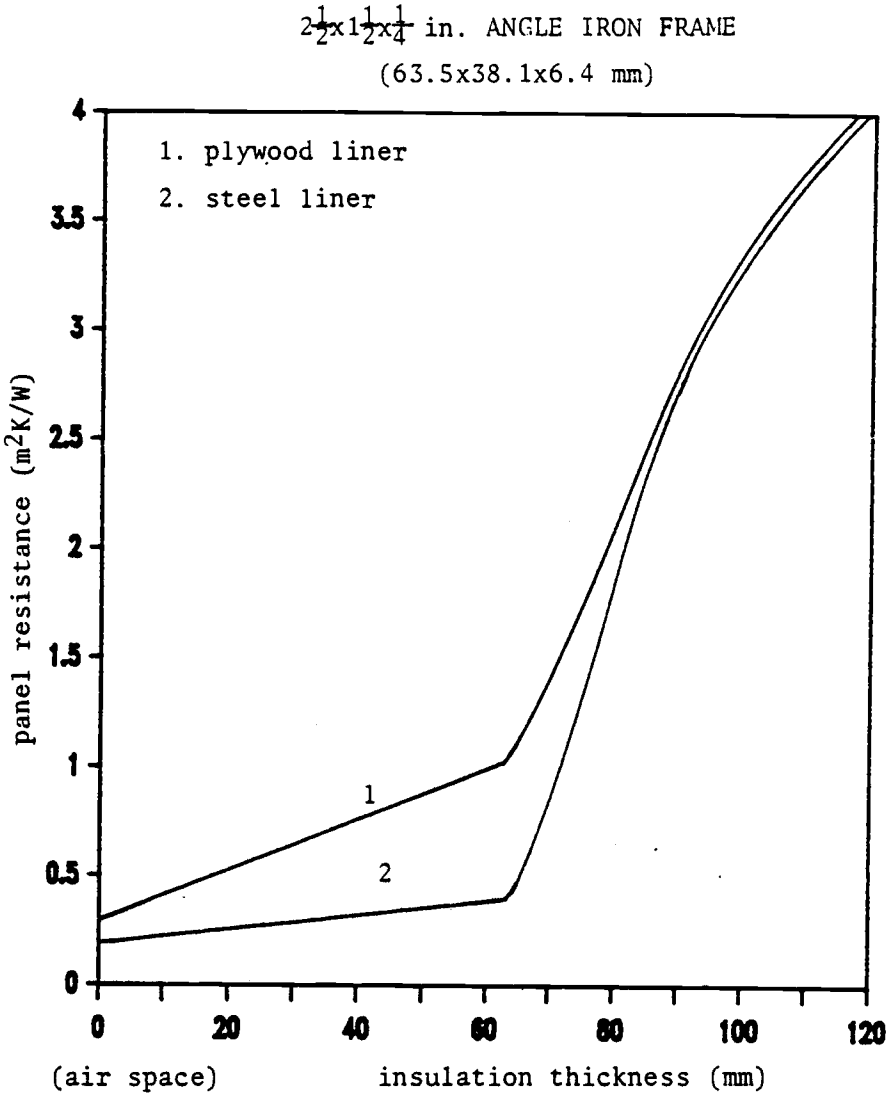

Fig. IV-4

PANEL RESISTANCE vs INSULATION THICKNESS

frame spacing: 381 mm (15 in.)

plywood liner thickness: 9.5 mm ($\frac{3}{8}$ in.)

steel liner thickness: 2.9 mm (11 gauge)

steel plate thickness: 4.8 mm ($\frac{3}{16}$ in.)

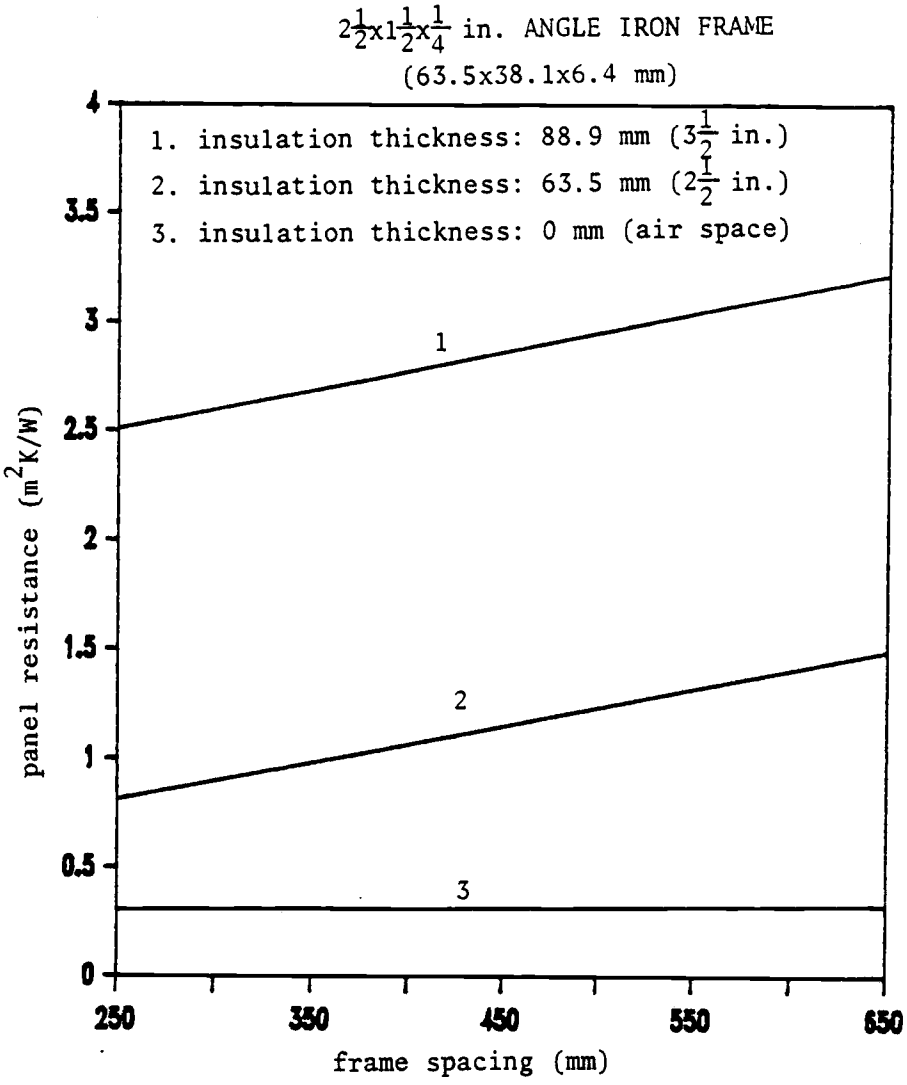

Fig. IV-5

PANEL RESISTANCE vs FRAME SPACING FOR A WALL SECTION WITH PLYWOOD LINER

plywood liner thickness: 9.5 mm ($\frac{3}{8}$ in.)

steel plate thickness: 4.8 mm ($\frac{3}{16}$ in.)

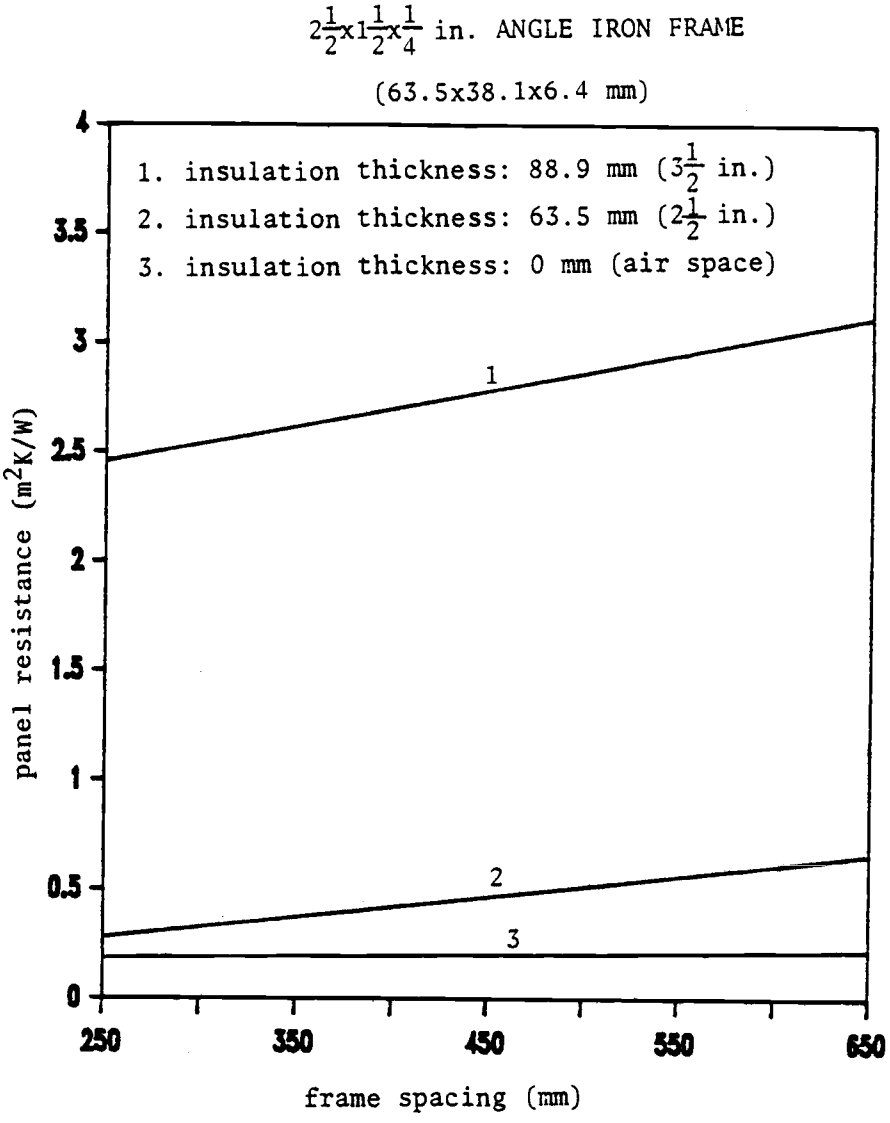

Fig. IV-6

PANEL RESISTANCE vs FRAME SPACING FOR A WALL SECTION WITH STEEL LINER

steel liner thickness: 2.9 mm (11 gauge)
steel plate thickness: 4.8 mm ($\frac{3}{16}$ in.)

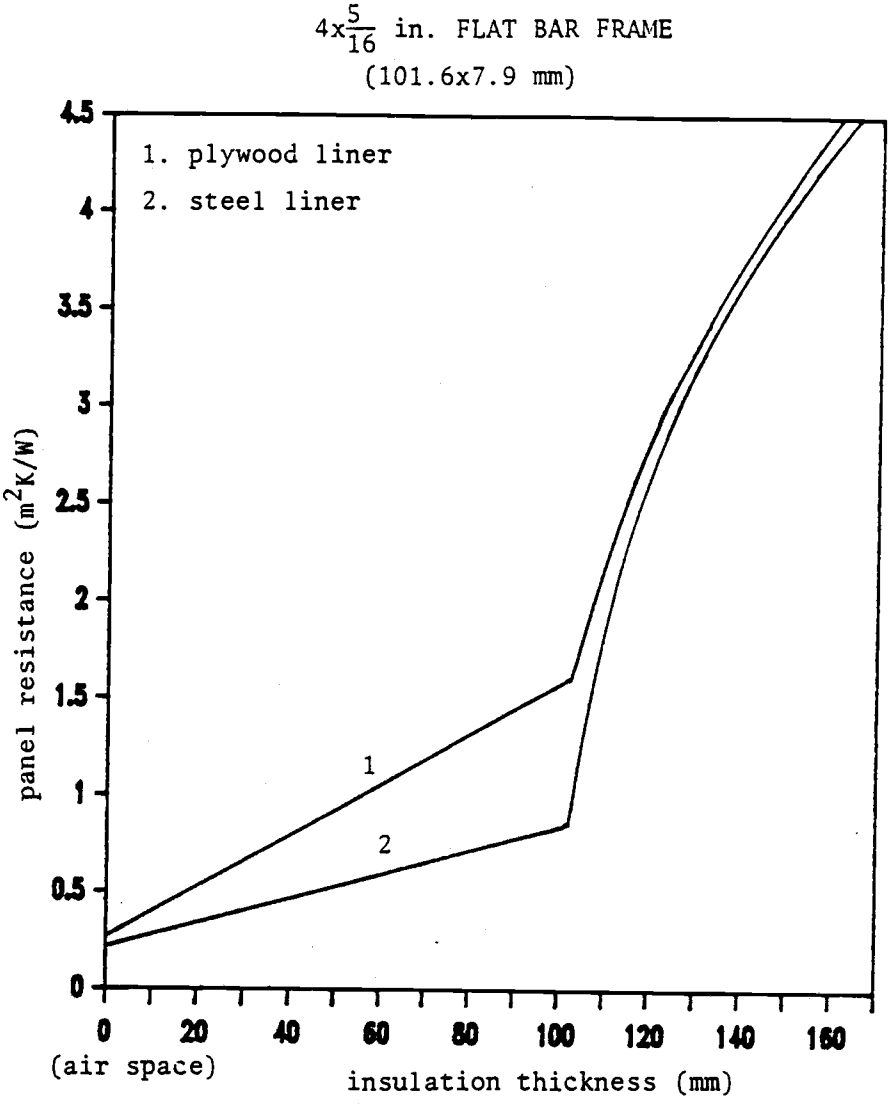

Fig. IV-7

PANEL RESISTANCE vs INSULATION THICKNESS

frame spacing: 381 mm (15 in.)

plywood liner thickness: 9.5 mm ($\frac{3}{8}$ in.)

steel liner thickness: 2.9 mm (11 gauge)

steel olate thickness: 4.8 mm ($\frac{3}{16}$ in.)

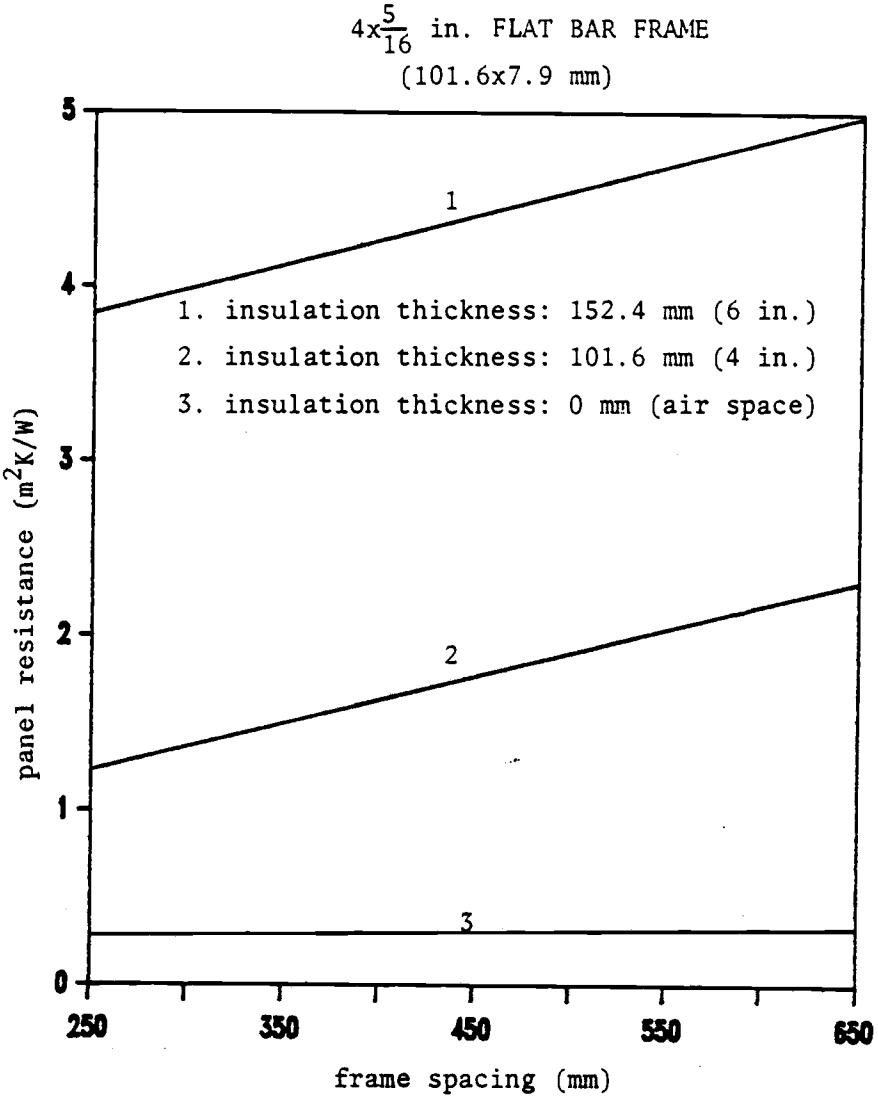

Fig. IV-8

PANEL RESISTANCE vs FRAME SPACING FOR A WALL SECTION WITH PLYWOOD LINER

plywood liner thickness: 9.5 mm ($\frac{3}{8}$ in.)
steel plate thickness: 4.8 mm ($\frac{3}{16}$ in.)

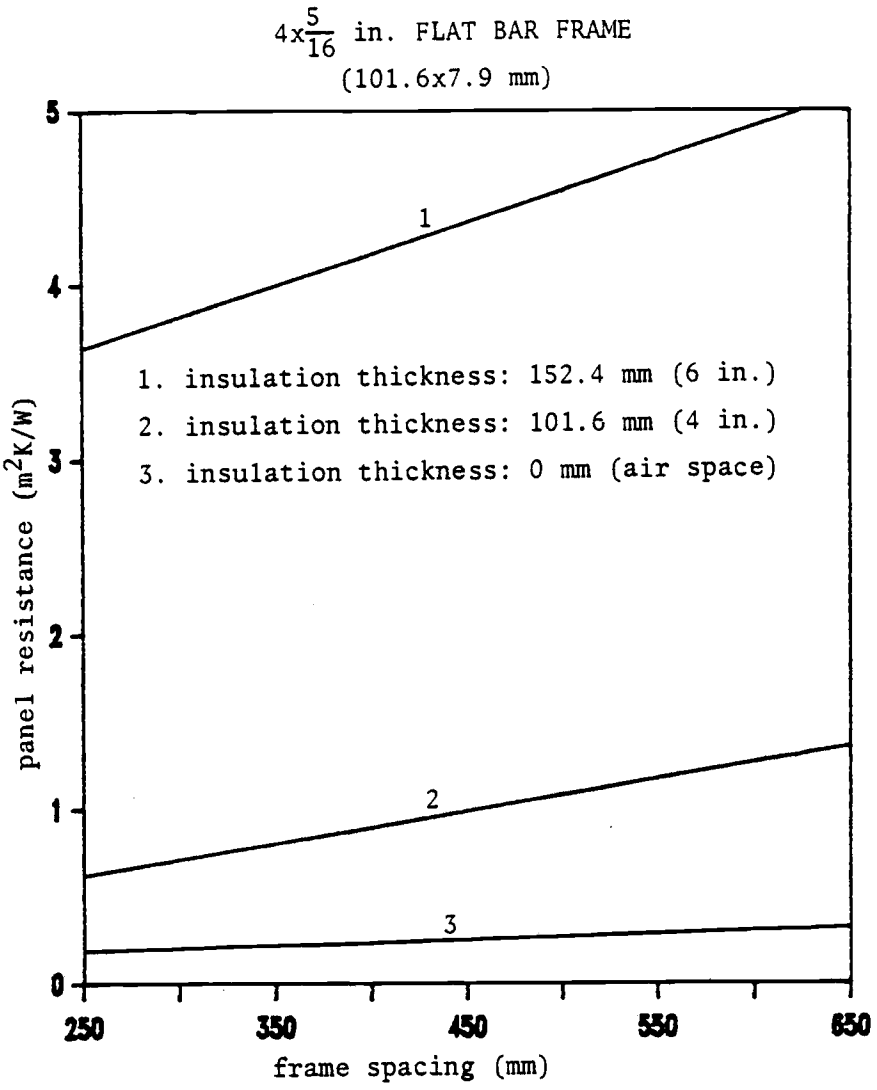

Fig. IV-9

PANEL RESISTANCE vs FRAME SPACING FOR A WALL SECTION WITH STEEL LINER

steel liner thickness: 2.9 mm (11 gauge)

steel plate thickness: 4.8 mm ($\frac{3}{16}$ in.)

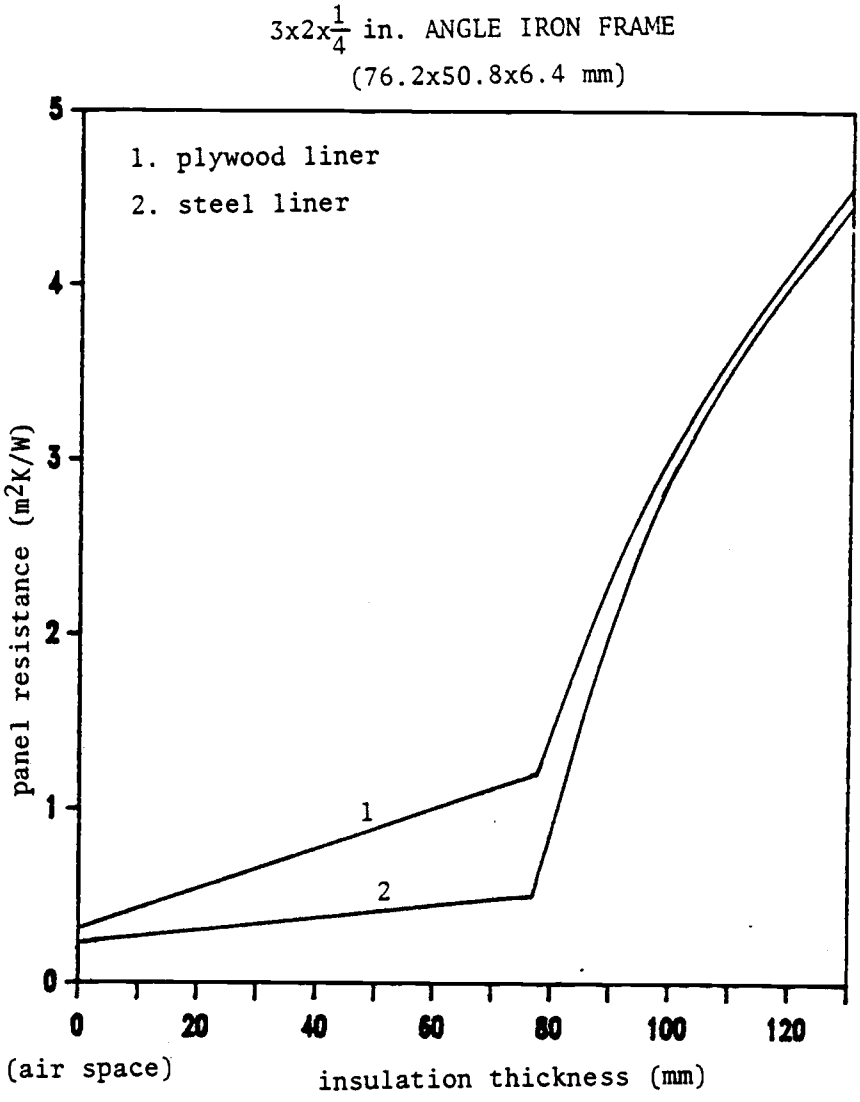

Fig. IV-10

PANEL RESISTANCE vs INSULATION THICKNESS

frame spacing: 457.2 mm (18 in.)
plywood liner thickness: 9.5 mm ($\frac{3}{8}$ in.)
steel liner thickness: 3.2 mm ($\frac{1}{8}$ in.)
steel plate thickness: 6.4 mm ($\frac{1}{4}$ in.)

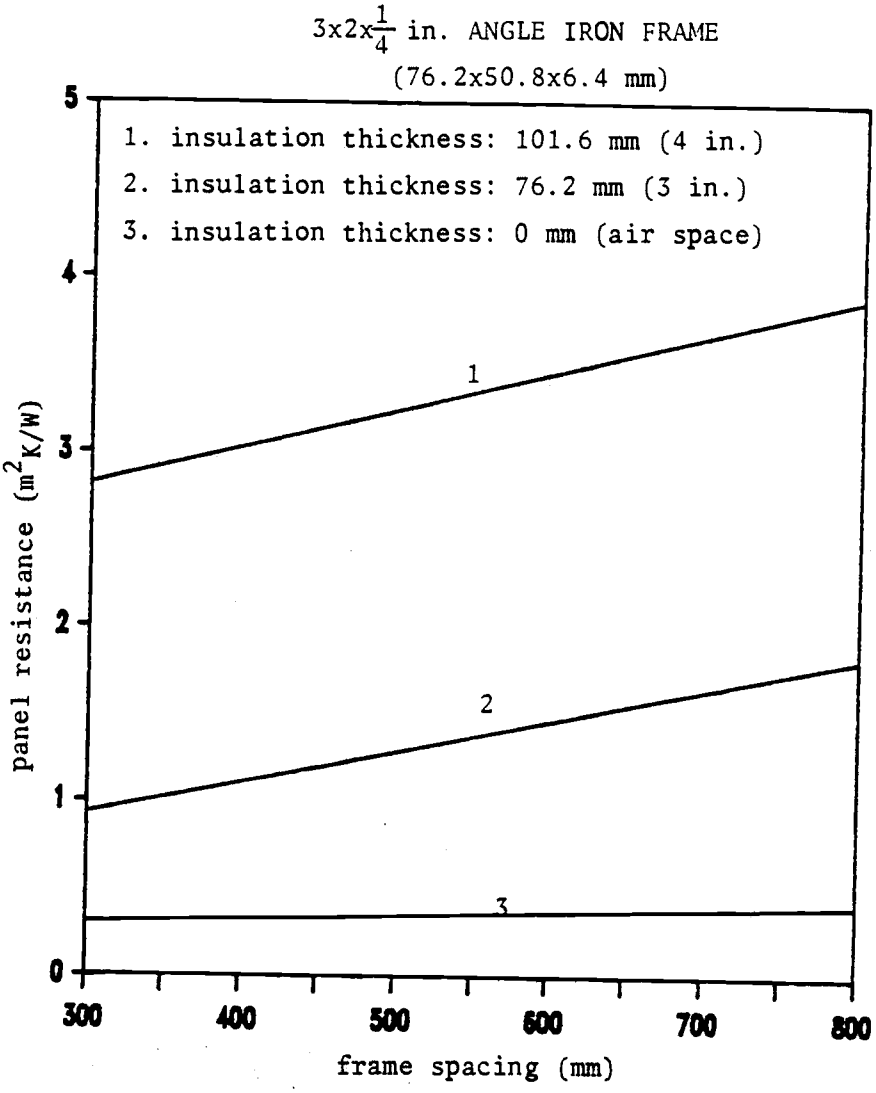

Fig. IV-11

PANEL RESISTANCE vs FRAME SPACING FOR A WALL SECTION WITH PLYWOOD LINER

plywood liner thickness: 9.5 mm ($\frac{3}{8}$ in.)
steel plate thickness: 6.4 mm ($\frac{1}{4}$ in.)

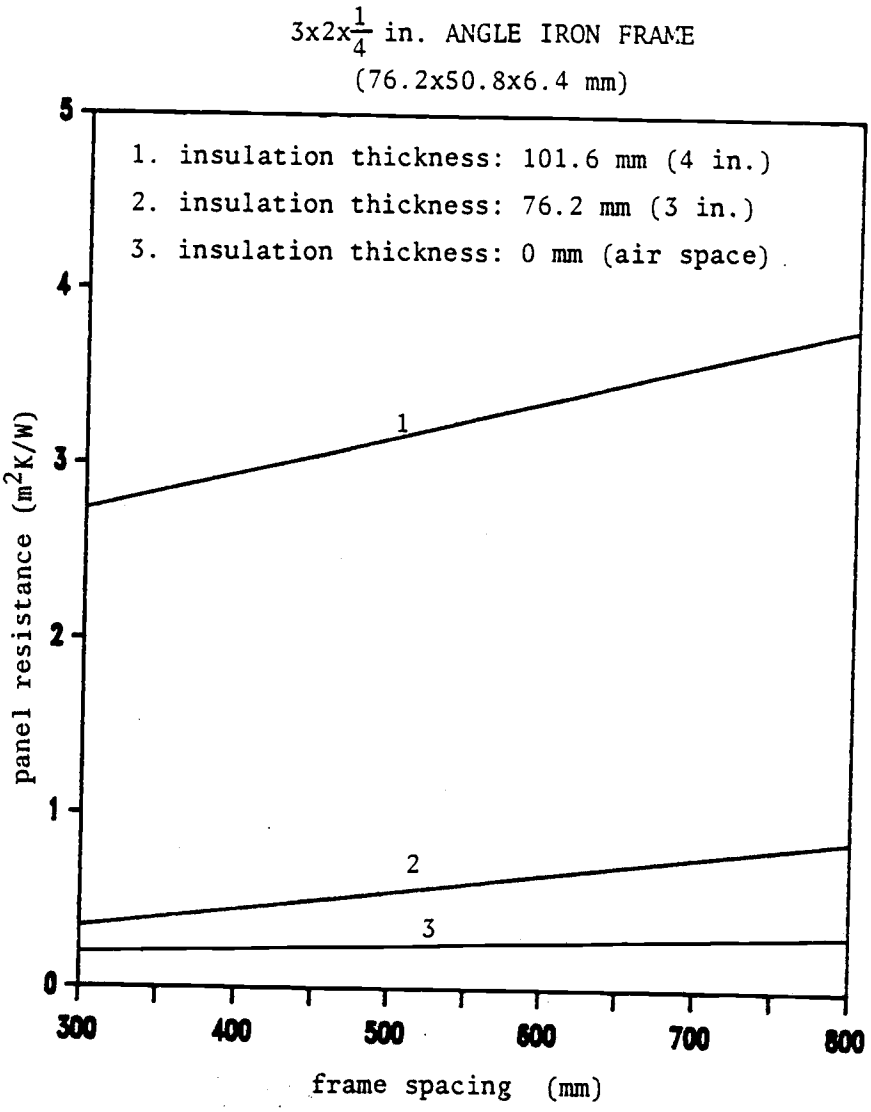

Fig. IV-12

PANEL RESISTANCE vs FRAME SPACING FOR A WALL SECTION WITH STEEL LINER

steel liner thickness: 3.2 mm ($\frac{1}{8}$ in.)

steel plate thickness: 6.4 mm ($\frac{1}{4}$ in.)

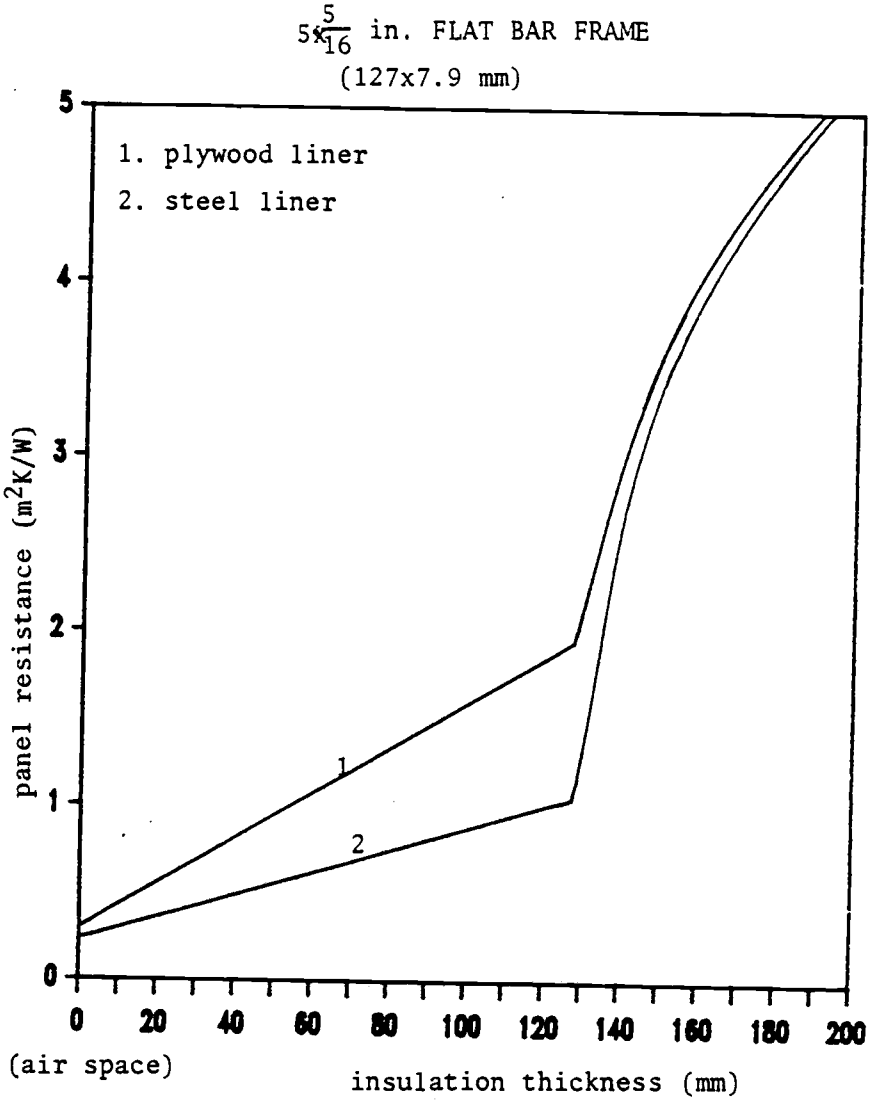

Fig. IV-13

PANEL RESISTANCE vs INSULATION THICKNESS

frame spacing: 457.2 mm (18 in.)

plywood liner thickness: 9.5 mm ($\frac{3}{8}$ in.)

steel liner thickness: 3.2 mm ($\frac{1}{8}$ in.)

steel plate thickness: 6.4 mm ($\frac{1}{4}$ in.)

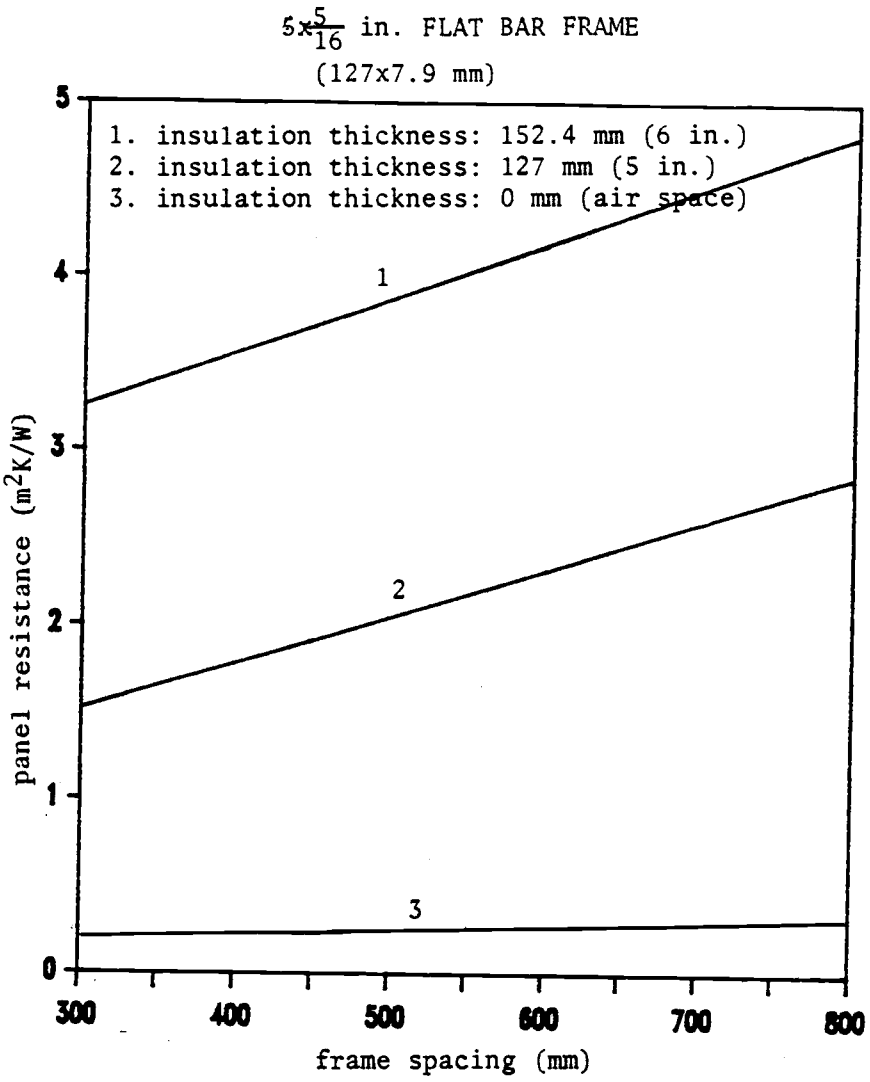

Fig. IV-14

PANEL RESISTANCE vs FRAME SPACING FOR A WALL SECTION WITH PLYWOOD LINER

plywood liner thickness: 9.5 mm ($\frac{3}{8}$ in.)
steel plate thickness: 6.4 mm ($\frac{1}{4}$ in.)

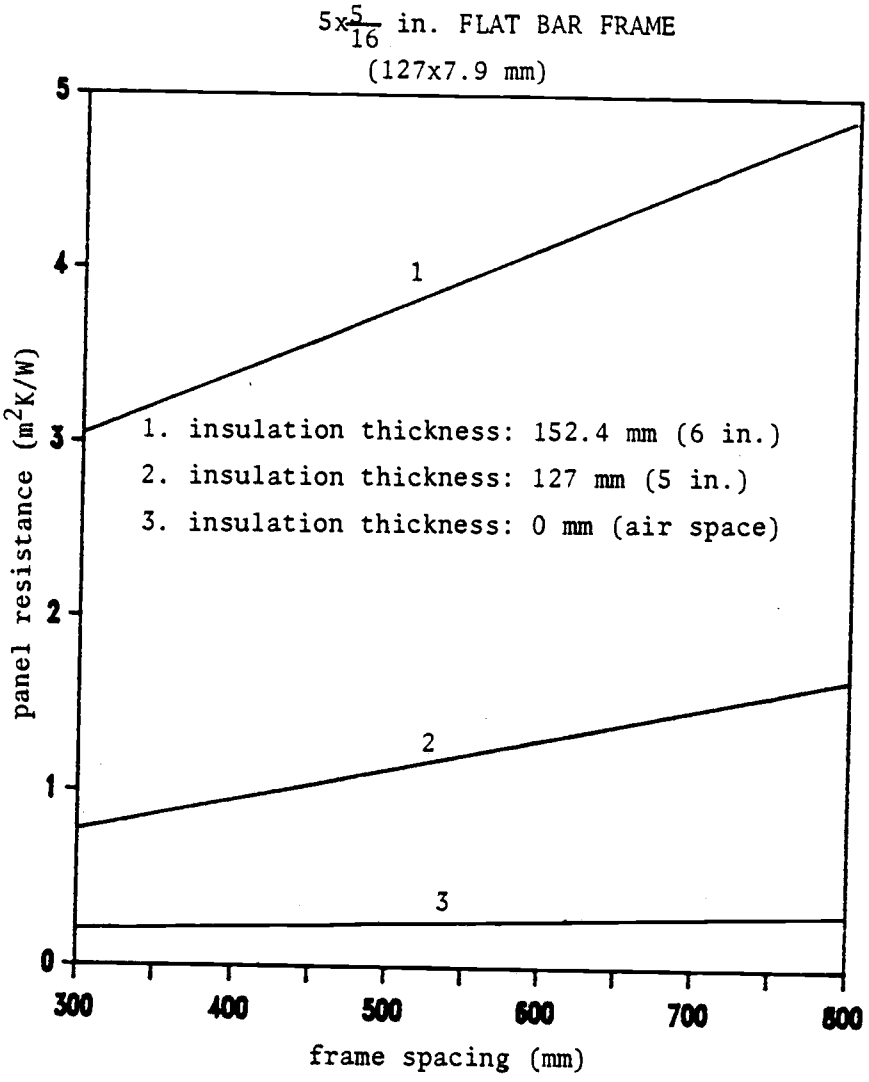

Fig. IV-15

PANEL RESISTANCE vs FRAME SPACING FOR
A WALL SECTION WITH STEEL LINER

steel liner thickness: 3.2 mm ($\frac{1}{8}$ in.)
steel plate thickness: 6.4 mm ($\frac{1}{4}$ in.)

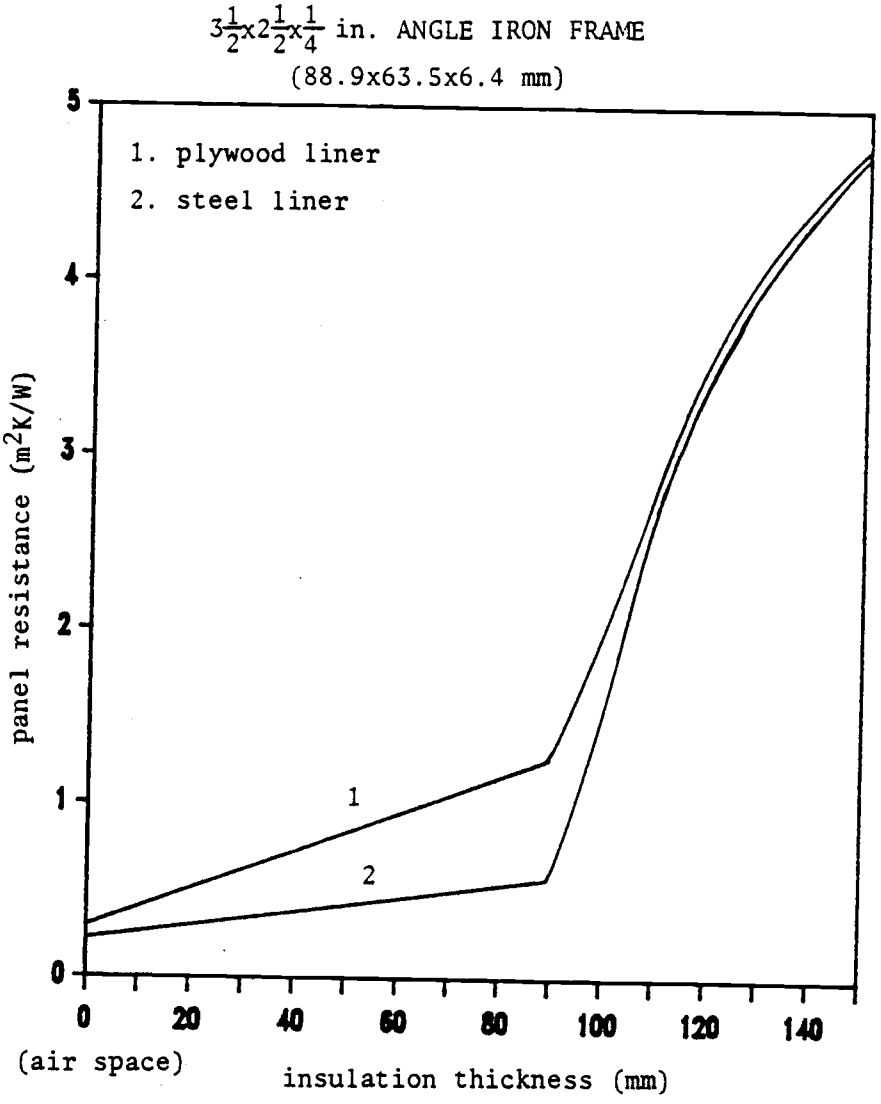

Fig. IV-16

PANEL RESISTANCE vs INSULATION THICKNESS

frame spacing: 533.4 mm (21 in.)

plywood liner thickness: 9.5 mm ($\frac{3}{8}$ in.)

steel liner thickness: 4.8 mm ($\frac{3}{16}$ in.)

steel plate thickness: 6.4 mm ($\frac{1}{4}$ in.)

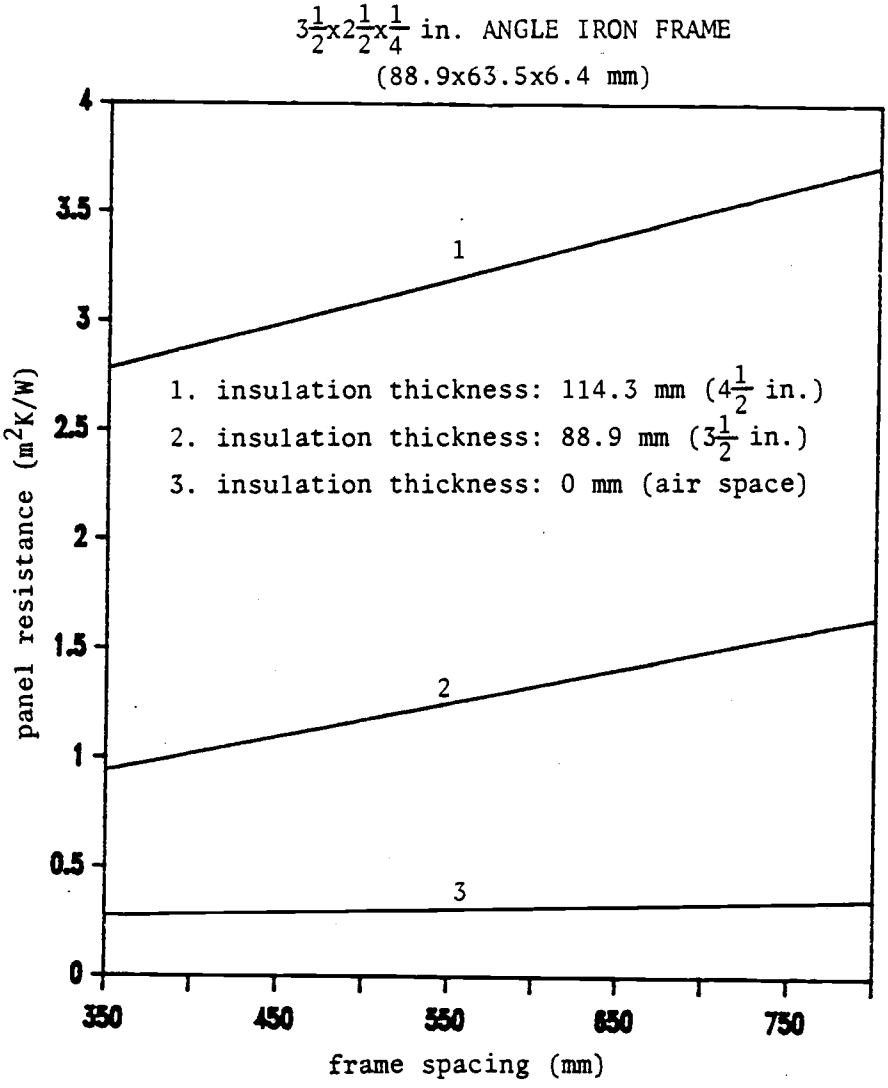

Fig. IV-17

PANEL RESISTANCE vs FRAME SPACING FOR
A WALL SECTION WITH PLYWOOD LINER

plywood liner thickness: 9.5 mm ($\frac{3}{8}$ in.)
steel liner thickness: 6.4 mm ($\frac{1}{4}$ in.)

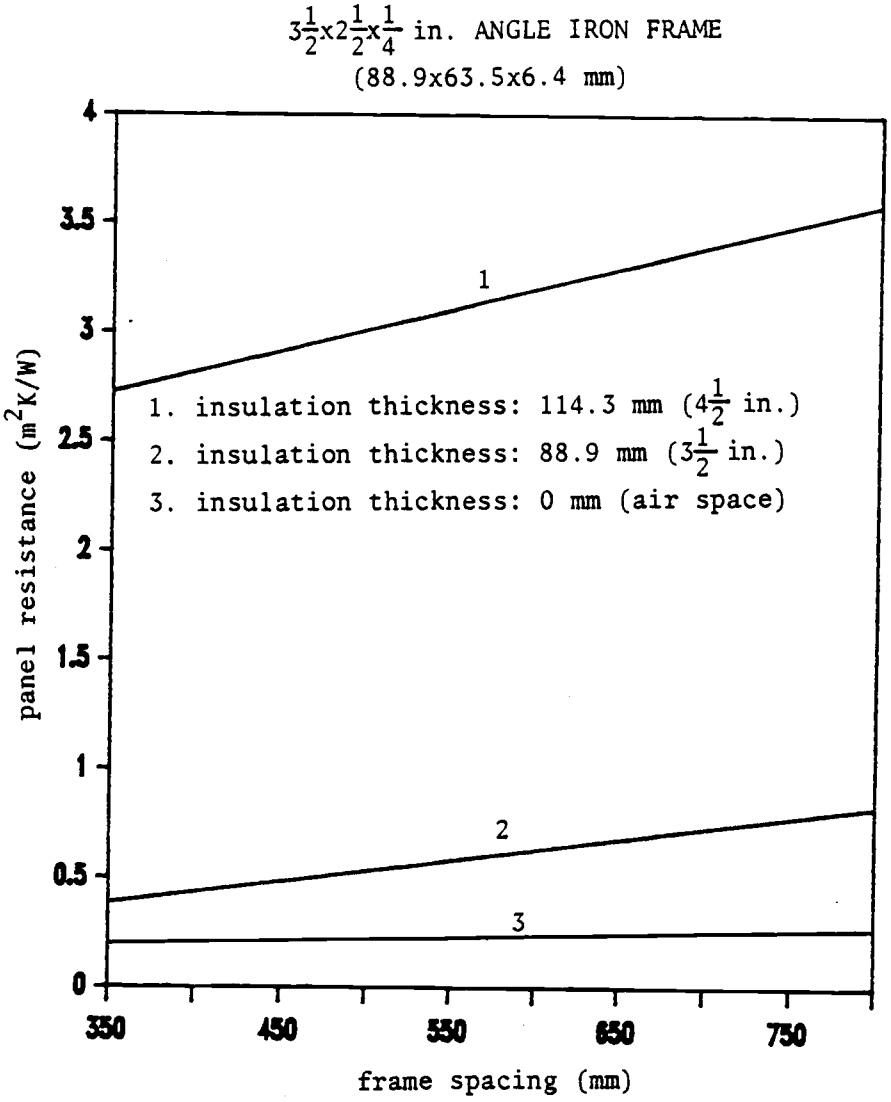

Fig. IV-18

PANEL RESISTANCE vs FRAME SPACING FOR
A WALL SECTION WITH STEEL LINER

steel liner thickness: 4.8 mm ($\frac{3}{16}$ in.)
steel plate thickness: 6.4 mm ($\frac{1}{4}$ in.)

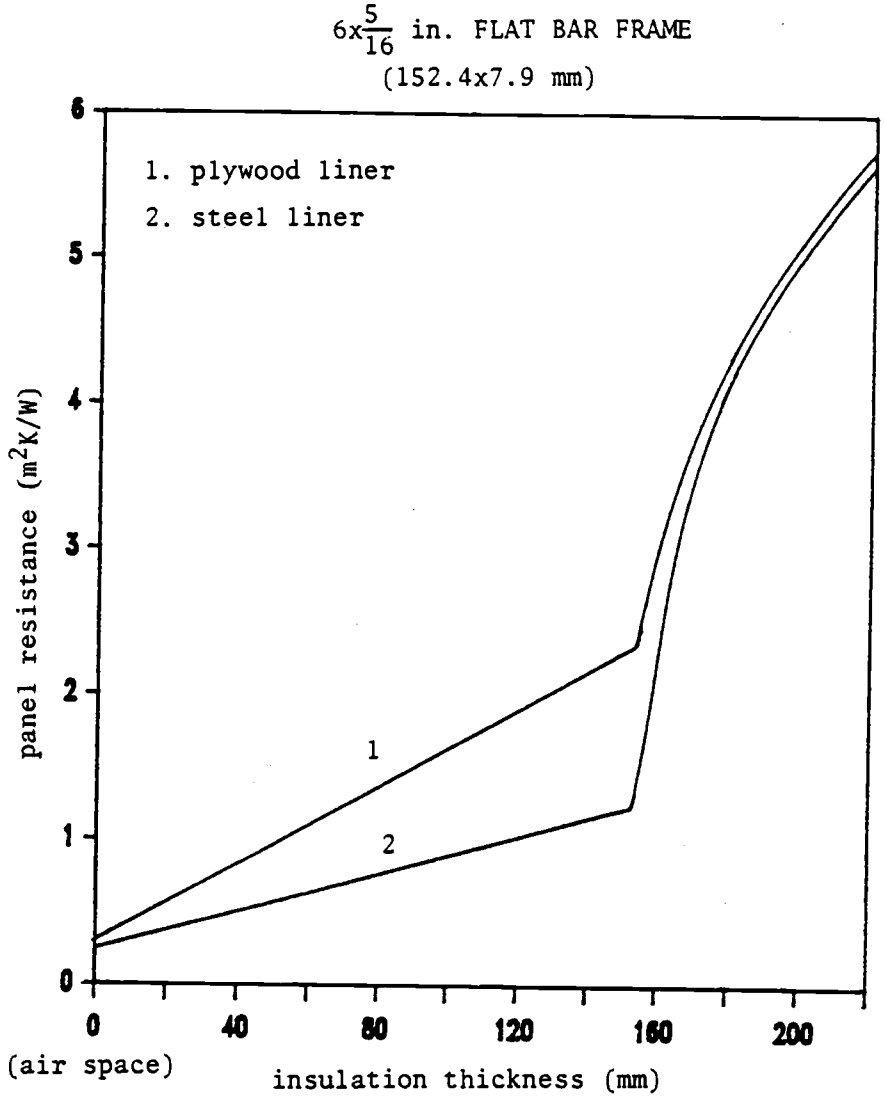

Fig. IV-19

PANEL RESISTANCE vs INSULATION THICKNESS

frame spacing: 533.4 mm (21 in.)
plywood liner thickness: 9.5 mm ($\frac{3}{8}$ in.)
steel liner thickness: 4.8 mm ($\frac{3}{16}$ in.)
steel plate thickness: 6.4 mm ($\frac{1}{4}$ in.)

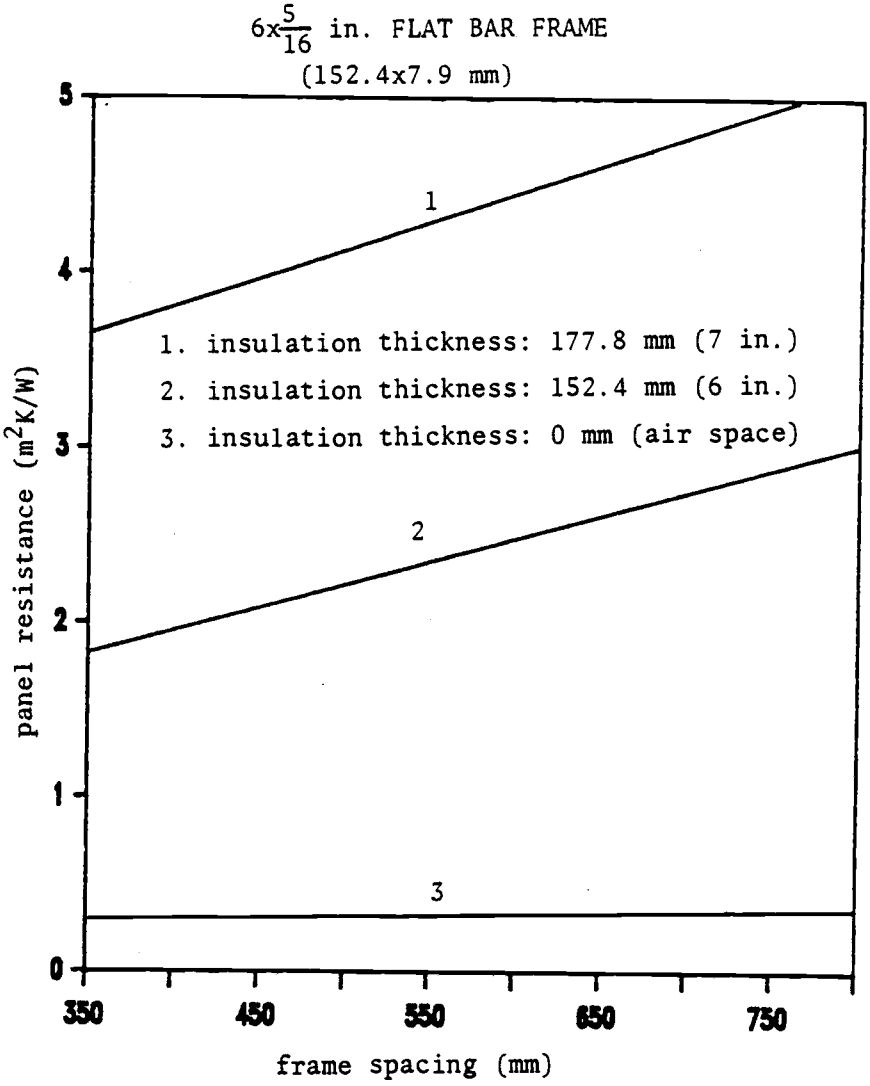

Fig. IV-20

PANEL RESISTANCE vs FRAME SPACING FOR
A WALL SECTION WITH PLYWOOD LINER

plywood liner thickness: 9.5 mm ($\frac{3}{8}$ in.)
steel plate thickness: 6.4 mm ($\frac{1}{4}$ in.)

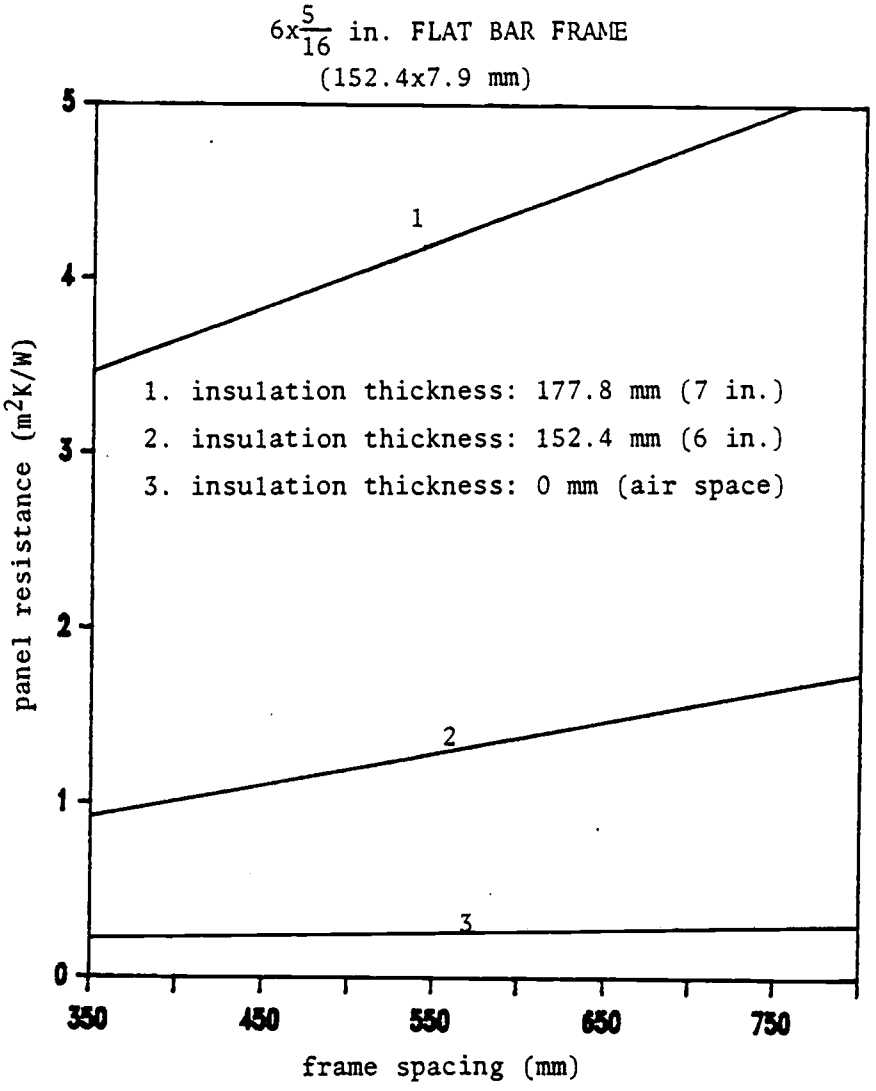

Fig. IV-21

PANEL RESISTANCE vs FRAME SPACING FOR A WALL SECTION WITH STEEL LINER

steel liner thickness: 4.8 mm ($\frac{3}{16}$ in.)

steel plate thickness: 6.4 mm ($\frac{1}{4}$ in.)

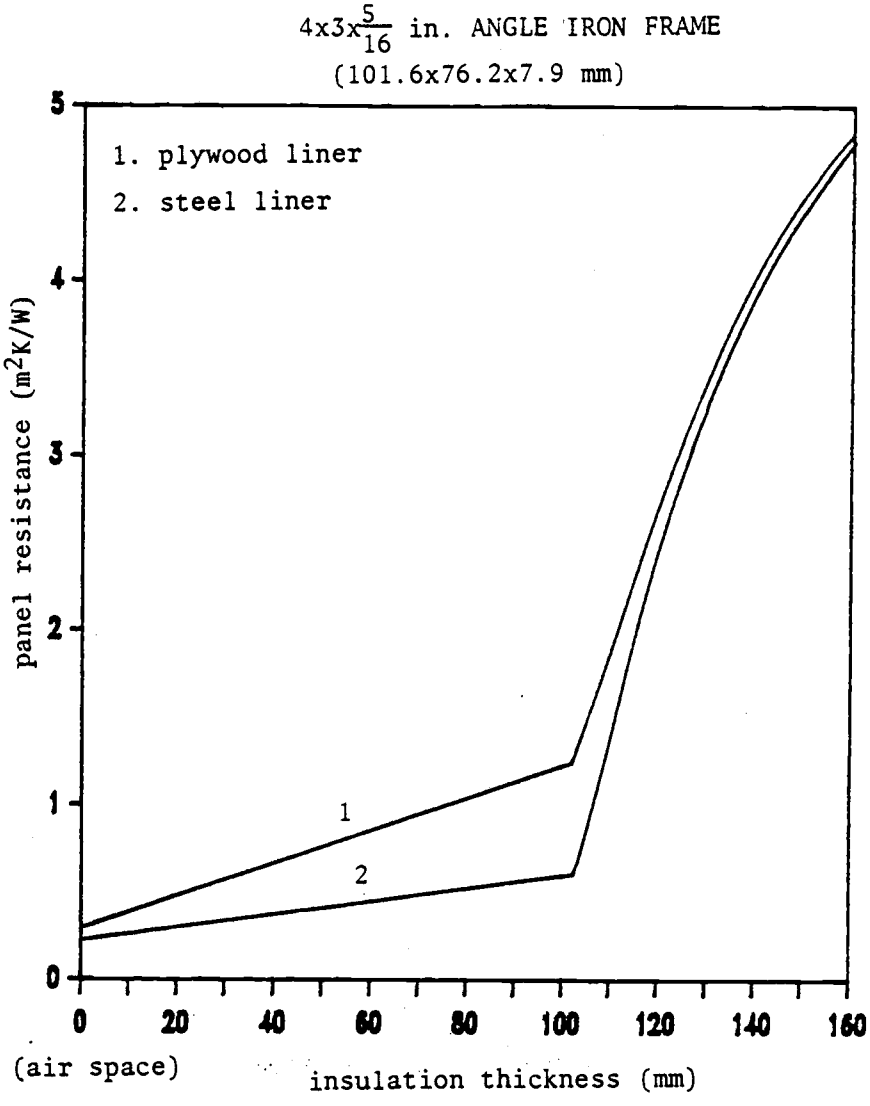

Fig. IV-22

PANEL RESISTANCE vs INSULATION THICKNESS

frame spacing: 558.8 mm (22 in.)

plywood liner thickness: 9.5 mm ($\frac{3}{8}$ in.)

steel liner thickness: 4.8 mm ($\frac{3}{16}$ in.)

steel plate thickness: 7.9 mm ($\frac{5}{16}$ in.)

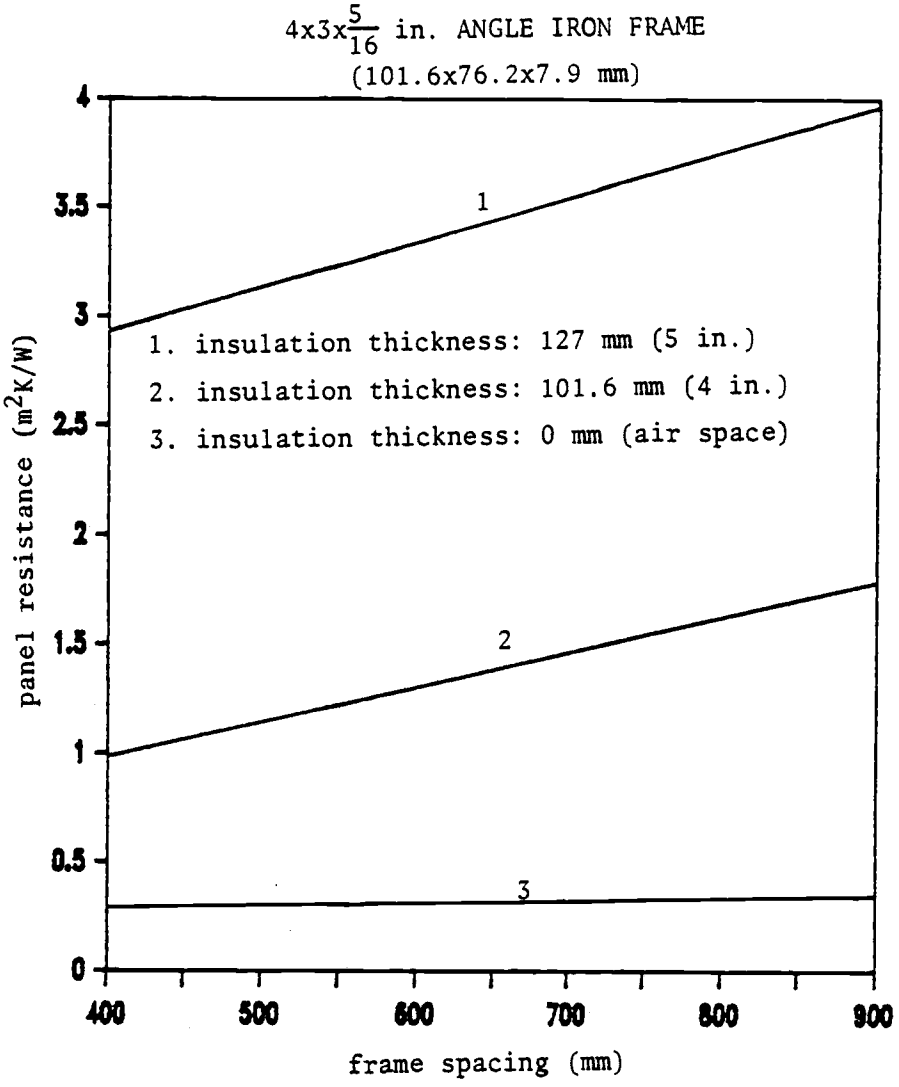

Fig. IV-23

PANEL RESISTANCE vs FRAME SPACING FOR A WALL SECTION WITH PLYWOOD LINER

plywood liner thickness: 9.5 mm ($\frac{3}{8}$ in.)
steel plate thickness: 7.9 mm ($\frac{5}{16}$ in.)

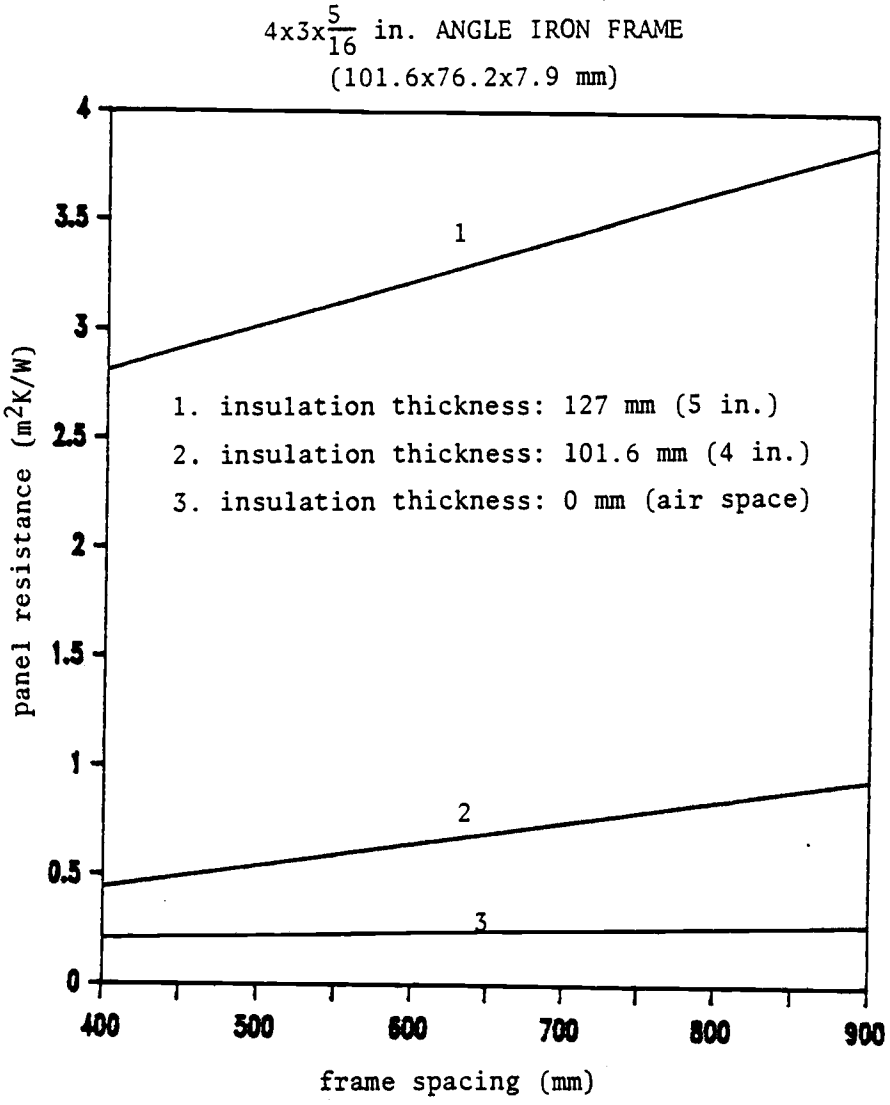

Fig. IV-24

PANEL RESISTANCE vs FRAME SPACING FOR
A WALL SECTION WITH STEEL LINER

steel liner thickness: 4.8 mm ($\frac{3}{16}$ in.)
steel plate thickness: 7.9 mm ($\frac{5}{16}$ in.)

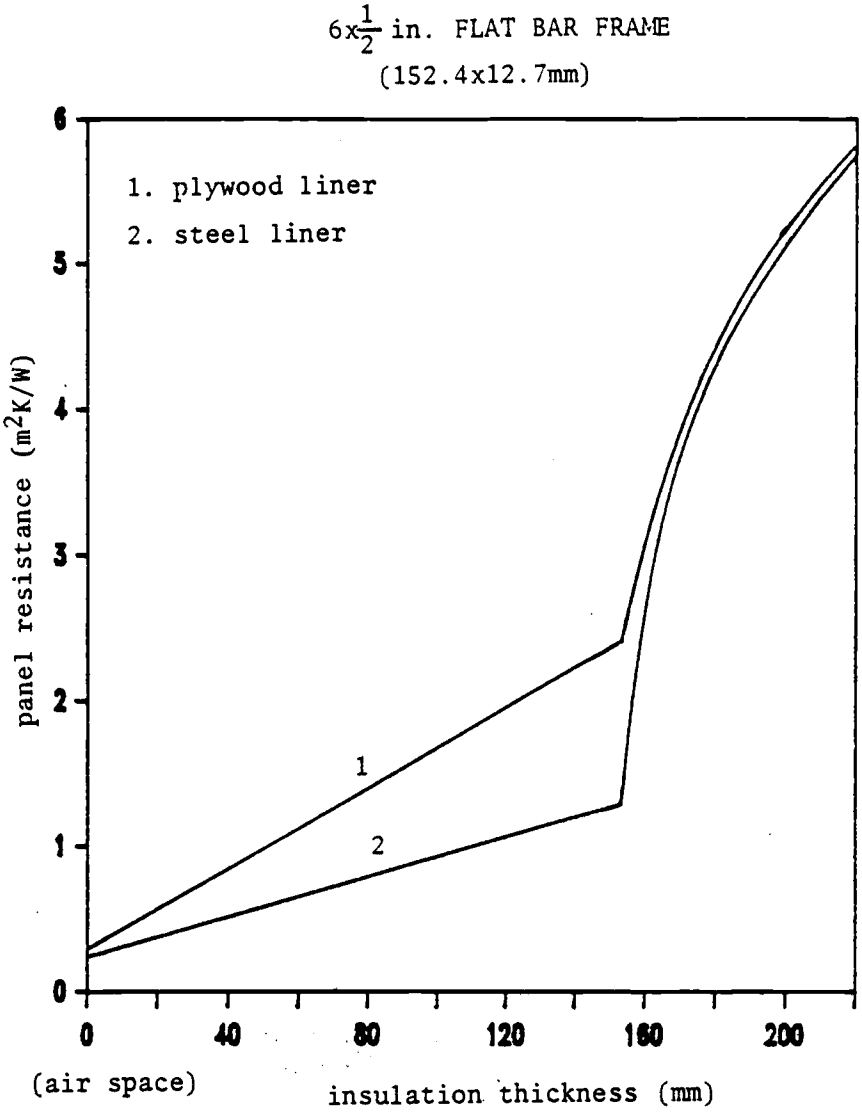

Fig. IV-25

PANEL RESISTANCE vs INSULATION THICKNESS

frame spacing: 558.8 mm (22 in.)
plywood liner thickness: 9.5 mm ($\frac{3}{8}$ in.)
steel liner thickness: 4.8 mm ($\frac{3}{16}$ in.)
steel plate thickness: 7.9 mm ($\frac{5}{16}$ in.)

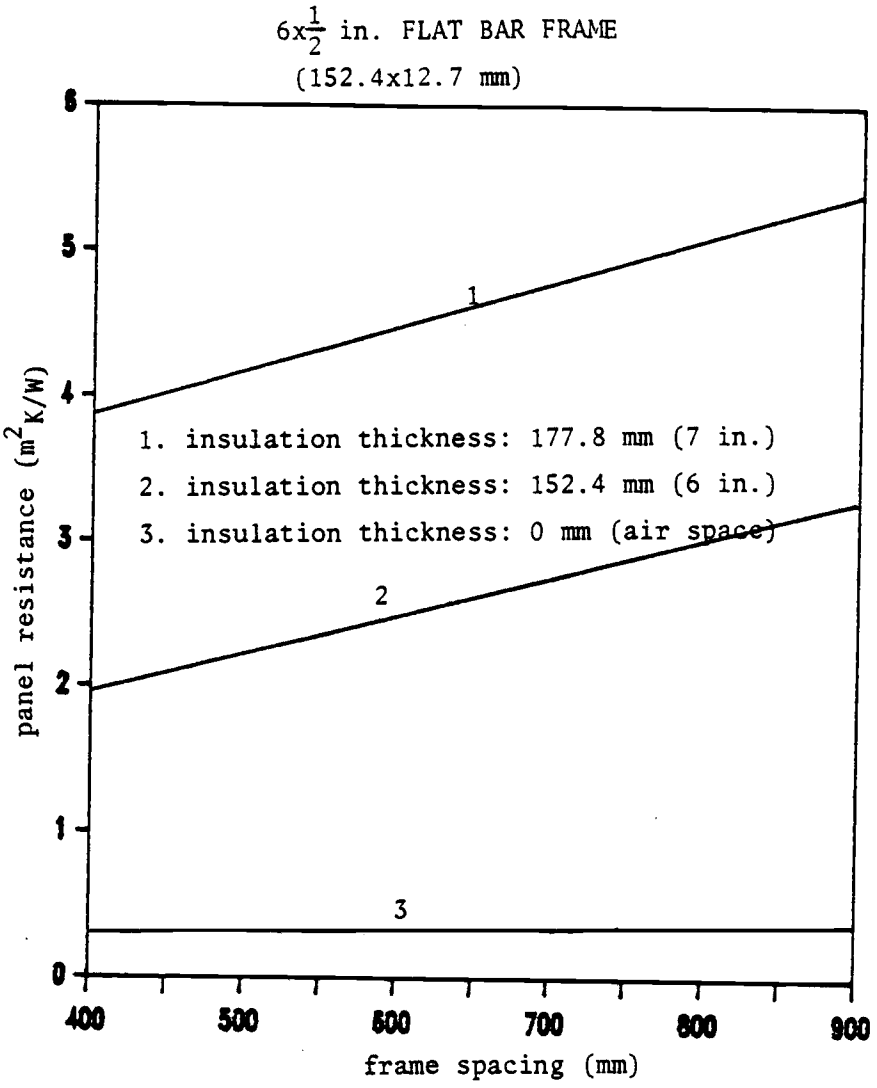

Fig. IV-26

PANEL RESISTANCE vs FRAME SPACING FOR
A WALL SECTION WITH PLYWOOD LINER

plywood liner thickness: 9.5 mm ($\frac{3}{8}$ in.)
steel plate thickness: 7.9 mm ($\frac{5}{16}$ in.)

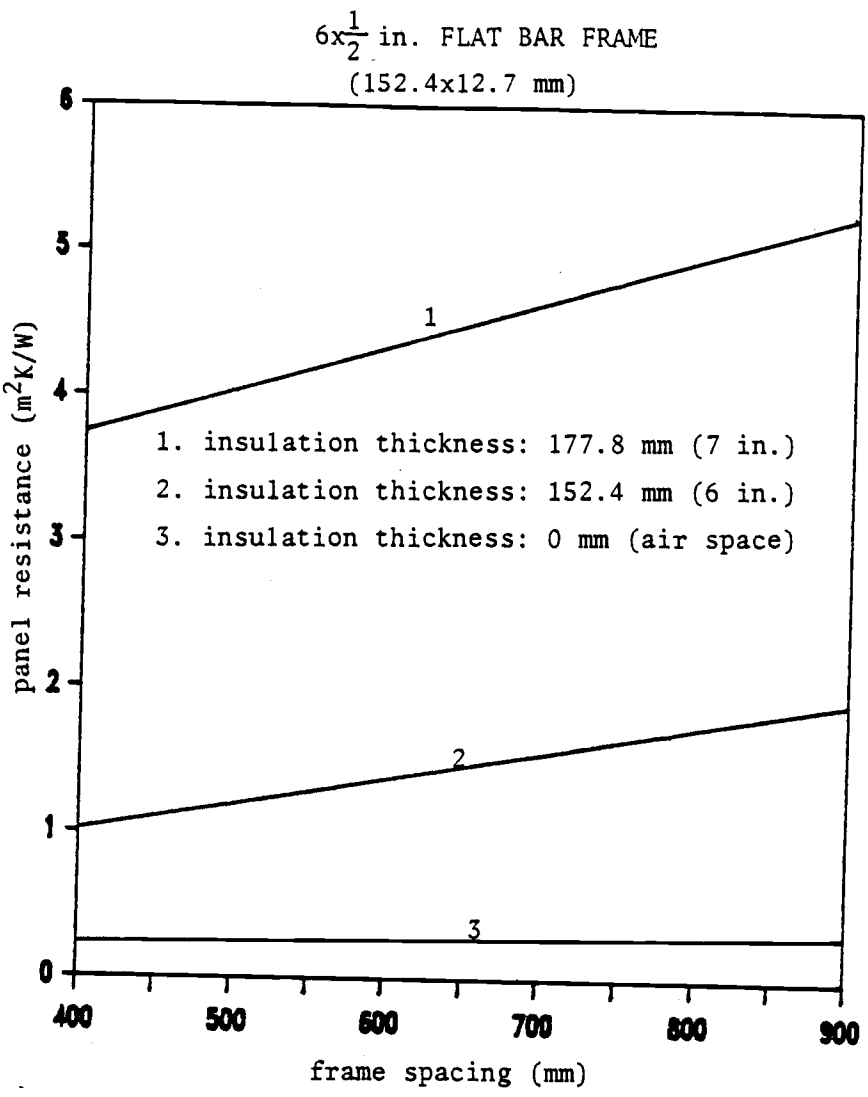

Fig. IV-27

PANEL RESISTANCE vs FRAME SPACING FOR
A WALL SECTION WITH STEEL LINER
steel liner thickness: 4.8 mm ($\frac{3}{16}$ in.)
steel plate thickness: 7.9 mm ($\frac{5}{16}$ in.)

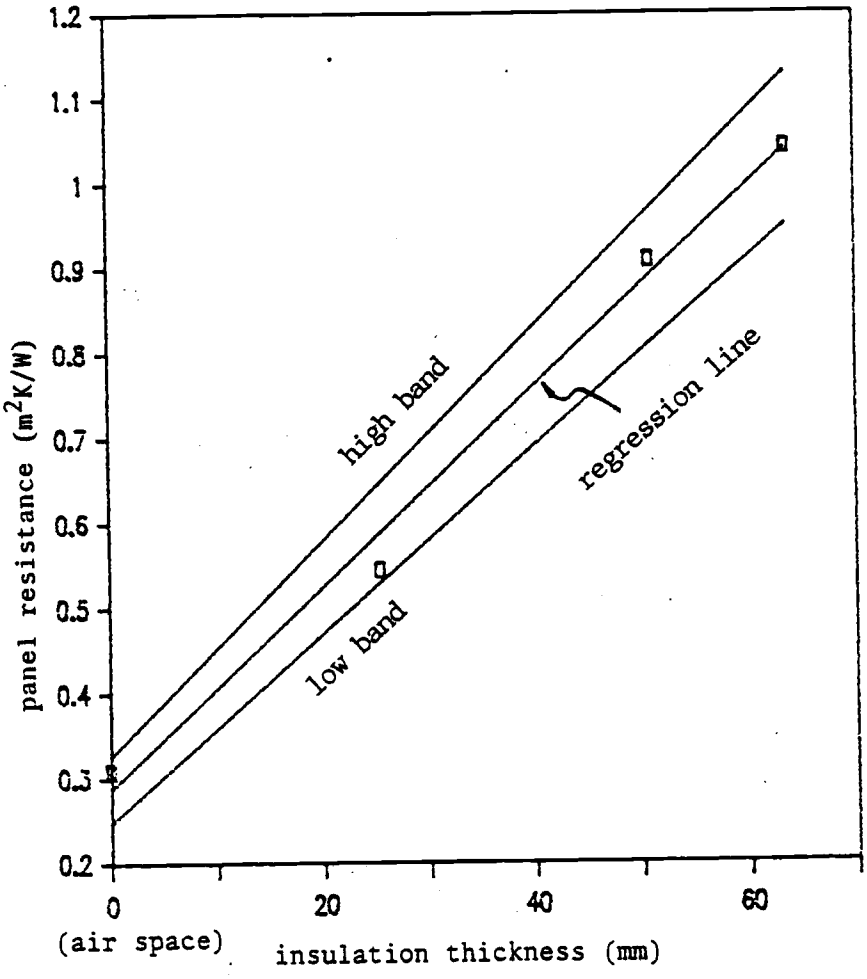

Fig. IV-28

THE LINEARITY OF PANEL RESISTANCE vs INSULATION THICKNESS FOR PANEL 1 WITH INSULATION THICKNESS LESS THAN THE FRAME DEPTH

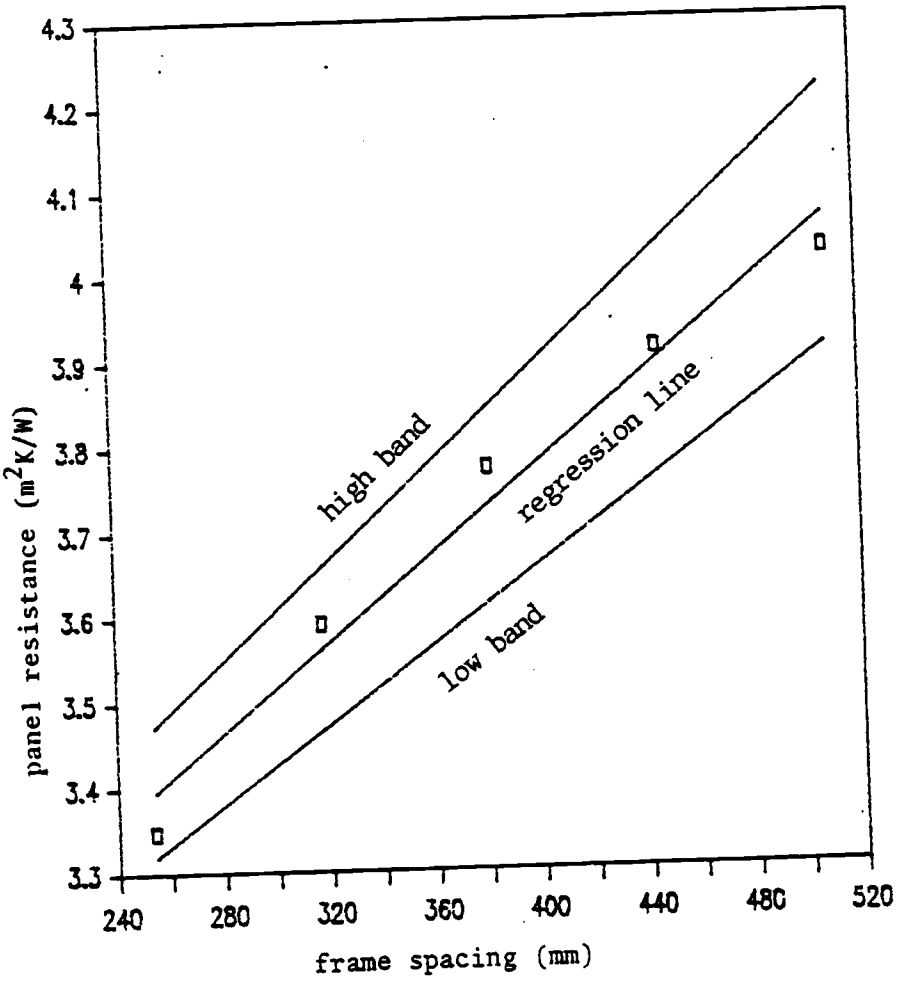

Fig. IV-29

THE LINEARITY OF PANEL RESISTANCE vs FRAME SPACING FOR PANEL 1

CHAPTER V. DISCUSSION

As described in the previous chapters, the numerical model agreed well with the experimental measurements. This allowed us to use program FD to predict panel resistance values for configurations not measured and to obtain 24 design curves for West Coast steel vessels. Further discussion on numerical modeling, experiments, and results is presented in this chapter.

V.1. Numerical Modeling

Since the steel frames penetrate the fish hold wall sections, the panel is considered to be a two-dimensional heat transfer body. This problem has been successfully solved by computer program FD. Most importantly, node centered mesh has been used to handle the interface between two materials. Without using this method, the problem is more difficult to solve. The disadvantage of this method relates to the difficulty of calculating the surface temperature distribution. Referring to Figure II-8, we can see that node i is located at one half of the grid space inward from the surface. However, this disadvantage can be easily overcome by calculating the surface temperature using the heat balance method. That is, the heat transfer from the air to the surface by convection is equal to the conduction from the surface to the point one half of a grid

space inward from the surface.

Since the steel frames penetrate the insulation layer, a field of thermal properties as functions of position is created. We assigned the different thermal properties to each small area which is represented by its centered node. The only requirement is that one must understand the grid system very well.

How to address the grid interval is another important consideration. The finer the grid assigned, the more accurate the result obtained. However, the tradeoff is increased computation effort, computer time, and memory. In computer program FD, finer grids have been used in the areas near frames. The reason is that great temperature gradients occur in these areas due to great differences of thermal conductivity between steel and other materials. Even using the finer grids, the temperature gradients in these areas are still large. Note for example, the top central area of Test Panel 3 (refer to Figure III-4. 3). To test adequaty of grid spacing, an even finer grid was tried, but no significant improvement resulted. Therefore, we can conclude that our grid system is appropriate.

V.2. Experiments

The experiments using the "Guarded hot box" were successful. According to personal contact with Dynatherm Engineering laboratory (13), evaluating the accuracy of

guarded hot box testing is difficult. National laboratories, include Dynatherm Engineering, have been involved in a "round-robin" testing program with other laboratories; testing has been in agreement within ±1% for one program and while ±4% for a second. However, in a more recent large scale "round-robin" program, the agreement between all laboratories was poorer, about ±8%. Based upon these comparisons and the personal experience of the laboratory personnel with similar type of panels, the overall accuracy of these fish hold panel measurements is estimated to be about ±4%.

V.3 Results

Both the test results and predictions indicate that insulation thickness is the most important factor affecting insulation effectiveness. The critical value is an insulation thickness equal to frame depth. Figures IV-4, 7, 10, 13, 16, 19, 22, and 25 show that panel resistance can be significantly improved if insulation thickness is greater than frame depth. For instance, from Figure IV-4, we can see a sudden change in the curves at an insulation thickness of 63.5 mm (2.5 in), which is equal to the frame depth. The same trend can be found for the seven other panel resistance vs insulation thickness curves. This tendency can be easily understood by seeing that the insulation layer beyond frame depth cuts off "heat bridges" to block heat flowing through the panel. For the case of

insulation thickness being less than or equal to the frame depth, the effectiveness of the insulation is poor. In other words, there is not a very good pay back for the cost of insulation.

Another important influence is the material used as the inside (or cold side) surface liner. The results show that use of different liner materials significantly affects panel resistance when insulation thickness is less than or equal to frame depth. Obviously, a plywood liner works better because it has lower thermal conductivity. However, as discussed in the preceding section, using a configuration with insulation thickness less than or equal to frame depth is not a good practice. In the case of another insulation layer being added beyond the frame, we find that the liner material is less important, or not important at all. This is especially true when the insulation thickness extends at least 25.4 mm (1 in) beyond the frame. Referring to the example Figure IV-4, we can see that the resistance of the panel with a plywood liner is significantly different from that of the panel with a steel liner at the point of 63.5 mm (2.5 in) insulation thickness. As the insulation thickness increases, the difference between the curves gets less and less, with the curves finally being close to identical beyond an insulation thickness of 25 mm (1 in) thicker than the frame depth.

Frame spacing is a very important factor for construction strength. However, all panel resistance-vs-frame-spacing curves show that frame spacing does not affect thermal resistance of panels as significantly as does insulation thickness. Therefore, frame spacing determination should satisfy construction strength requirements first, as it is less important from the view of insulation effectiveness. The same conclusion can be reached for the determination of other dimensions, such as frame thickness, steel plate thickness, etc. The panel resistance corresponding to a practical variation of frame and steel skin thicknesses were calculated using program FD. Figure V-1 shows the effect of frame thickness for Panels 1 and 2. The maximum variation of panel resistance caused by the use of different frame thicknesses is about 11%. Figure V-2 shows the effect of steel skin thickness for Panels 1 and 2. The maximum variation of panel resistance caused by the use of different steel skin thickness is less than 1%.

Various fasteners for insulation lining are used in shipyard practice. As described in Chapter III, fasteners were also used to hold insulation lining in construction of the two test assemblies for the "Guarded hot box" experiment. Results of Table IV-1 show that the calculated resistances are always greater than the test results. This is probably due to the fact that fastener effects on the

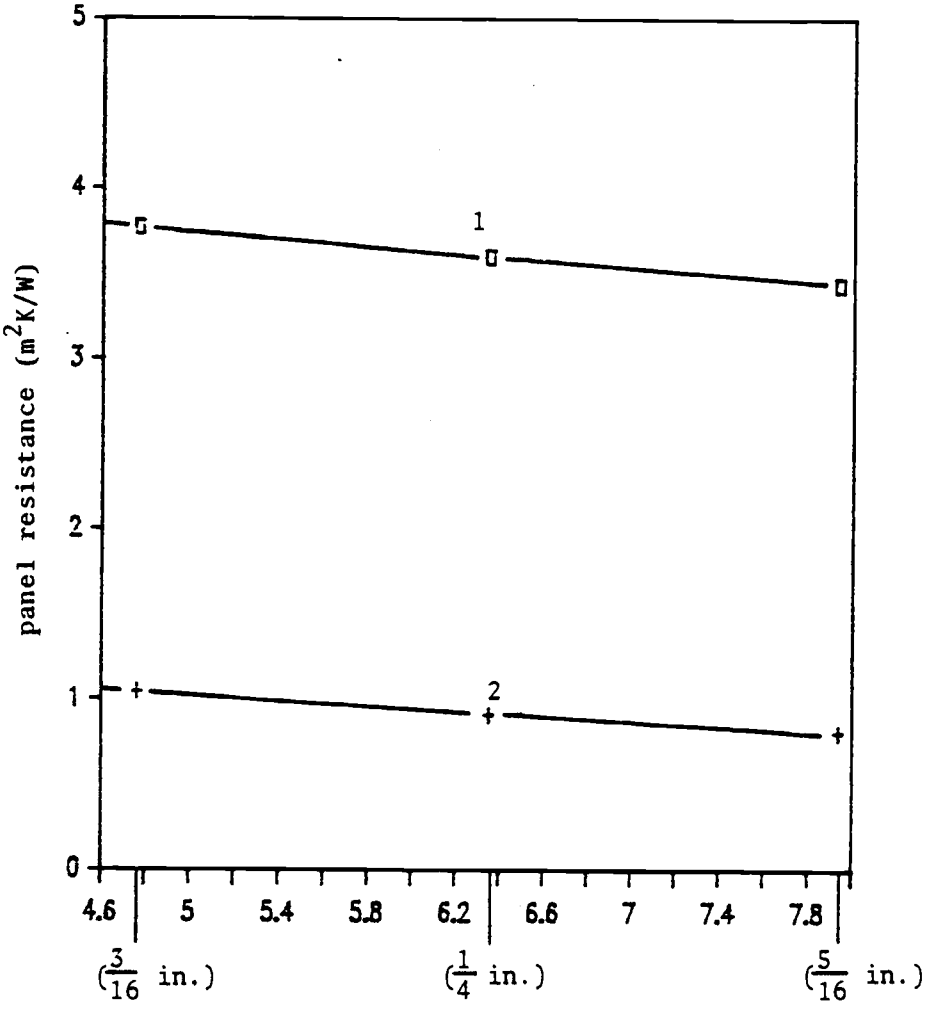

Fig. V-1

FRAME THICKNESS EFFECT

1. construction of Panel 1.
2. construction of Panel 2.

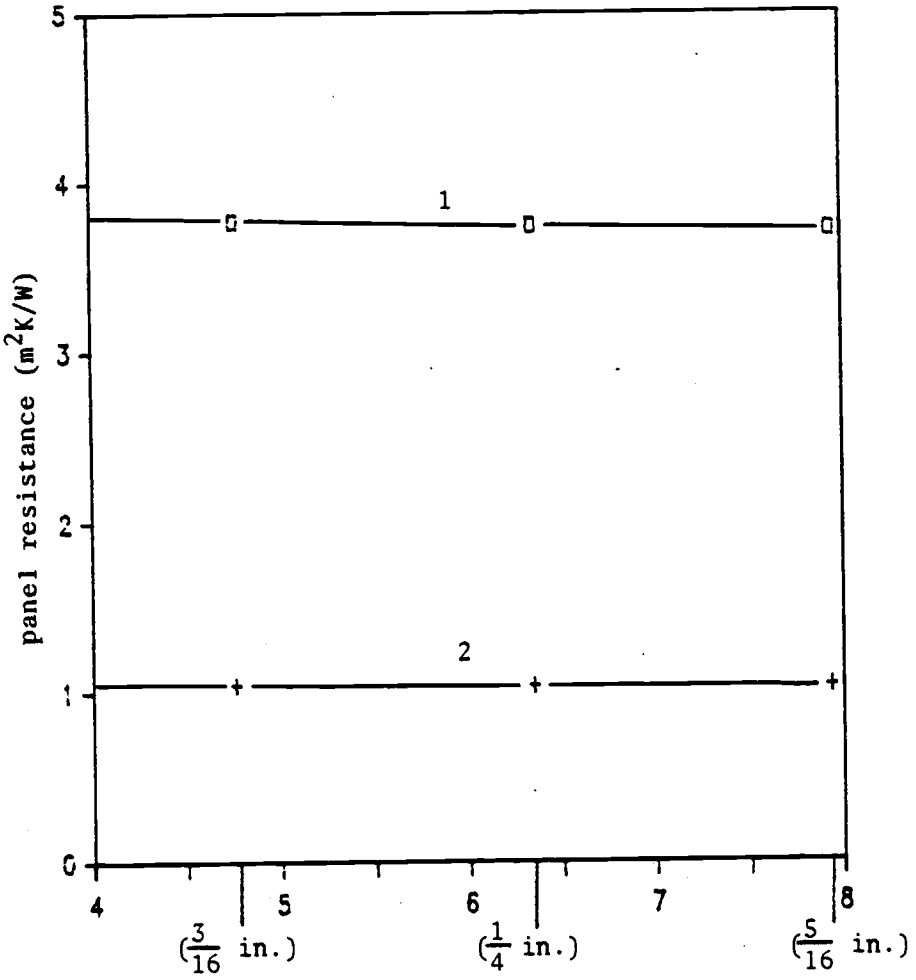

Fig. V-2

STEEL SKIN THICKNESS EFFECT

1. construction of Panel 1.
2. construction of Panel 2.

heat transfer through the panel are not considered in Program FD. Munton and Stott (28) reported that 5% heat leakage should be added to allow for the effect of fasteners. Their estimate is probably applicable in practice.

Another term to be considered is the weld effect. Chapter III described how the steel skin was welded to the frames. Thermocouples were installed both on welds and in un-welded areas for checking weld effects. Test results show that temperatures on weld seams are close to those in un-welded areas (refer to Appendix 4), supporting the assumption that contact resistance due to non-continuous weld is not significant.

An experimental model for predicting heat leakage through steel vessel wall sections, known as the Joelson equation (18 and 32), was mentioned in Chapter I. Here, this equation is further compared with our numerical modeling results. Joelson equation is presented as

$$C=\frac{k\times 10^3}{S}\left[\frac{F}{d-D}+\frac{S-F-1.7D}{d}+3\log\left(\frac{d+0.6D}{d-D}\right)\right]$$

Where the symbols are illustrated in Figure V-3 and defined as:

C=thermal conductance, in W/m^2K

k=thermal conductivity, in W/mK

S=frame spacing, in mm

F=width of frame face, in mm

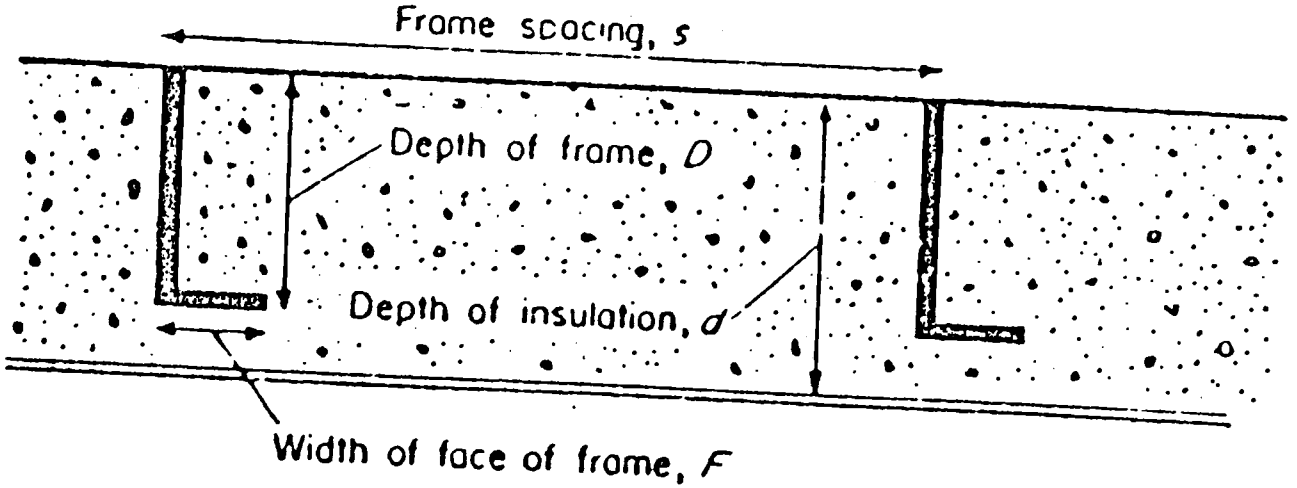

Fig. V-3

SYMBOLS USED IN JOELSON EQUATION (28)

D=depth of frame, in mm

d=depth of insulation, in mm.

An example application is for the case of a 14 m (45 ft) vessel with angle iron frames, k=0.023 W/mK (aged value of urethane foam); S=381 mm; F=38.1 mm; D=63.5 mm; and d=114.3 mm. Joelson's equation would predict panel conductance to be 0.255773 W/mK and panel resistance (the reciprocal of conductance) about 3.91 mK/W. This agrees well with the numerically-predicted value of 3.89 mK/W. Similar agreement also holds true for other sizes of vessels. Therefore, we can say that Joelson's equation is a good predicting model for practical use. However, the limitation is that the equation can only be applied for angle iron frames and requires the insulation thickness d to be greater than the frame depth D.

Estimation of the accuracy of results is necessary but difficult. The maximum error given in Table IV-1 is +9.5% compared to the test result. If 5% can be taken out to allow for the fasteners effect, the error left is about +5%. Additionally, the error of the "guarded hot box" test is about ±4% and the maximum error caused by linear assumptions is ±11.4%. Therefore, the accuracy can be estimated to be about ±13% from the square root of the sum of squares.

CHAPTER VI. CONCLUSIONS AND RECOMMENDATIONS

VI.1. Conclusions

The following specific conclusions were drawn from this research:

1. Insulation thickness plays a very important role in the thermal performance of steel vessel wall sections. The critical point is when insulation thickness is equal to frame depth. Poor insulation effectiveness will be obtained if the insulation layer is less than or equal to the frame depth. The best configuration is one in which insulation thickness is at least 25 mm (1 in) greater than the frame depth.

2. Material used as a cold side (or inside) liner has an important effect on insulation effectiveness if insulation thickness is less than or equal to the frame depth. A plywood liner is a good choice under this condition. However, it becomes less important, or not important at all, if insulation thickness is at least 25 mm (1 in) greater than frame depth.

3. To allow for the effect of fasteners, 5% heat leakage should be added according to Munton and Stott report.(28) Their estimate agrees with the numerical modeling results of this project and is applicable in practice.

4. Frame spacing has less effect on heat leakage than the insulation thickness. The importance of the thickness of frame and steel skin is even less.

5. Both finite element and finite difference methods work well to predict heat leakage through fish hold wall sections, but the finite difference method is easier to apply. Twenty-four thermal resistance curves for various frame sizes were obtained by applying the finite difference model. These curves will provide basic information on the design of fish hold wall sections for steel vessels. The accuracy of these curves is about ±13%.

6. Joelson's empirical equation is a good model for predicting heat leakage through fish hold wall sections. The limitation of this equation is that it can be applied only to angle iron frames for the case of insulation thickness greater than the frame depth.

VI.2. Recommendations for Future Research

Construction of fish hold wall sections varies with different parts of steel vessels, such as bulkheads, decks, floors, etc. For instance, heat leakage through a concrete floor is quite different from the situation we have analysed in this project. The use of a numerical model to predict heat leakage through such wall sections has not been reported in any literature known to the author. A better understanding of thermal performance of

these different constructions is necessary for improving our ablility to predict total heat leakage through the whole vessel.

In this research, all conclusions were drawn from the view of thermal performance. For instance, we conclude that the best configuration is the one with insulation thickness being greater than the frame depth. The tradeoff is that the more insulation installed, the higher the cost and the less volume left for the fish hold. Therefore, an optimization procedure is necessary to balance these opposing effects. If this research could be accomplished, a standard design of steel vessel wall section would naturely be set up. This would greatly benefit architects, engineers, builders, refrigeration contractors, and insulation contractors, as well as fishermen.

REFERENCES

1. ABS (American Bureau of Shipping). "Rules for Building and Classing steel vessels under 61 meter (200 feet) in Length." New York, 1983.
2. Adame, J. A., and D. F. Rogers. "Computer-Aided Heat Transfer Analysis" McGraw-Hill Book Co. 1973.
3. ASTM (American Society for Testing and Materials). "STP470-Manual on the Use of Thermocouples in Temperature Measurement." ASTM, Philadelphia. 1970.
4. ASTM (American Society for Testing and Materials). "Standard Test Method for Steady-State Thermal Performance of Building Assemblies by Means of A Guarded Hot Box." ASTM Designation: C 236-80.
5. ASTM (American Scociety for Testing and Materials). "Steady-state Thermal Transmission Properties by Means of Guarded Hot Plate." ASTM Designation: C 177-76.
6. ASHRAE (American Society of Heating Refrigeration and Air Conditioning Engineers). "Fundamentals." ASHRAE Handbook. 1981.
7. Barfuet, F. J. Naval Architect, Portland, Oregon. Personal communication. 1984.
8. Braun, M. "Differential Equations and Their Applications." 2nd. Edition. Springer-Verlay, New York Inc. 1978.

9. Carnahan, B., H. A. Luther and J. O. Wilkes. "Applied Numerical Methods." John Wiley and Sons. Inc. 1969.

10. Croft, D. R. and D. G. Lilley. "Heat Transfer Calculations Using Finite Difference Equations." Applied Science Publishers LTD. London. 1977.

11. Eckert, E. R. G. and T. J. Goldstein. "Measurements in Heat Transfer." 2nd. Edition. McGraw Hill. 1976.

12. Emerson, P. C. Parker C. Emerson & Associates, Lake Oswego, Oregon. Personal communication. 1984.

13. Funkhouser, J. B. Dynatherm Engineering Laboratory, Lino Lakes, Minnesota. Personal communication. 1985.

14. Glaser et al., P. E. "Thermal Insulation System, A Survey." NASA Spec. Publ. NASA SP-5027 (1967).

15. Gougus, A. Y. and Y. Paker. "Thermal Bridge Factor." From: Heat and Mass Transfer in Refrigeration System and in Air Conditioning. PP 203-210; Proceedings of Meeting of Commission B-1, B-2, E-1, of the International Insititute of Refrigeration. Freudenstadt. 1972.

16. Hanson, H. C. "Steel and Wood Scantling Tables (West Coast of U.S.A.)" From "Fishing Boats of the World: 2" Fishing News (Book) Ltd. 1960.

17. Huebner, K. H. and E. A. Thornton. "The Finite Element Method For Engineers." 2nd. Edition. John Wiley and Sons. 1982.

18. Joelson, E. "Die Berechung Von Schiffsisolierungen."

Zit. ges. Kalte-Ind., 1930 Vol.37, P.229; 1931, Vol.38, P.8 and 23. (As referenced in Munton and Stott (28) and Stott (32).)

19. Kaplan, W. "Advanced Methematics for Engineers." Addison-Wesley Publishing Co. Inc. 1981.

20. Kolbe, E. R. Agricultural Engineering Department, Oregon State University, Corvallis, Oregon. Personal Communication. 1986.

21. Kuehn, T. H. "Temperature and Heat Flow Measurements from An Insulated Concrete Bermed Wall and Adjacent Floor." Vol. 104, Journal of Solar Energy Engineering. 1982.

22. Kuehn, T. H. and E. A. B. Maldonado. "A Finite Difference Transient Heat Conduction Program for Studying the Thermal Performance of Composite Building Envelopes." Engineering Research Institute, Iowa State University. Ames. 1980.

23. Kuehn, T. H. "Field Heat-Transfer Measurements and Life-Cycle Cost Analysis of Four-Frame Wall Constructions." V.88, Pt.1, For Inclusion in ASHRAE Transactions. 1982.

24. MacCallum, W. A. "Fish Handling and Hold Construction in the North Altantic Trawlers." Fisheries Research Board of Canada Bulletin No. 103. 1955a.

25. MacCallum, W. A. "Jacketed, Refrigerated Fish Holds." In Fishing Boats of the World: 230-232. J. O. Traung,

ed. Fishing News Books Ltd. Farnham. 1955b.

26. MacCallum, W. A. "The Fish Room - Engineering and Architecture." In Fishing Boats of the World 2: 208-226. J. O. Traung, ed. Fishing News Books Ltd. Surrey. 1960.

27. Merritt, J. H., E. Kolbe, and W. Robertson. "Refrigeration Storage of Fish at Sea with Particular Reference to Thermal Insulation." Research Report under Contract with Canadian Department of Fisheries Technology, Technical University of Nova Scotia. Halifax. 1981.

28. Munton, R. and J. R. Stott. "Refrigeration at Sea." 2nd. Edition. Applied Science Publishing Co. London. 1978.

29. SABROE MARINE Inc. Various Advertizing Literatures Plus Personal Communications. 1985.

30. Segerlind, L. J. "Applied Finite Element Analysis." John Wiley and Sons. 1976.

31. SNAME (Society of Naval Architects and Marine Engineers). "Thermal Insulation Report." Technical and Research Bulletin 4-7. SNAME, New York. 1963.

32. Stott, J. R. Refrigeration and Air Conditioning Consultant, Surry, UK. Personal Communication. 1985.

33. Trent, D. S. and J. R. Welty. "A Summary of Numerical Methods for Solving Transient Heat Conduction Problems." Bulletin No.49, Engineering Experiment Station, Oregon

State University. 1974.

34. Welty, J.R. "Engineering Heat Transfer." John Wiley and Sons. 1978.

35. Welty, J. R., C. E. Wicks and R. E. Wilson. "Fundamentals of Momentum, Heat, and Mass Transfer." John Wiley and Sons. 1984.

36. Wilsky, J. Sause Brothers & Towing Inc. Coos Bay, Oregon. Personal Communication. 1985.

37. Wilson, E. L., K. J. Bathe, and F. E. Peterson. "Finite Element Analysis of Linear and Nonlinear Heat Transfer." Nuclear Engineering and Design 29(1974)110-124. North Holland Publishing Co. 1974.

APPENDICES

APPENDIX 1 LISTING OF THE FINITE ELEMENT PROGRAM

1.1. GRID

```
      PROGRAM GRID(TAPE50,TAPE 52,OUTPUT,TAPE 51=OUTPUT)
C*****************************
C       GRID AND HT ARE FINITE ELEMENT PROGRAM FOR SOLVING
C       FISH HOLD WALL SECTION PROBLEM.  THESE PROGRAMS ARE
C       MODIFICATIONS OF EXISTING CODES FROM REFERENCE 30.
C       THE VARIABLES IN THESE TWO PROGRAMS ARE DEFINED AS:
C       A: THE COLUMM VECTOR CONTAINING {PHI}, {F} AND [K]
C          OF THE MATRIX EQUATION [K]{PHI}={F}.
C       AR2: TWO TIME THE ELEMENT AREA.
C       AR4: FOUR TIME THE ELEMENT AREA.
C       B: COEFFICIENT THAT OCCUR DURING THE EVALUATION OF
C          THE ELEMENT MATRIX.
C       C: SAME AS B.
C       CK: THERMAL CONDUCTIVITY OF INSULATION MATERIAL.
C       CK1: THERMAL CONDUCTIVITY OF STEEL.
C       CK2: THERMAL CONDUCTIVITY OF PLYWOOD.
C       COND: THERMAL CONDUCTIVITY OF THE ELEMENT.
C       CONV1: CONVECTIVE COEFFICIENT AT COLD SURFACE.
C       CONV2: CONVECTIVE COEFFICIENT AT WARM SURFACE.
C       EF: ELEMENT FORCE VECTOR.
C       ESM: ELEMENT STIFFNESS MATRIX.
C       H: CONVECTIVE COEFFICIENT OF THE ELEMENT.
C       IN: NUMBER OF THE INPUT DEVICE.
C       IO: NUMBER OF THE OUTPUT DEVICE.
C       INBP: NUMBER OF BOUNDARY POINTS.
C       INGR: NUMBER OF REGIONS.
C       JGF: A POINT INDICATING THE LAST STORAGE LOCATION
C            FOR {PHI} IN THE COLUMM ARRAY A.
C      JGSM: SAME AS JGF BUT FOR {F}.
C      JEND: SAME AS JGF BUT FOR [K].
C      NCL: NUMBER OF LOADING CASES.
C      NCOL: NUMBER OF COLUMMS OF NODES.
C      NE: TOTAL NUMBER OF ELEMENT.
C      NEL: NUMBER OF AN INDIVIDUAL ELEMENT.
C      NDN: GLOBAL NODE NUMBER USED TO DEFINE THE
C           QUADRILATERAL.
C      NGR: REGION NUMBER.
C      NROWS: NUMBER OF ROWS OF NODES.
C      NS: ELEMENT NODE NUMBER.
C      LBOT: THE LAST BOUNDARY REGION NUMBER AT BUTTOM.
C      LTOP: THE LAST BOUNDARY REGION NUMBER AT TOP.
C      TAMB1: AIR TEMPERATURE AT THE COLD SURFACE.
C      TAMB2: AIR TEMPERATURE AT THE WARM SURFACE.
C      TITLE: A DESCRIPTIVE STATEMENT OF THE PROBLEM BEING
C             SOLVED.
C      X: X COORDINATES OF THE ELEMENT NODES (COUNTER
C         CLOCKWISE).
```

```
C       XP: X COORDINATES.
C       XRG: X COORDINATES FOR A REGION NODE.
C       Y: Y COORDINATES OF THE ELEMENT NODES (COUNTER
C          CLOCKWISE).
C       YP: Y COORDINATES.
C       YRG: Y COODINATES FOR A REGION NODE.
C*****************************
C
        DIMENSION TITLE(10),XP(100),YP(100),H(200),COND(200)
        DIMENSION TINF(200),XRG(9),YRG(9),N(8),NNN(200)
        DIMENSION NN(21,21),YC(21,21),XC(21,21)
        DIMENSION NNRB(20,4,21),JT(20,4),LB(3),NE(200)
        DIMENSION NDN(8),ICOMP(4,4),XE(200),YE(200),NR(4)
        REAL N
        DATA ICOMP/-1,1,1,-1,1,-1,-1,1,1,-1,-1,1,-1,1,1,-1/
        DATA IN/50/,IO/51/,IP/52/,NBW/0/,NB/0/,NEL/0/
        DATA YMAX/0.546/,YMIN/0/,XXX/0.6120/,CK/0.0133/
        DATA CK1/24.8/,CK2/0.0667/,CONV1/1.11/,CONV2/0.99/
        DATA TAMB1/2.4/,TAMB2/59.8/
C*********************
C       INPUT AND OUTPUT OF TITLE, CONTROL PARAMETER,GLOBL
C       COORDINATES AND CONNECTITVITY DATA
C*********************
        READ(IN,999) TITLE
 999    FORMAT(10A8)
        READ(IN,*)LTOP,LBOT
        READ(IN,*)INRG,INBP
        READ(IN,*)(XP(I),I=1,INBP)
        READ(IN,*)(YP(I),I=1,INBP)
        DO 2 I=1,INRG
 2      READ(IN,*)NGR,(JT(NGR,J),J=1,4)
        WRITE(IO,36) TITLE
 36     FORMAT(1H1////1X,10A8//1X,'GLOBAL COORDINATES'//1X,
     C          'NUMBER      X           Y')
        WRITE(IO,30) (I,XP(I),YP(I),I=1,INBP)
 30     FORMAT(2X,I3,7X,F7.2,5X,F7.2)
        WRITE(IO,37) LTOP,LBOT
  37    FORMAT(//1X,'BOUNDARY REGION CONTROL',2X,2I10)
        WRITE(IO,21)
  21    FORMAT(//1X,'CONNECTIVITY DATA'/1X,
     C          'REGION',3X,'ONE   TWO   THREE   FOUR')
        DO 26 I=1,INRG
 26     WRITE(IO,22) I,(JT(I,J),J=1,4)
 22     FORMAT(2X,I3,14X,4(I2,5X))
C
C       LOOP ON THE REGION TO GENERATE THE ELEMENTS
C
        DO 16 KK=1,INRG
        READ(IN,*)NRG,NROWS,NCOL,NDN
        WRITE(IO,18)NRG,NROWS,NCOL,(NDN(I),I=1,8)
  18    FORMAT(1H1///1X,'***REGION',I3,'***'//10X,I2,
     C  'ROWS',10X,
```

```
     C  I2,' COLUMNS'//10X,'BOUNDARY NODE NUMBERS',10X,8I5)
C
C        GENERATION OF THE ELEMENT NODAL COORDINATES
C
         DO 5 I=1,8
         II=NDN(I)
         XRG(I)=XP(II)
    5    YRG(I)=YP(II)
         XRG(9)=XRG(1)
         YRG(9)=YRG(1)
         TR=NROWS-1
         DETA=2./TR
         TR=NCOL-1
         DSI=2./TR
         DO 12 I=1,NROWS
         TR=I-1
         ETA=1.-TR*DETA
         DO 12 J=1,NCOL
         TR=J-1
         SI=-1.+TR*DSI
         N(1)=-0.25*(1.-SI)*(1.-ETA)*(SI+ETA+1.)
         N(2)=0.50*(1.-SI**2)*(1.-ETA)
         N(3)=0.25*(1.+SI)*(1.-ETA)*(SI-ETA-1.)
         N(4)=0.5*(1.+SI)*(1.-ETA**2)
         N(5)=0.25*(1.+SI)*(1.+ETA)*(SI+ETA-1.)
         N(6)=0.50*(1.-SI**2)*(1.+ETA)
         N(7)=0.25*(1.-SI)*(1.+ETA)*(ETA-SI-1.)
         N(8)=0.50*(1.-SI)*(1.-ETA**2)
         XC(I,J)=0.0
         YC(I,J)=0.0
         DO 12 K=1,8
         XC(I,J)=XC(I,J)+XRG(K)*N(K)
   12    YC(I,J)=YC(I,J)+YRG(K)*N(K)
C
C        GENERATION OF THE REGION NODE NUMBERS
C
         KN1=1
         KS1=1
         KN2=NROWS
         KS2=NCOL
         DO 50 I=1,4
         NRT=JT(NRG,I)
         IF (NRT.EQ.0.OR.NRT.GT.NRG) GOTO 50
         DO 56 J=1,4
   56    IF(JT(NRT,J).EQ.NRG) NRTS=J
         K=NCOL
         IF (I.EQ.2.OR.I.EQ.4) K=NROWS
         JL=1
         JK=ICOMP(I,NRTS)
         IF (JK.EQ.-1) JL=K
         DO 44 J=1,K
         GO TO(45,46,47,48),I
```

```
   45     NN(NROWS,J)=NNRB(NRT,NRTS,JL)
          KN2=NROWS-1
          GOTO 44
   46     NN(J,NCOL)=NNRB(NRT,NRTS,JL)
          KS2=NCOL-1
          GOTO 44
   47     NN(1,J)=NNRB(NRT,NRTS,JL)
          KN1=2
          GOTO 44
   48     NN(J,1)=NNRB(NRT,NRTS,JL)
          KS1=2
   44     JL=JL+JK
   50     CONTINUE
          IF (KN1.GT.KN2)GOTO 105
          IF (KS1.GT.KS2) GOTO 105
          DO 10 I=KN1,KN2
          DO 10 J=KS1,KS2
          NB=NB+1
   10     NN(I,J)=NB
C
C         STORAGE OF THE BOUNDARY NODE NUMBER
C
          DO 42 I=1,NCOL
          NNRB(NRG,1,I)=NN(NROWS,I)
   42     NNRB(NRG,3,I)=NN(1,I)
          DO 43 I=1,NROWS
          NNRB(NRG,2,I)=NN(I,NCOL)
   43     NNRB(NRG,4,I)=NN(I,1)
C
C         OUTPUT OF THE REGION NODE NUMBER
C
          WRITE(IO,49)
   49     FORMAT(//1X,'REGION NODE NUMBER'/)
          DO 52 I=1,NROWS
   52     WRITE(IO,53)(NN(I,J),J=1,NCOL)
   53     FORMAT(1X,25I5)
C
C         DIVISION INTO TRIANGULAR ELEMENT
C
   105    WRITE(IO,55)
   55     FORMAT(//2X,'NEL  NODE NUMBERS',4X,4HX(1),3X,4HY(1),
      C   3X,4HX(2),3X,4HY(2),3X,4HX(3),3X,4HY(3),4X,4HCONV,
      C   4X,4HCOND,4X,4HTINF)
          K=1
          DO 54 I=1,NROWS
          DO 54 J=1,NCOL
          XE(K)=XC(I,J)
          YE(K)=YC(I,J)
          NE(K)=NN(I,J)
   54     K=K+1
          L=NROWS-1
          DO 15 I=1,L
```

```
      DO 15 J=2,NCOL
      DIAG1=SQRT((XC(I,J)-XC(I+1,J-1))**2+(YC(I,J)-
     C YC(I+1,J-1))**2)
      DIAG2=SQRT((XC(I+1,J)-XC(I,J-1))**2+(YC(I+1,J)-
     C YC(I,J-1))**2)
      NR(1)=NCOL*I+J-1
      NR(2)=NCOL*I+J
      NR(3)=NCOL*(I-1)+J
      NR(4)=NCOL*(I-1)+J-1
      DO 15 IJ=1,2
      NEL=NEL+1
      IF ((DIAG1/DIAG2).GT.1.02) GOTO 41
      J1=NR(1)
      J2=NR(IJ+1)
      J3=NR(IJ+2)
      GOTO 40
   41 J1=NR(IJ)
      J2=NR(IJ+1)
      J3=NR(4)
   40 LB(1)=IABS(NE(J1)-NE(J2))+1
      LB(2)=IABS(NE(J2)-NE(J3))+1
      LB(3)=IABS(NE(J1)-NE(J3))+1
      DO 107 IK=1,3
      IF (LB(IK).LE.NBW) GOTO107
      NBW=LB(IK)
      NELBW=NEL
  107  CONTINUE
      IF(YE(J3).GT.YMAX)THEN
       COND(NEL)=CK2
      ELSE IF(YE(J1).EQ.YMIN)THEN
            COND(NEL)=CK1
           ELSE IF(XE(J1).EQ.XXX.AND.YE(J3).LE.0.3490)THEN
                 COND(NEL)=CK1
                ELSE
                 COND(NEL)=CK
       END IF
C
C      NNN IS A NUMBER OF WHICH SIDE INVOLVED WITH
C      CONVECTRION
C
      IF (YE(J2).GT.YMAX)THEN
       H(NEL)=CONV1
       TINF(NEL)=TAMB1
       NNN(NEL)=2
      ELSE IF(YE(J2).EQ.YMIN)THEN
            H(NEL)=CONV2
            TINF(NEL)=TAMB2
            NNN(NEL)=1
           ELSE
            H(NEL)=0
            TINF(NEL)=0
            NNN(NEL)=0
```

```
      END IF
      WRITE(IO,301) NEL,NE(J1),NE(J2),NE(J3),
     C  XE(J1),YE(J1),
     C  XE(J2),YE(J2),XE(J3),YE(J3),H(NEL),COND(NEL),
     C  TINF(NEL)
301   FORMAT(1X,4I4,3X,6F7.3,1X,3F8.3)
      WRITE(IP,303) NEL,NE(J1),NE(J2),NE(J3),XE(J1),
     C  YE(J1),XE(J2),
     C  YE(J2),XE(J3),YE(J3),H(NEL),COND(NEL),
     C  TINF(NEL),NNN(NEL)
303   FORMAT(4I4,6F8.4,3F8.4,I2)
 15   CONTINUE
 16   CONTINUE
      WRITE(IO,51) NBW,NELBW
 51   FORMAT(///1X,'BANDWIDTH QUANTITY IS',I4,'CALCULATED

     C  IN',1X,'ELEMENT',I4)
      STOP
      END
```

1.2. HT

```
      PROGRAM HT(TAPE52,TAPE53,TAPE54,OUTPUT)
      DIMENSION NS(3),ESM(3,3),EF(3),X(3),Y(3),B(3),C(3)
      DIMENSION ISIDE(2),A(20000),PHI(3)
      COMMON/TLE/TITLE(20)
      REAL LG
C
      DATA IN/52/,ID/53/,IO/54/,NCL/1/,ID1/0/
      DATA NP/99/,NE/160/,NBW/25/
C
C  NP-NUMBER OF GLOBAL NODE, NE-NUMBER OF ELEMENTS, NBW-
C  BAND WIDTH
C
C  CALCULATION OF POINTERS AND INITIALIZATION OF THE COLUMN
C  VECTOR A
C
      JGF=NP*NCL
      JGSM=JGF*2
      JEND=JGSM+NP*NBW
      DO 13 I=1 ,JEND
 13   A(I)=0.0
C
C  OUTPUT OF TITLE
C
      WRITE(IO,4)
  4   FORMAT(1H1////1X,'HT FOR FISH HOLD WALL SECTIONS'//)
C***************
C  ASSMBLYING OF THE GLOBAL STIFFNESS MATRIX AND GLOBAL
C  FORCE MATRIX
C***************
C
C  INPUT AND ECHO PRINT OF ELEMENT DATA
C
      DO 7 KK=1,NE
      READ(IN,19)NEL,NS(1),NS(2),NS(3),X(1),Y(1),X(2),
     C Y(2),X(3),Y(3),H,COND,TINF,ISIDE(1)
 19   FORMAT(4I4,6F8.4,3F8.4,I2)
      WRITE(IO,23)NEL,NS(1),NS(2),NS(3),X(1),Y(1),X(2),
     C Y(2),X(3),Y(3),H,COND,TINF,ISIDE(1)
  23  FORMAT(4I4,6F8.4,3F8.4,I2)
C
C  CALCULATION OF CONDUCTITVITY MATRIX
C
      B(1)=Y(2)-Y(3)
      B(2)=Y(3)-Y(1)
      B(3)=Y(1)-Y(2)
      C(1)=X(3)-X(2)
      C(2)=X(1)-X(3)
      C(3)=X(2)-X(1)
```

```
      AR4=(X(2)*Y(3)+X(3)*Y(1)+X(1)*Y(2)-X(2)*Y(1)
     C      -X(3)*Y(2)-X(1)*Y(3))*2.
      DO 5 I=1,3
      EF(I)=0.0
      DO 5 J=1,3
    5 ESM(I,J)=(COND*B(I)*B(J)+COND*C(I)*C(J))/AR4
C
C  CALCULATION OF THE CONVECTION RELATED QUANTITIES
C
      DO 10 I=1,2
      IF(ISIDE(I).LE.0) GOTO 8
      J=ISIDE(I)
      WRITE(IO,12)J,NEL
   12 FORMAT(1X,20HCONVECTION FROM SIDE,I2,11H OF
     C ELEMENT,I4)
      K=J+1
      IF(J.EQ.3) K=1
      LG=SQRT((X(K)-X(J))**2+(Y(K)-Y(J))**2)
      HL=H*LG
      EF(J)=EF(J)+HL*TINF/2
      EF(K)=EF(K)+HL*TINF/2
      ESM(J,J)=ESM(J,J)+HL/3
      ESM(J,K)=ESM(J,K)+HL/6
      ESM(K,J)=ESM(J,K)
   10 ESM(K,K)=ESM(K,K)+HL/3
C
C  INSERTION OF THE ELEMENT PROPERTIES INTO THE GLOBAL
C  STIFFNESS MATRIX
C
    8 DO 17 I=1,3
      II=NS(I)
      DO 15 J=1,NCL
      J5=(NCL+J-1)*NP+II
   15 A(J5)=A(J5)+EF(I)
      DO 17 J=1,3
      JJ=NS(J)
      JJ=JJ-II+1
      IF(JJ)17,17,16
   16 J5=JGSM+(JJ-1)*NP+II
      A(J5)=A(J5)+ESM(I,J)
   17 CONTINUE
    7 CONTINUE
      CALL BDYVAL(A(JGSM+1),A(JGF+1),NP,NBW,NCL)
      CALL DCMPBD(A(JGSM+1),NP,NBW)
      CALL SLVBD(A(JGSM+1),A(JGF+1),A(1),NP,NBW,NCL,ID1)
C***************
C  CALCULATION OF THE ELEMENT RESULTS
C***************
C
C  INPUT OF THE ELEMENT DATA
C
      REWIND(UNIT=52)
```

```
      DO 86 KK=1,NE
      READ(IN,21)NEL,NS(1),NS(2),NS(3),X(1),Y(1),X(2),Y(2),
     C     X(3),Y(3),H,COND,TINF,ISIDE(1)
 21   FORMAT(4I4,6F8.4,3F8.4,I2)
      IF(NEL.LT.0)     STOP
      IF(KK.GT.1) GOTO 50
      WRITE(IO,80)
 80   FORMAT(1H1,//////1X,'ELEMENT RESULTS'//6X,'ELEMENT',
     C 1X,'         GRAD(X)          GRAD(Y)          AVG

     C TEMP')
C
C  RETRIEVAL OF THE NODAL VALES FOR THE ELEMENT
C            CALCULATION OF THE AVERAGE TEMPERATURE
C
 50   J1=JGSM+NEL
      A(J1)=0.0
C
      DO 20 I=1,3
      II=NS(I)
      PHI(I)=A(II)
 20   A(J1)=A(J1)+PHI(I)/3
C
C  CALCULATION AND OUTPUT OF THE TEMPERATURE GRADIENTS
C
      B(1)=Y(2)-Y(3)
      B(2)=Y(3)-Y(1)
      B(3)=Y(1)-Y(2)
      C(1)=X(3)-X(2)
      C(2)=X(1)-X(3)
      C(3)=X(2)-X(1)
      AR2=(X(2)*Y(3)+X(3)*Y(1)+X(1)*Y(2)-X(2)*Y(1)-X(3)
     C     *Y(2)-X(1)*Y(3))
 52   GRADX=0.0
      GRADY=0.0
      DO 29 I=1,3
      GRADX=GRADX+B(I)*PHI(I)/AR2
 29   GRADY=GRADY+C(I)*PHI(I)/AR2
 86   WRITE(IO,85)NEL,GRADX,GRADY,A(J1)
 85   FORMAT(8X,I3,4(5X,E12.5))
      IF(IPCH.EQ.0) STOP
      J2=JGSM+1
      STOP
      END
C***************
C     BDYVAL
C***************
      SUBROUTINE BDYVAL(GSM,GF,NP,NBW,NCL)
      DIMENSION GSM(NP,NBW),GF(NP,NCL),IB(6),BV(6)
      COMMON/TLE/TITLE(20)
      DATA IN/52/,IO/54/
C  INPUT OF THE NODAL FORCE VALUES
```

```
C
      WRITE(IO,201)
  201 FORMAT(/1X,15HBOUNDARY VALUES//1X,12HNODAL FORCES)
      DO 216 JM=1,NCL
      ID1=0
      INK=0
  202 DO 288 IJ=1,6
      IB(IJ)=0
      BV(IJ)=0
 288  CONTINUE
      ID=0
      DO 204 L=1,6
      IF(IB(L).LE.0) GOTO 205
      ID=ID+1
      I=IB(L)
  204 GF(I,JM)=BV(L)+GF(I,JM)
      GOTO 206
  205 INK=1
      IF(ID.EQ.0) GOTO 216
  206 IF(ID1.EQ.1) GOTO 222
      WRITE(IO,217)JM
  217 FORMAT(1X,12HLOADING CASE,I2)
  222 WRITE(IO,207)(IB(L),BV(L),L=1,ID)
  207 FORMAT(1X,6(I3,E14.5,2X))
      IF(INK.EQ.1) GOTO 216
      ID1=1
      GOTO 202
C
C  INPUT OF THE PRESCRIBED NODAL VALUES
C
  216 CONTINUE
      WRITE(IO,208)
  208 FORMAT(////,1X,'PRESCRIBED NODAL VALUES')
      INK=0
  209 DO 299 IK=1,6
      IB(IK)=0
      BV(IK)=0
 299  CONTINUE
      ID=0
      DO 221 L=1,6
      IF(IB(L).LE.0) GOTO 215
      ID=ID+1
      I=IB(L)
      BC=BV(L)
C
C  MODIFICATION OF THE GLOBAL STIFFNESS MATRIX AND THE
C          GOLBAL FORCE MATRIX USING THE METHOD OF DELETION
C          OF ROWS AND COLUMNS
C
      K=I-1
      DO 211 J=2,NBW
      M=I+J-1
```

```
      IF(M.GT.NP) GOTO 210
      DO 218 JM=1,NCL
218   GF(M,JM)=GF(M,JM)-GSM(I,J)*BC
      GSM(I,J)=0.0
210   IF(K.LE.0) GOTO 211
      DO 219 JM=1,NCL
219   GF(K,JM)=GF(K,JM)-GSM(K,J)*BC
      GSM(K,J)=0.0
      K=K-1
211   CONTINUE
212   IF(GSM(I,1).LT.0.05) GSM(I,1)=500000.
      DO 220 JM=1,NCL
220   GF(I,JM)=GSM(I,1)*BC
221   CONTINUE
      GOTO 214
C
C  OUTPUT OF THE BOUNDARY VALUES,(BV)
C
215   INK=1
      IF(ID.EQ.0) RETURN
214   WRITE(IO,207)(IB(L),BV(L),L=1,ID)
      IF(INK.EQ.1)RETURN
      GOTO 209
      END
C
C
C****************
C  DCMPBD
C***************
C
      SUBROUTINE DCMPBD(GSM,NP,NBW)
      DIMENSION GSM(NP,NBW)
      IO=54
      NP1=NP-1
      DO 226 I=1,NP1
      MJ=I+NBW-1
      IF(MJ.GT.NP)MJ=NP
      NJ=I+1
      MK=NBW
      IF((NP-I+1).LT.NBW)MK=NP-I+1
      ND=0
      DO 225 J=NJ,MJ
      MK=MK-1
      ND=ND+1
      NL=ND+1
      DO 225 K=1,MK
      NK=ND+K
225   GSM(J,K)=GSM(J,K)-GSM(I,NL)*GSM(I,NK)/GSM(I,1)
226   CONTINUE
      RETURN
      END
C
```

```
C
C***************
C  SLVBD
C***************
C
      SUBROUTINE SLVBD(GSM,GF,X,NP,NBW,NCL,ID)
      DIMENSION GSM(NP,NBW),GF(NP,NCL),X(NP,NCL)
      IO=54
      NP1=NP-1
      DO 265 KK=1,NCL
      JM=KK
C
C  DECOMPOSITION OF THE COLUMN VECTOR GF()
C
      DO 250 I=1,NP1
      MJ=I+NBW-1
      IF(MJ.GT.NP) MJ=NP
      NJ=I+1
      NJ=I+1
      L=1
      DO 250 J=NJ,MJ
      L=L+1
250   GF(J,KK)=GF(J,KK)-GSM(I,L)*GF(I,KK)/GSM(I,1)
C
C  BACKWARD SUBSTITUTION FOR DETERMINATION OF X( )
C
      X(NP,KK)=GF(NP,KK)/GSM(NP,1)
      DO 252 K=1,NP1
      I=NP-K
      MJ=NBW
      IF((I+NBW-1).GT.NP)MJ=NP-I+1
      SUM=0.0
      DO 251 J=2,MJ
      N=I+J-1
251   SUM=SUM+GSM(I,J)*X(N,KK)
252   X(I,KK)=(GF(I,KK)-SUM)/GSM(I,1)
C
C  OUTPUT OF THE CALCULATION NODAL VALUES
C
      IF(ID.EQ.1) GOTO 265
      WRITE(IO,260)KK
260   FORMAT(1H1,//////1X,26HNODAL VALUES, LOADING

     C  CASE,I2)
      WRITE(IO,254)(I,X(I,KK),I=1,NP)
254   FORMAT(1X,I3,E14.5,3X,I3,E14.5,3X,I3,E14.5,3X,I3,
     C       E14.5,3X,I3,E14.5)
265   CONTINUE
      RETURN
      END
```

APPENDIX 2 LISTING OF THE FINITE DIFFERENCE PROGRAM

```
      PROGRAM FD
C*************************************************************
C     THIS IS A PROGRAM USING FINITE DIFFERENCES METHOD TO
C     MODEL STEADY-STATE HEAT TRANSFER OF FISH HOLD WALL
C     SECTIONS.  IT DEALS WITH VARIOUS DX AND DY VALUES
C     IN TWO DIMENSIONS, AND VARIOUS THERMAL PROPERTIES
C     OF STEEL, PLYWOOD AND FOAM INSULATION.  TEMPERATURE
C     DISTRIBUTION IS COMPUTED BY USING GAUSS-SEIDEL
C     ITERATION.  ALL UNITS ARE IN S.I. SYSTEM.
C     IN ADDITION TO THE EXPLANATION IN THE PROGRAM,
C     OTHER VARIABLES ARE DEFINED AS:
C        H1,H2: CONVECTIVE COEFFICENTS OF COLD AND WARM
C               SURFACES.  THEY ARE NEEDED WHEN CONVECTION
C               CONDITIONS ARE KNOWN SO THAT PANEL
C               TRANSMITTANCE CAN BE CALCULATED.  OTHERWISE,
C               THEY CAN BE CHOSEN ARBITRARILY AND THEY WILL
C               NOT INFLUENCE THE CALCULATION OF PANEL
C               RESISTANCE.
C        TBS,TTS: TEMPERATURES AT COLD AND WARM SURFACES.
C        K1: MILD STEEL CONDUCTIVITY, 42.9 W/mK.
C        K2: PLYWOOD CONDUCTIVITY, 0.1155 W/mK.
C        K3: URETHANE FOAM CONDUCTIVITY, 0.023 W/mK.
C        RC: CONTACT RESISTANCE, 5.17 K/W (METAL-TO-PLYWOOD)
C                                0 K/W (METAL-TO-METAL)
C        EPS: CONVERGENCE CRITERIA, 0.001
C*************************************************************
      DIMENSION T(19,20),DX(19),DY(20),K(19,20),A(19,20,4)
      DIMENSION TBS(19),TTS(19)
      REAL K1,K2,K3,K4,H1,H2,K
      WRITE(*,100)
 100  FORMAT(/1X,'THE CALCULATION RESULTS'//)
C     INPUT DATA
C     M AND N ARE MAX. NODE NUMBERS IN X AND Y DIRECTION
      M=19
      WRITE(*,11)
  11  FORMAT('ENTER N')
      READ(*,*)N
C     XL IS OVERALL LENGTH
      WRITE(*,12)
 12   FORMAT('  ENTER XL  ')
      READ(*,*)XL
C     INPUT DIFFERENT SPACE INTERVAL IN X AND Y DIRECTIONS
      WRITE(*,13)
 13   FORMAT('  ENTER DX1, DX2, DX3  ')
      READ(*,*)DX1,DX2,DX3
      WRITE(*,14)
 14   FORMAT( '   ENTER DY1, DY2, DY3')
      READ(*,*)DY1,DY2,DY3
C     INPUT DIFFERENT THERMAL PROPERTIES FOR DIFFERENT
```

```
C   MATERIALS
        WRITE(*,15)
C       K4 IS URETHANE BOARD CONDUCTIVITY ONLY FOR
C       CALCULATING TEST PANELS, SET K4=K3 FOR PREDICTION.
 15     FORMAT('ENTER K1,K2,K3,K4')
        READ(*,*)K1,K2,K3,K4
        H1=5.6215
        H2=6.3029
C       RC IS CONTACT RESISTANCE
        WRITE(*,16)
 16     FORMAT(' ENTER RC ')
        READ(*,*)RC
C       SET COLD AND WARM AIR TEMPERATURES, INITIAL GUESS
C       TEMPERATURE,
C       CRITERIA VALUE FOR ITERATION AND HEAT BALANCE CHECK
        TTB=-16.4444
        TBB=15.4444
        TIN=0.0
        EPS=0.001
        QMAX=0.5
C       SET DX AND DY FOR NODES
        DO 1 I=1,M
        IF(I.EQ.7.OR.I.EQ.13)THEN
        DX(I)=DX2
        ELSEIF(I.GE.8.AND.I.LE.12)THEN
        DX(I)=DX1
        ELSE
        DX(I)=DX3
        ENDIF
 1      CONTINUE
        DO 2 J=1,N
        IF(J.GE.5.AND.J.LE.9)THEN
        DY(J)=DY2
        ELSEIF(J.GE.14.AND.J.LE.16)THEN
        DY(J)=DY3
        ELSE
        DY(J)=DY1
        ENDIF
 2      CONTINUE
C       SET CONDUCTIVITY (K) VALUES FOR DIFFERENT MATERIALS
        DO 3 I=1,M
        DO 3 J=1,N
        IF(J.EQ.2)THEN
        K(I,J)=K1
        ELSEIF(J.GE.12.AND.J.LE.17)THEN
        K(I,J)=K4
        ELSEIF(J.GE.18)THEN
        K(I,J)=K2
        ELSEIF(I.EQ.10.AND.J.LE.11)THEN
        K(I,J)=K1
        ELSE
        K(I,J)=K3
```

```
      ENDIF
 3    CONTINUE
C     ASSIGN INTERNODE CONDUCTANCE
      DO 4 I=2,M-1
      DO 4 J=2,N-1
      R1=0.5*DX(I)/(K(I,J)*DY(J))
      R2=0.5*DX(I-1)/(K(I-1,J)*DY(J))
      A(I,J,1)=1/(R1+R2)
      R1=0.5*DX(I)/(K(I,J)*DY(J))
      R2=0.5*DX(I+1)/(K(I+1,J)*DY(J))
      A(I,J,2)=1/(R1+R2)
      R1=0.5*DY(J)/(K(I,J)*DX(I))
      IF(J.EQ.2)THEN
      R2=1/(H1*DX(I))
      ELSE
      R2=0.5*DY(J-1)/(K(I,J-1)*DX(I))
      ENDIF
      IF(I.EQ.10.AND.J.EQ.12)THEN
      A(I,J,3)=1/(R1+R2+RC)
      ELSE
      A(I,J,3)=1/(R1+R2)
      ENDIF
      R1=0.5*DY(J)/(K(I,J)*DX(I))
      IF(J.EQ.N-1)THEN
      R2=1/(H2*DX(I))
      ELSE
      R2=0.5*DY(J+1)/(K(I,J+1)*DX(I))
      ENDIF
      IF(I.EQ.10.AND.J.EQ.11)THEN
      A(I,J,4)=1/(R1+R2+RC)
      ELSE
      A(I,J,4)=1/(R1+R2)
      ENDIF
 4    CONTINUE
C     ASSIGN INITIAL GUESS AND CONVECTIVE BOUNDARY
C     TEMPERATURES
      DO 5 I=1,M
      DO 5 J=1,N
      IF(J.EQ.1)THEN
      T(I,J)=TBB
      ELSEIF(J.EQ.N)THEN
      T(I,J)=TTB
      ELSE
      T(I,J)=TIN
      ENDIF
 5    CONTINUE
C     EPS IS CRITERIA VALUE FOR CONVERGENE
 6    SEPS=0.0
      TCHECK=T(10,10)
C     START ITERATION
 50   DO 80 I=2,M-1
      DO 80 J=2,N-1
```

```
      B=A(I,J,1)+A(I,J,2)+A(I,J,3)+A(I,J,4)
      C1=A(I,J,1)/B
      C2=A(I,J,2)/B
      C3=A(I,J,3)/B
      C4=A(I,J,4)/B
      TEMP=T(I,J)
      T1=C1*T(I-1,J)+C2*T(I+1,J)+C3*T(I,J-1)+C4*T(I,J+1)
      T(I,J)=T(I,J)+1.6*(T1-T(I,J))
C     SET LHS AND RHS ADIABATIC BOUNDARIES
      T(M-1,J)=T(2,J)
         T(1,J)=T(2,J)
      T(M,J)=T(M-1,J)
      SEPS=SEPS+ABS(TEMP-T(I,J))
 80   CONTINUE
      SEPS=SEPS/((M-2)*(N-2))
      IF(SEPS.GE.EPS)THEN
      GOTO 6
      ELSE
C     CHECK HEAT FLOW BALANCE
      QQ1=0.0
      QQ2=0.0
      DO 7 I=2,M-1
      X=K(I,2)/(0.5*DY(2))
      Y=K(I,N-1)/(0.5*DY(N-1))
      TBS(I)=X*T(I,2)/(X+H1)+H1*TBB/(X+H1)
      TTS(I)=Y*T(I,N-1)/(Y+H2)+H2*TTB/(Y+H2)
      IF(I.EQ.2.OR.I.EQ.M-1)THEN
      Q1=0.5*H1*DX(I)*(TBB-TBS(I))
      Q2=0.5*H2*DX(I)*(TTS(I)-TTB)
      ELSE
      Q1=H1*DX(I)*(TBB-TBS(I))
      Q2=H2*DX(I)*(TTS(I)-TTB)
      ENDIF
      QQ1=QQ1+Q1
      QQ2=QQ2+Q2
  7   CONTINUE
      DQ=ABS(QQ1-QQ2)
      IF(DQ.GE.QMAX)THEN
      GOTO 6
      ELSE
      ENDIF
 140  WRITE(*,200)SEPS
      ENDIF
 200  FORMAT(/1X,'CRITERIA=',F7.6/)
      QQ=(QQ1+QQ2)/2
      QQ=QQ1/XL
C     CALCULATE WARM SURFACE AVERAGE TEMPERATURE
      TW=TBB-QQ/H1
C     CALCULATE COLD SURFACE AVERAGE TEMPERATURE
      TC=TTB+QQ/H2
C     CALCULATE THERMAL TRANSMITTANCE (U VALUE)
      U=QQ/(TBB-TTB)
```

```
C       CALCULATE PANEL CONDUCTANCE (C VALUE)
        C=QQ/(TW-TC)
C       CALCULATE PANEL RESISTANCE (R VALUE)
        R=1/C
        WRITE(*,210)
 210    FORMAT(1X,'TEMPERATURE DISTRIBUTION'/)
        WRITE(*,300)((T(I,J),I=2,M-1),J=1,N)
        WRITE(*,220)
 220    FORMAT(1X,'COLD SURFACE TEMPERATURES'/)
        WRITE(*,300)(TTS(I),I=2,M-1)
        WRITE(*,240)
 240    FORMAT(1X,'WARM SURFACE TEMPERATURES'/)
        WRITE(*,300)(TBS(I),I=2,M-1)
        WRITE(*,8)QQ
  300   FORMAT(1X,7F11.4,/3X,7F11.4,/3X,3F11.4)
  8     FORMAT(1X,'HEAT FLUX=',F9.6,1X,'W/M^2'/)
        WRITE(*,230)TW
 230    FORMAT(1X,'AVERAGE WARM SURFACE
     C          TEMP.=',F8.4,1X,'C'/)
        WRITE(*,250)TC
 250    FORMAT(1X,'AVERAGE COLD SURFACE
     C          TEMP.=',F8.4,1X,'C'/)
        WRITE(*,260)U
 260    FORMAT(1X,'THERMAL TRANSMITTANCE,
     C          U=',F6.4,1X,'W/M^2-K'/)
        WRITE(*,270)C
 270    FORMAT(1X,'PANEL CONDUCTANCE, C=',F6.4,1X,'W/M^2-
     C          K'/)
        WRITE(*,280)R
 280    FORMAT(1X,'PANEL RESISTANCE, R=',F6.4,1X,'M^2-
     C          K/W'/)
        STOP
        END
```

APPENDIX 3 CALCULATING EQUATIONS GIVEN BY ASTM FOR "GUARDED HOT BOX" TECHNIQUE (4)

$U=q/A(t_h-t_c)$

$C=q/A(t_1-t_2)$

$R=(t_1-t_2)A/q$

$R_u=(t_h-t_c)A/q=r_c+R+r_h$

$r_h=(t_2-t_c)A/q$

$r_c=(t_2-t_c)A/q$

$h_h=q/A(t_h-t_1)$

$h_c=q/A(t_2-t_c)$

$k=qL/A(t_1-t_2)$

Where,

k=thermal conductivity, W/(m K),

C=thermal conductance, W/(m^2 K),

h=surface conductance, W/(m^2 K),

U=thermal transmittance, W/(m^2 K),

q=heat flux (time rate of heat flow through area A), W/m^2,

Q=time rate of heat flow, total input to the metering box, W,

A=area normal to heat flow, m^2,

L=length of path of heat flow (thickness of specimen), m,

r=surface resistance, m^2K/W,

R=thermal resistance, m^2K/W,

R_u=overall thermal resistance, m^2K/W,

t_h=average temperature of air 75 mm or more from the hot surface, K,

t_1=area weighted average temperature of hot surface, K,

t_2=area weighted average temperature of cold surface,K,

t_c=average temperature of air 75 mm from or more from cold surface, K.

APPENDIX 4 EXPERIMENTAL DATA

Temperatures measured during "Guarded Hot Box" tests are reported in the following pages. For Tests 1, 2, 3, 6 and 7, there are three figures for each test describing thermocouple locations and measured values for internal, cold surface, and warm surface, respectively. For Tests 4, 5 and 8, there are only two figures for each test since the internal thermocouples were removed with insulation materials. These two figures describe the thermocouple locations and measured temperatures for cold and warm surface, respectively. All of these figures are identical to those received from Dynatherm Engineering laboratory except that units have been converted into SI system.

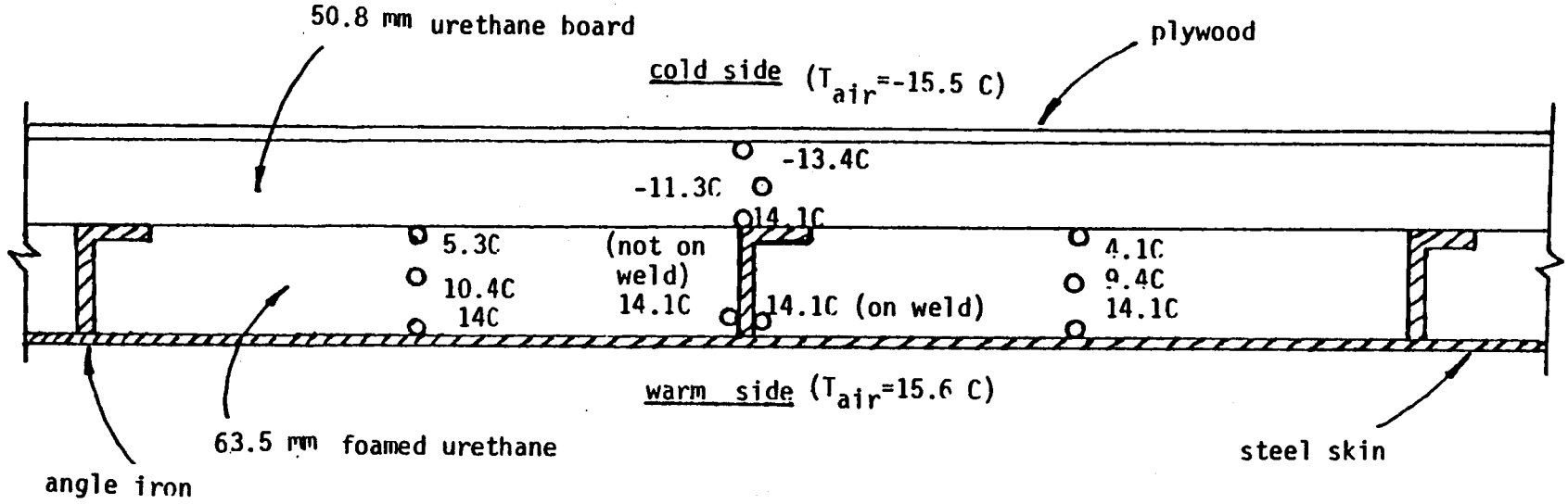

Fig. 1
INTERNAL TEMPERATURES AND THERMOCOUPLE LOCATIONS
Panel 1 Tested as Submitted

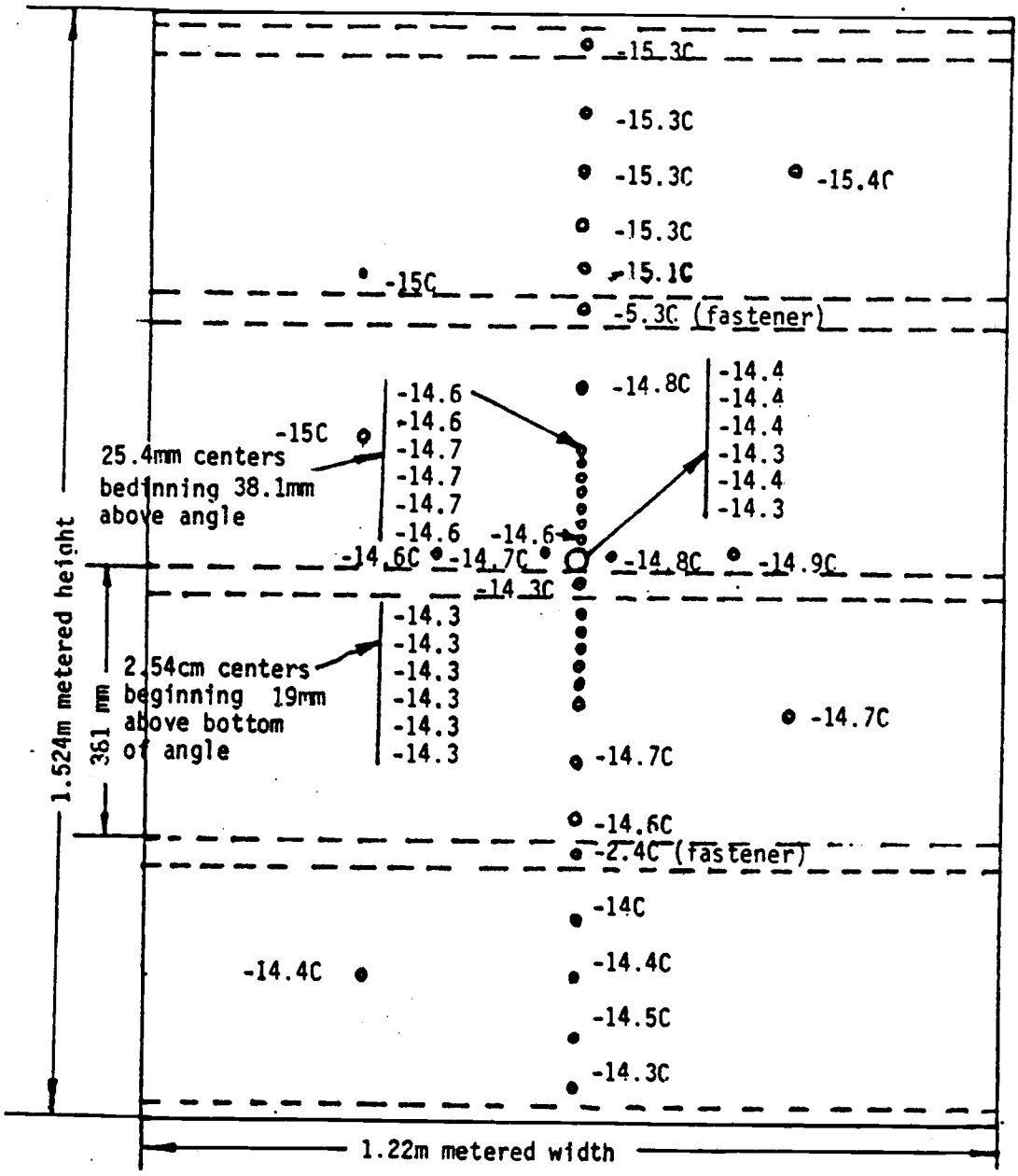

Fig. 2
COLD SURFACE TEMPERATURES AND THERMOCOUPLE LOCATIONS
Panel 1 Tested as Submitted

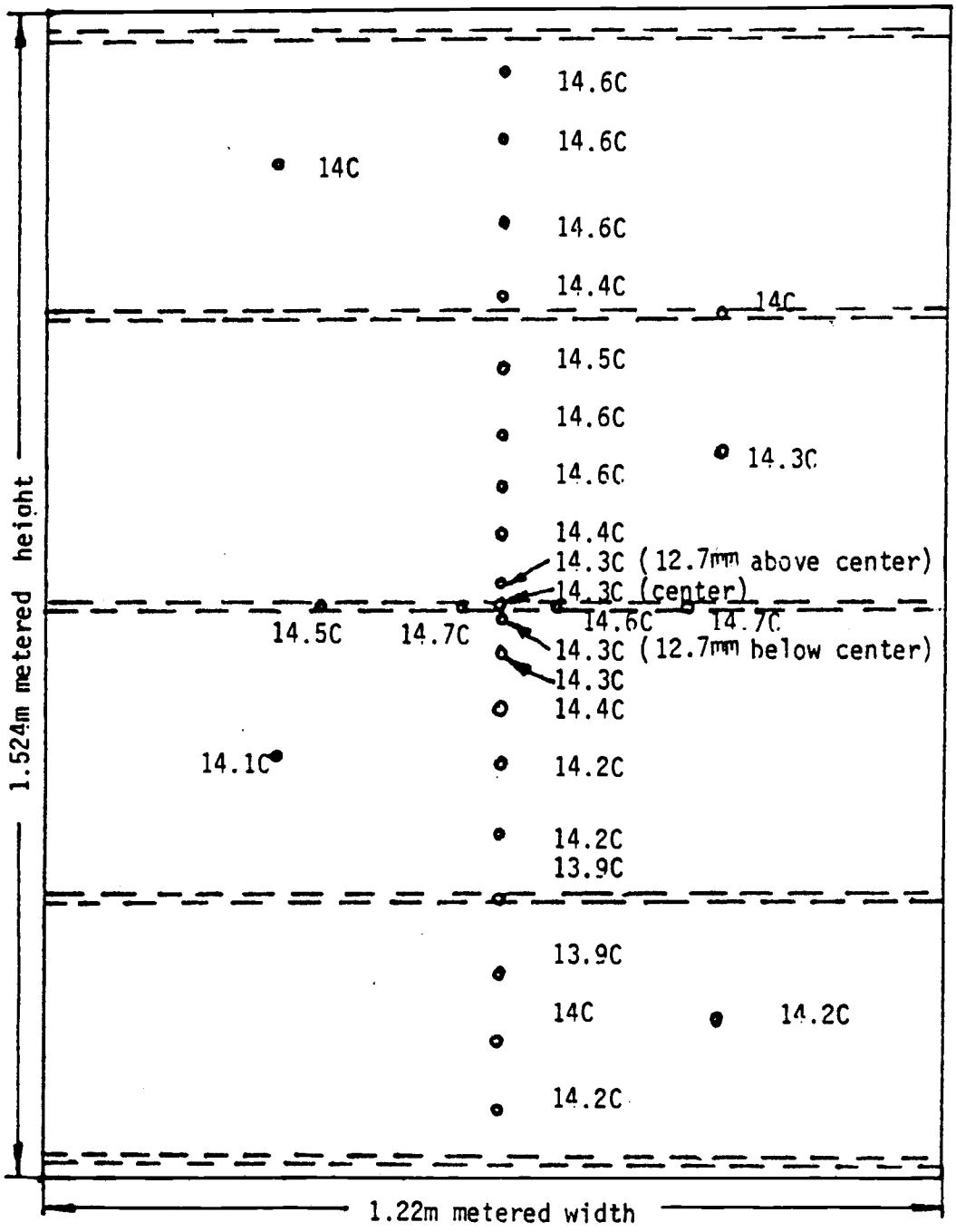

Fig.3
WARM SURFACE TEMPERATURES AND THERMOCOUPLE LOCATIONS
Panel 1 Tested as Submitted

Note: Thermocouples #4 and #5 were taped to the cold side surface of the foamed urethane. Thermocouples #3 and #9 were placed slightly under the cold side surface of the urethane and thus provided warmer temperature readings.

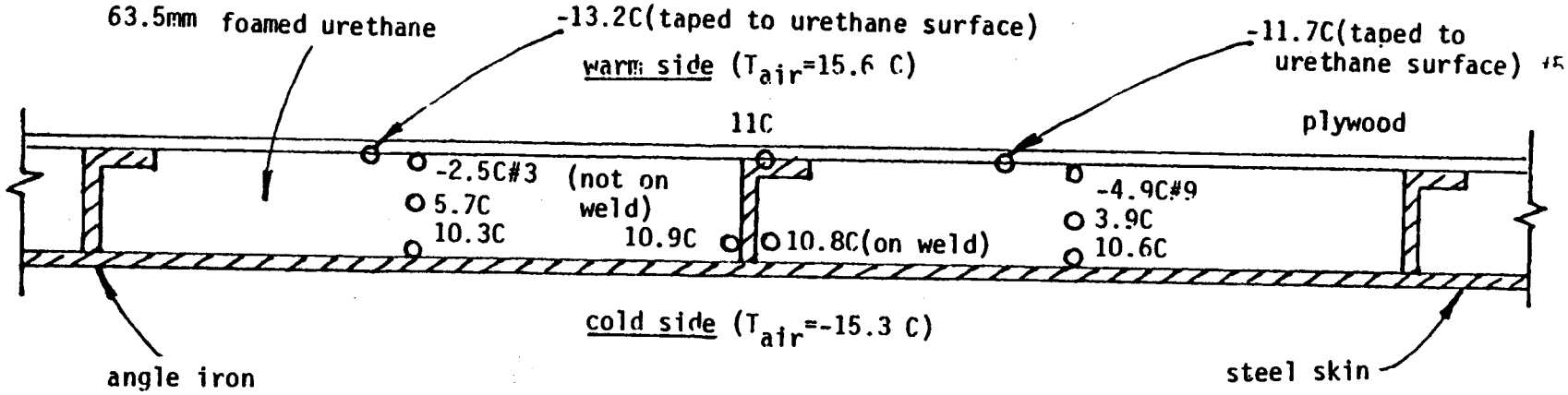

Fig.4
INTERNAL TEMPERATURES AND THERMOCOUPLE LOCATIONS
Panel 2: Plywood Secured to Cold Side of Angle Iron

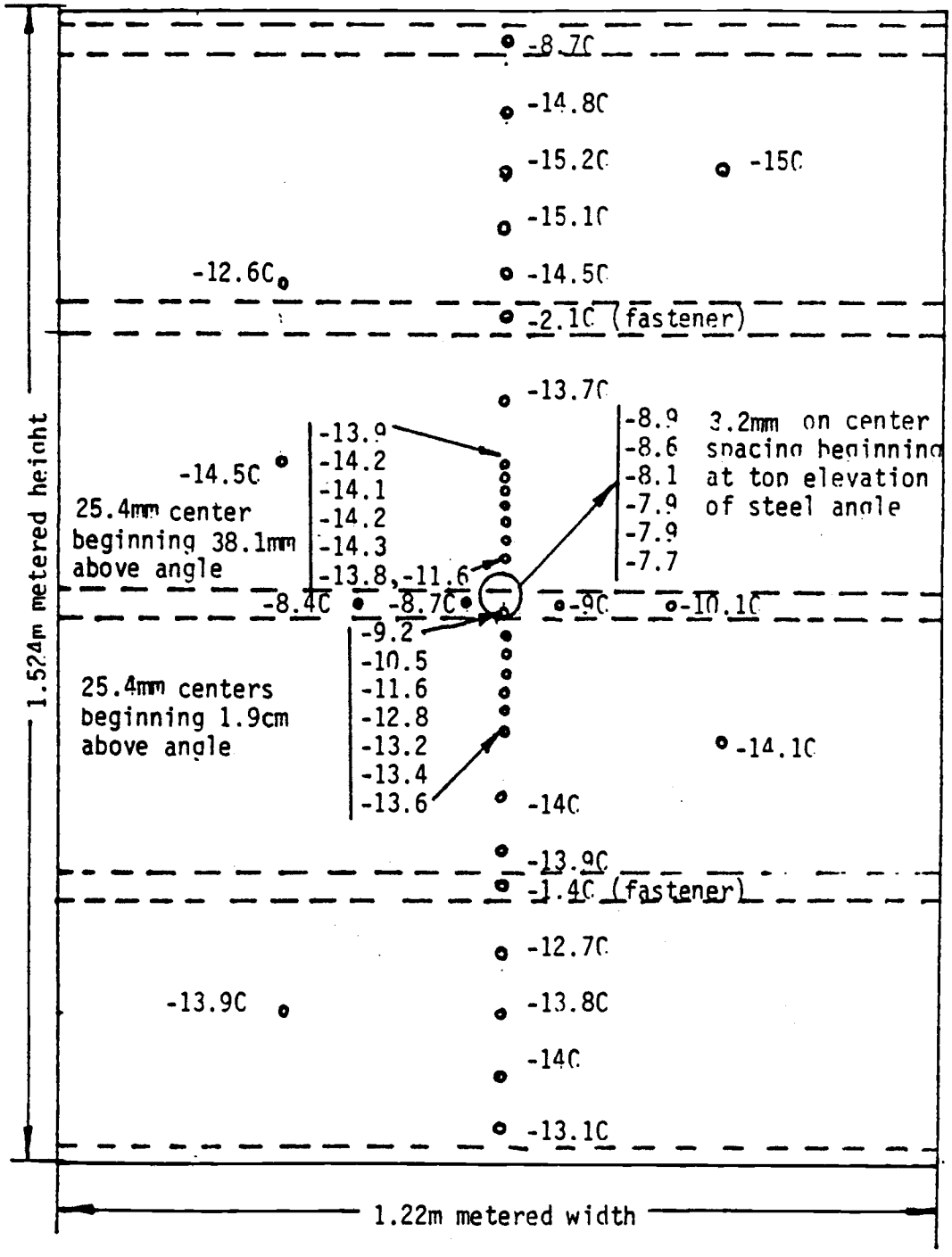

Fig.5
COLD SURFACE TEMPERATURES AND THERMOCOUPLE LOCATIONS
Panel 2: 50.8mm board insulation removed, plywood installed directly to angle iron, 63.5mm foamed urthane in place

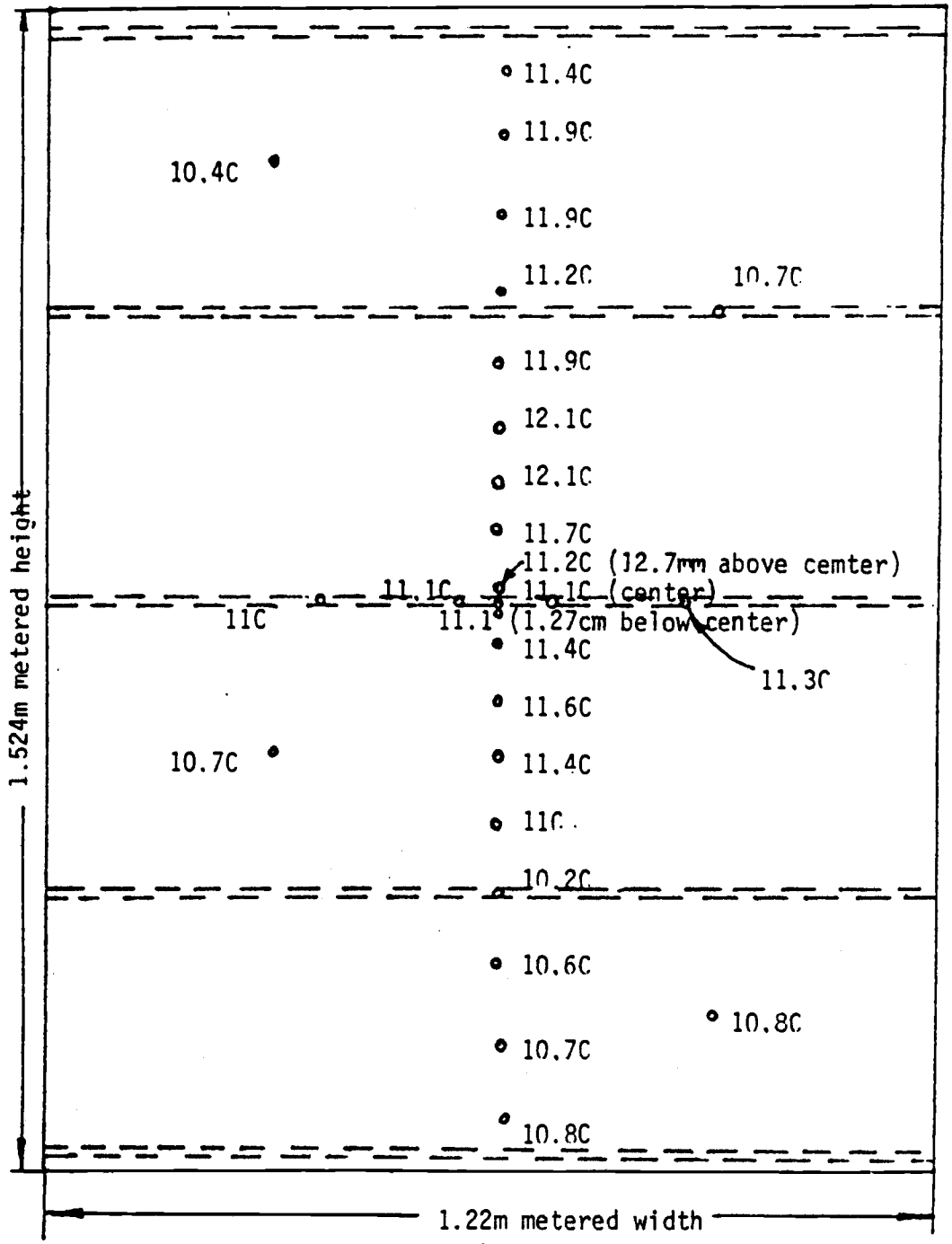

Fig.6
COLD SURFACE TEMPERATURES AND THERMOCOUPLE LOCATION
Panel 2: 50.8mm board insulation removed, plywood installed directly to angle iron, 63.5mm foamed urethane in place

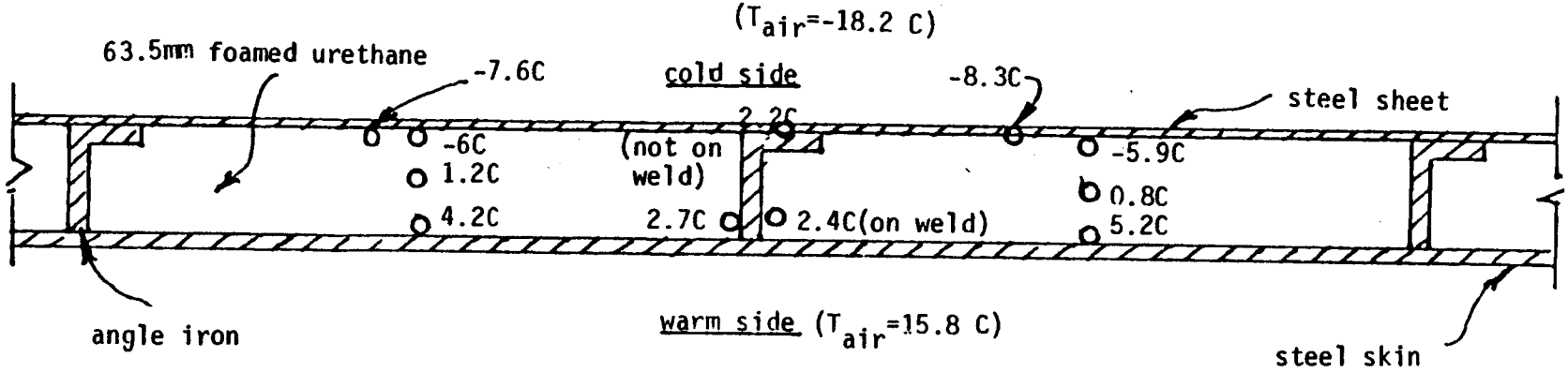

Fig.7
INTERNAL TEMPERATURES AND THERMOCOUPLE LOCATIONS
Panel 3: steel sheet secured to cold side of angle irons

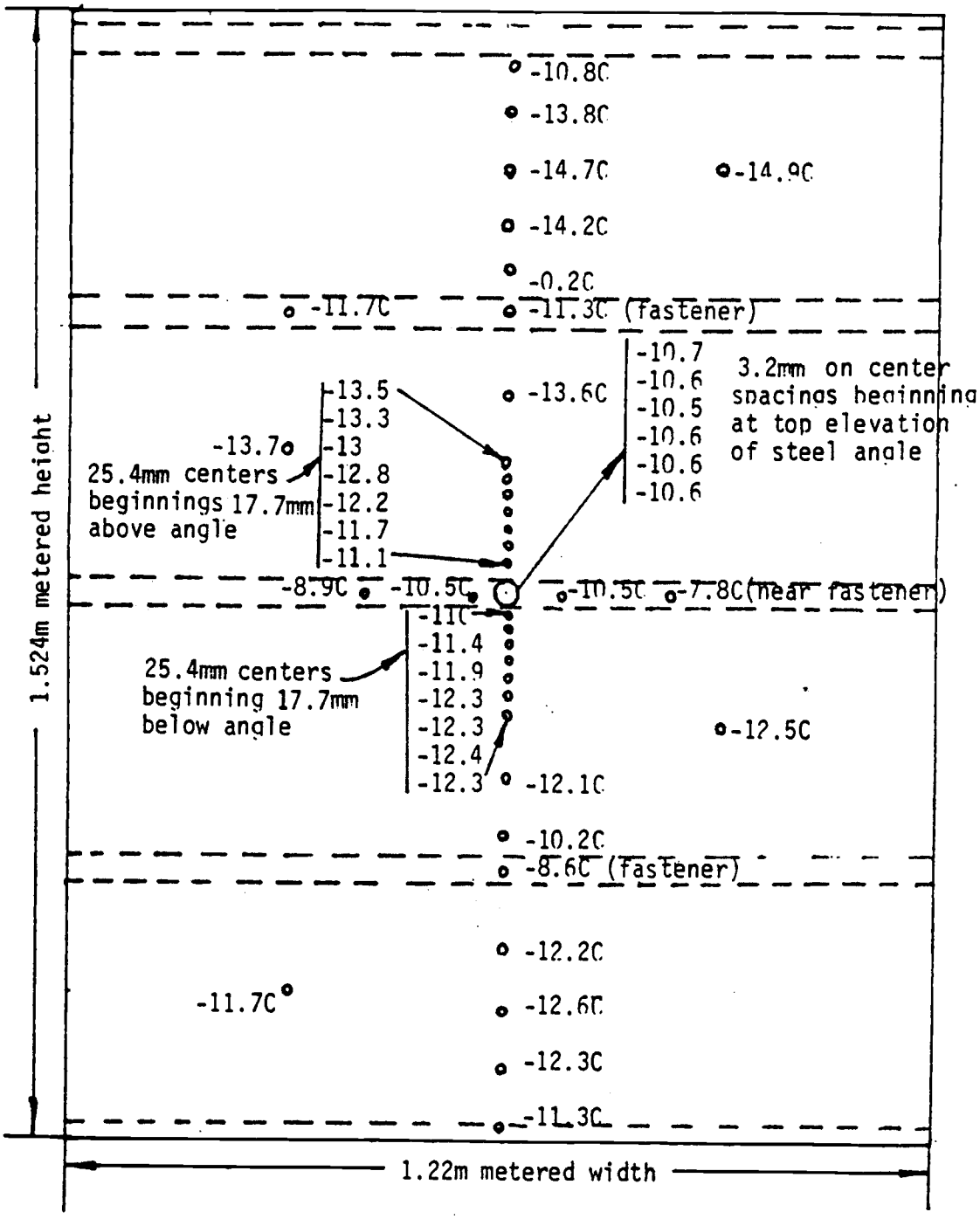

Fig.8
COLD SURFACE TEMPERATURES AND THERMOCOUPLE LOCATIONS
Panel 3: 50.8mm board insulation removed, steel sheet installed directly to angle iron, 63.5mm foamed urethane in place

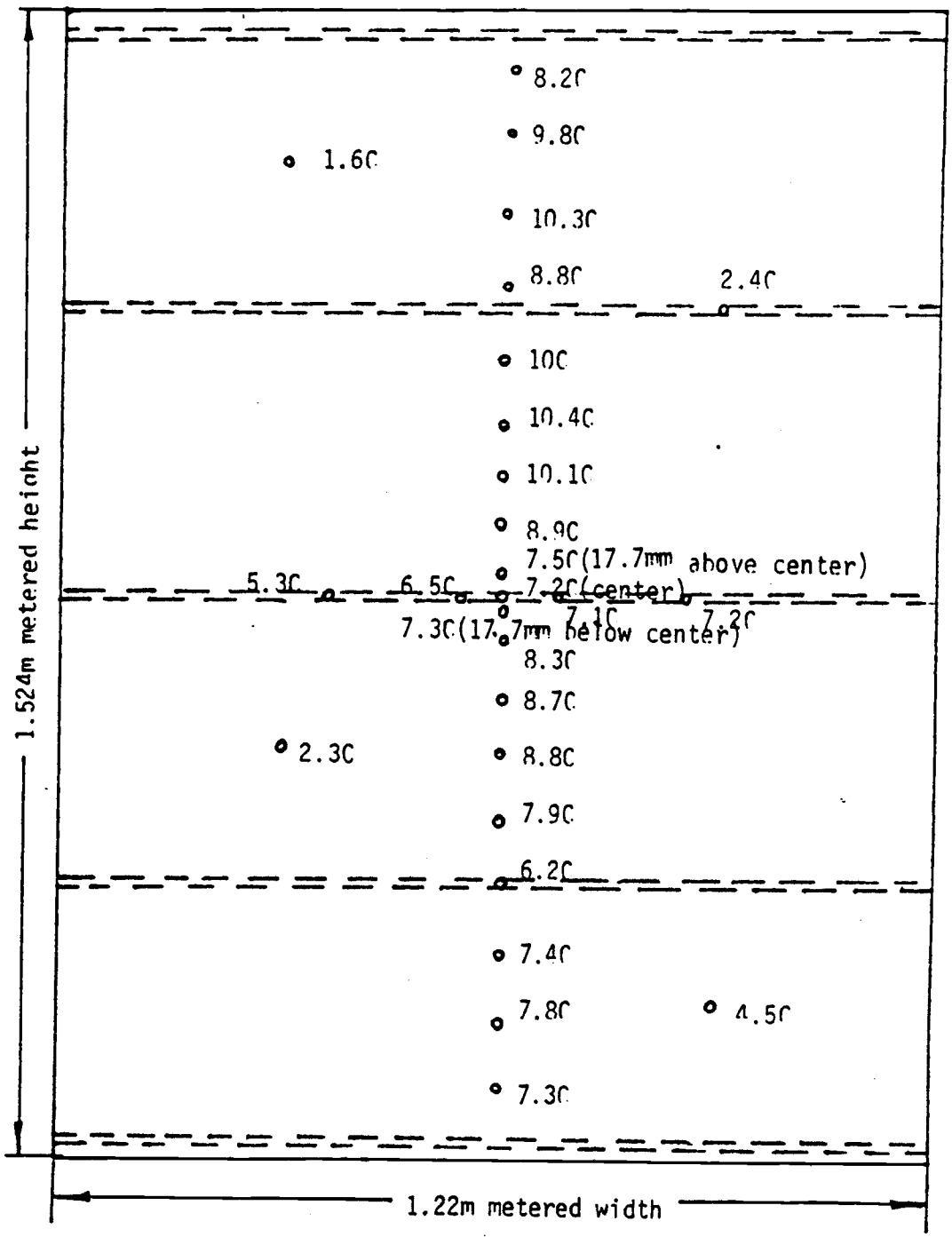

Fig.9
WARM SURFACE TEMPERATURES AND THERMOCOUPLE LOCATIONS
Panel 3: 50.8mm board insulation removed, steel sheet installed directly to angle iron, 63.5mm foamed urethane in place

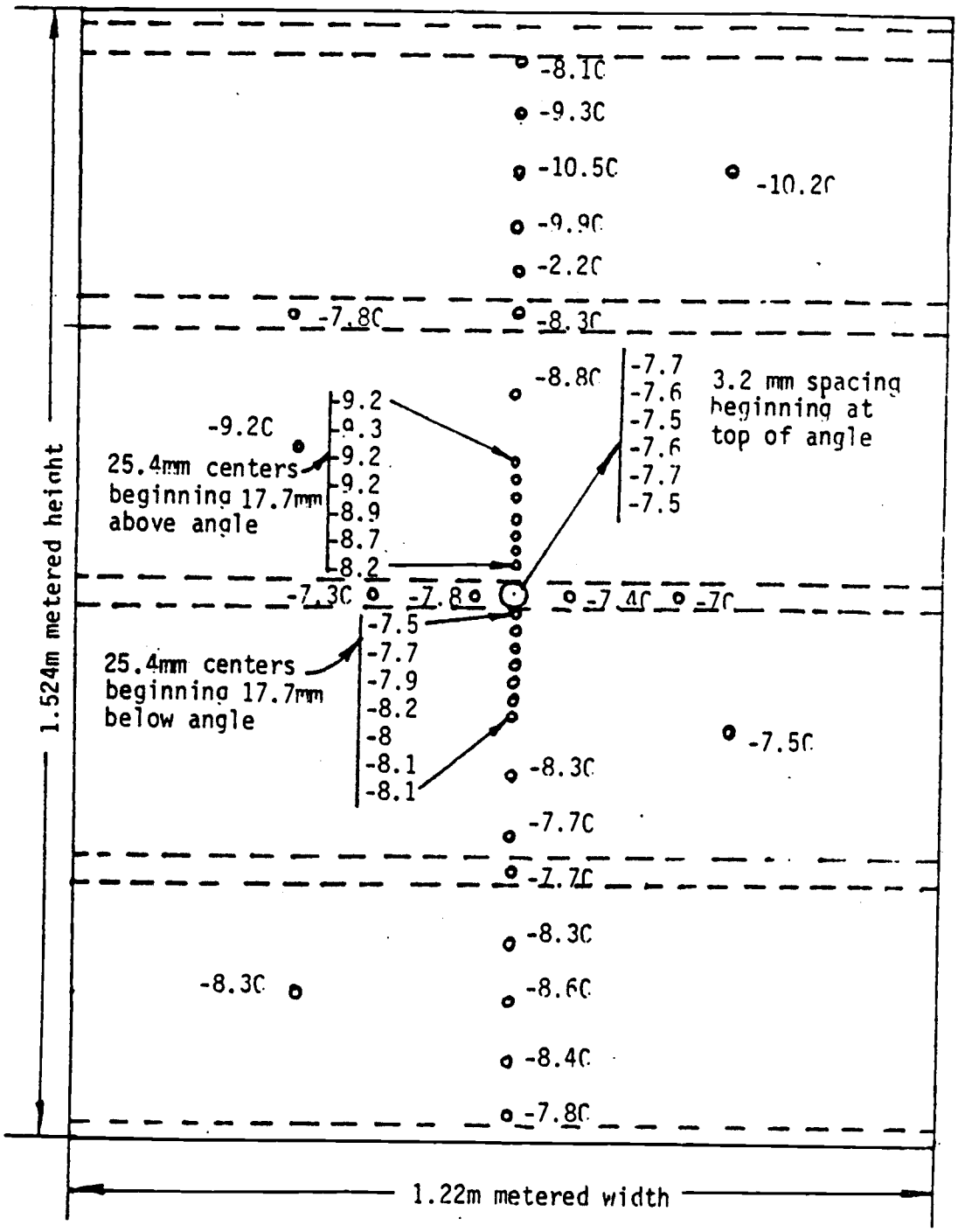

Fig.10
COLD SURFACE TEMPERATURE AND THERMOCOUPLE LOCATIONS
Panel 4: all insulation material removed, steel sheet installed to panel cold side

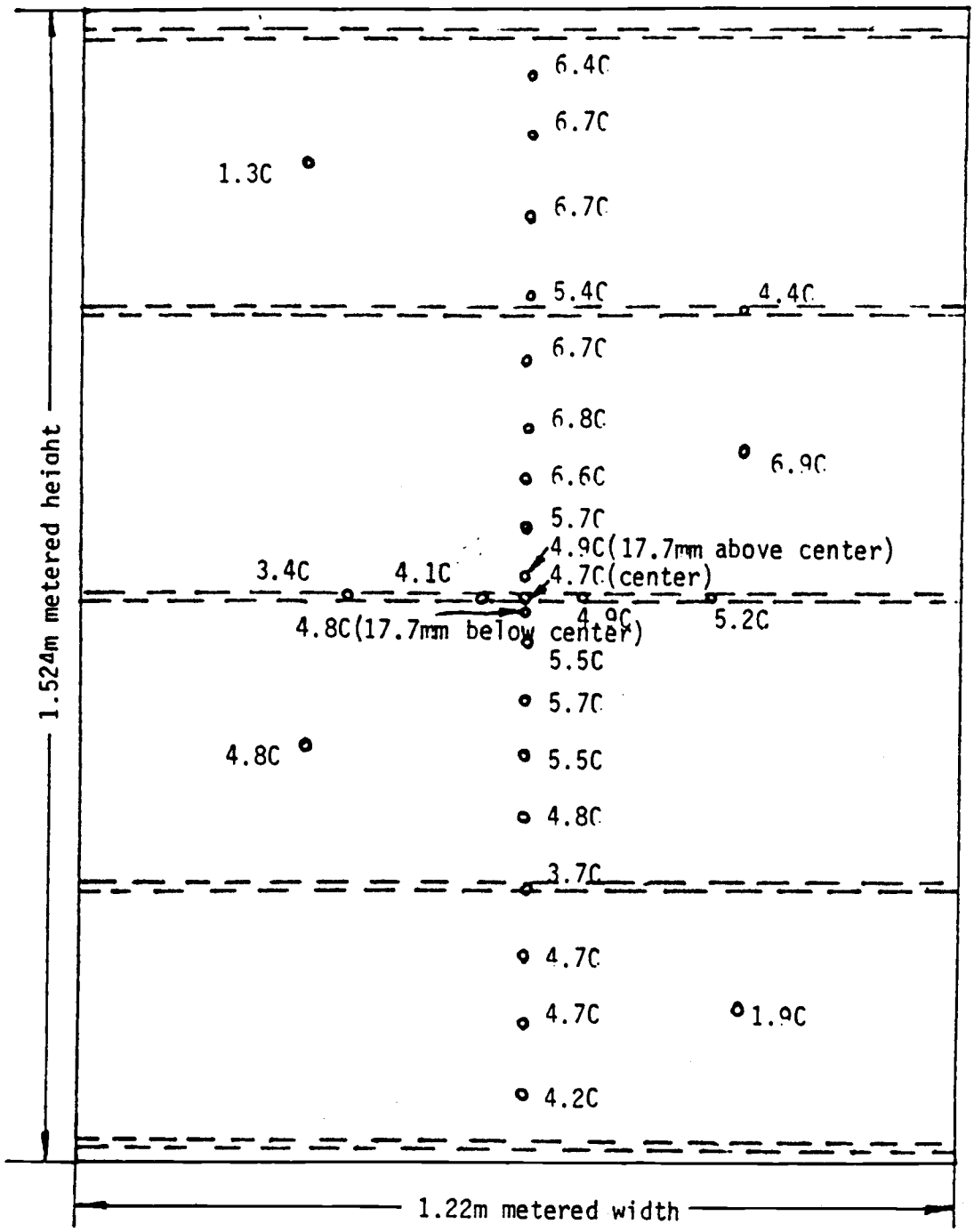

Fig.11
WARM SURFACE TEMPERATURES AND THERMOCOUPLE LOCATIONS

Panel 4: all insulation material removed, steel sheet installed to panel cold side

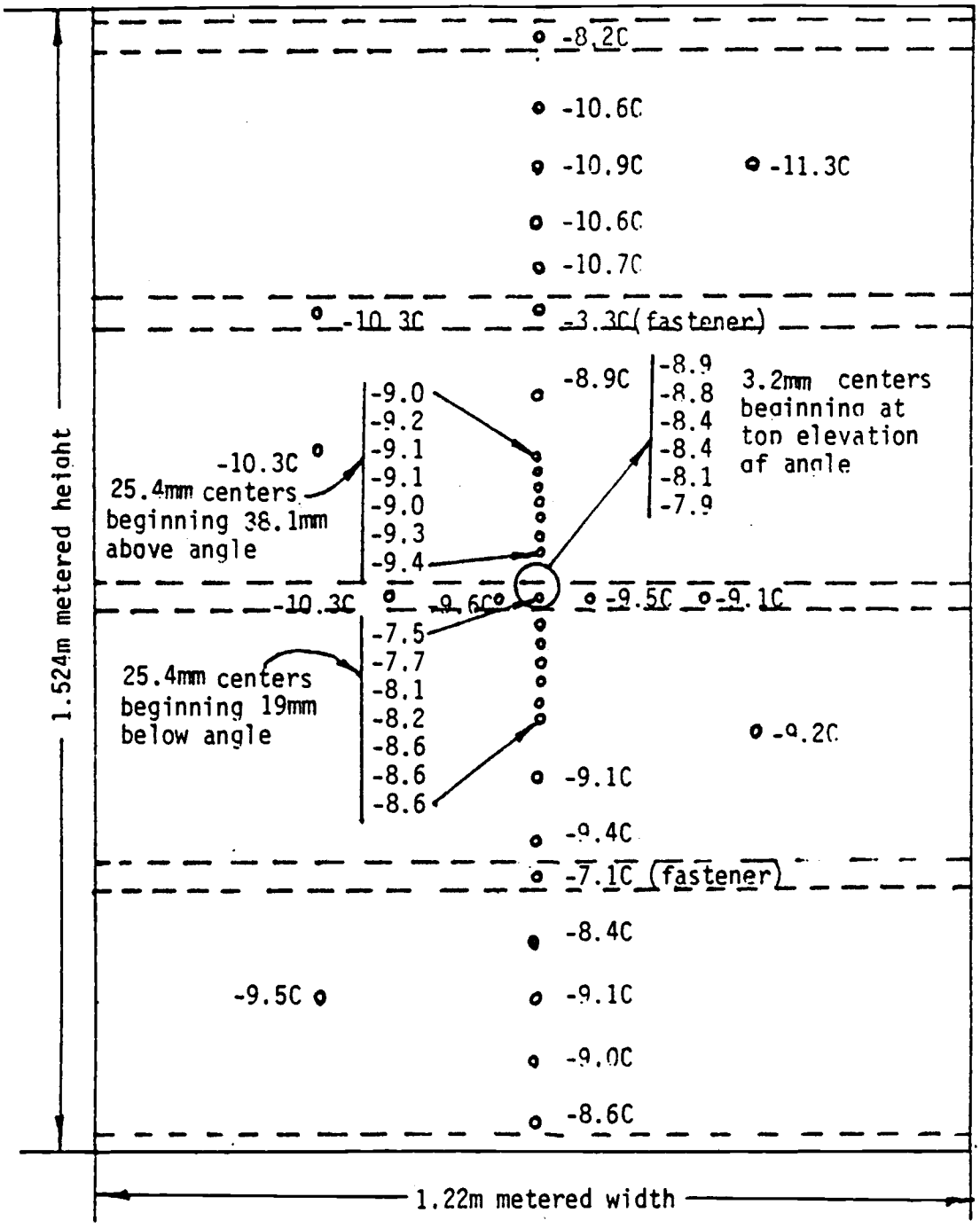

Fig.12
COLD SURFACE TEMPERATURES AND THERMOCOUPLE LOCATIONS
Panel 5: all insulation material removed, plywood sheet installed to panel cold side

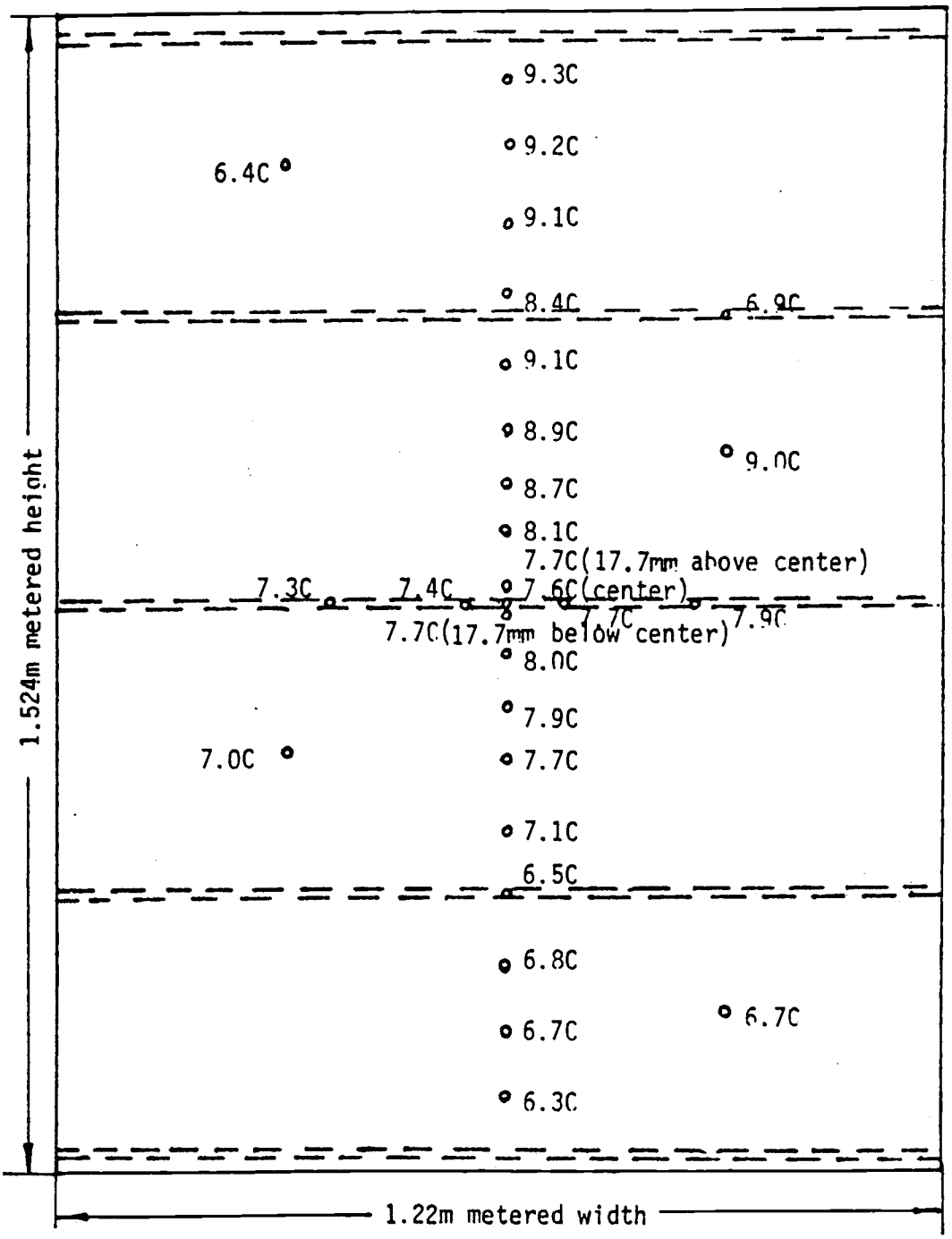

Fig.13
WARM SURFACE TEMPERATURES AND THERMOCOUPLE LOCATIONS
Panel 5: all insulation material removed, plywood sheet installed to panel cold side

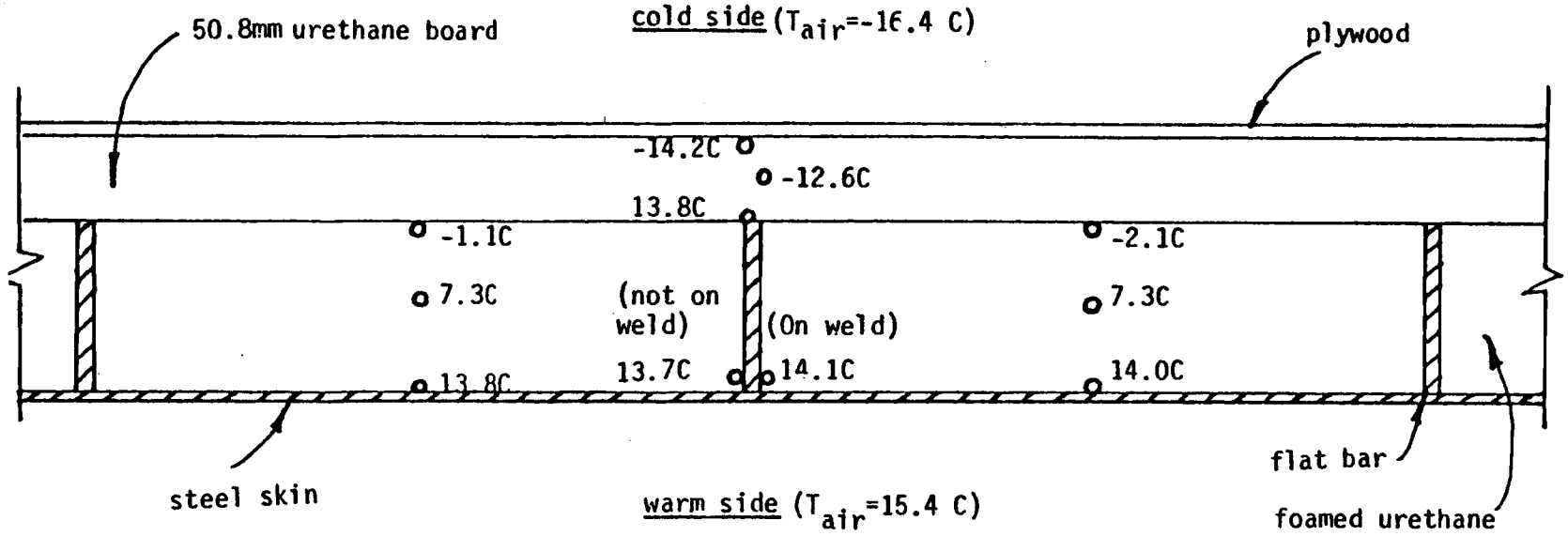

Fig.14
INTERNAL TEMPERATURES AND THERMOCOUPLE LOCATIONS
Panel 6 tested as submitted

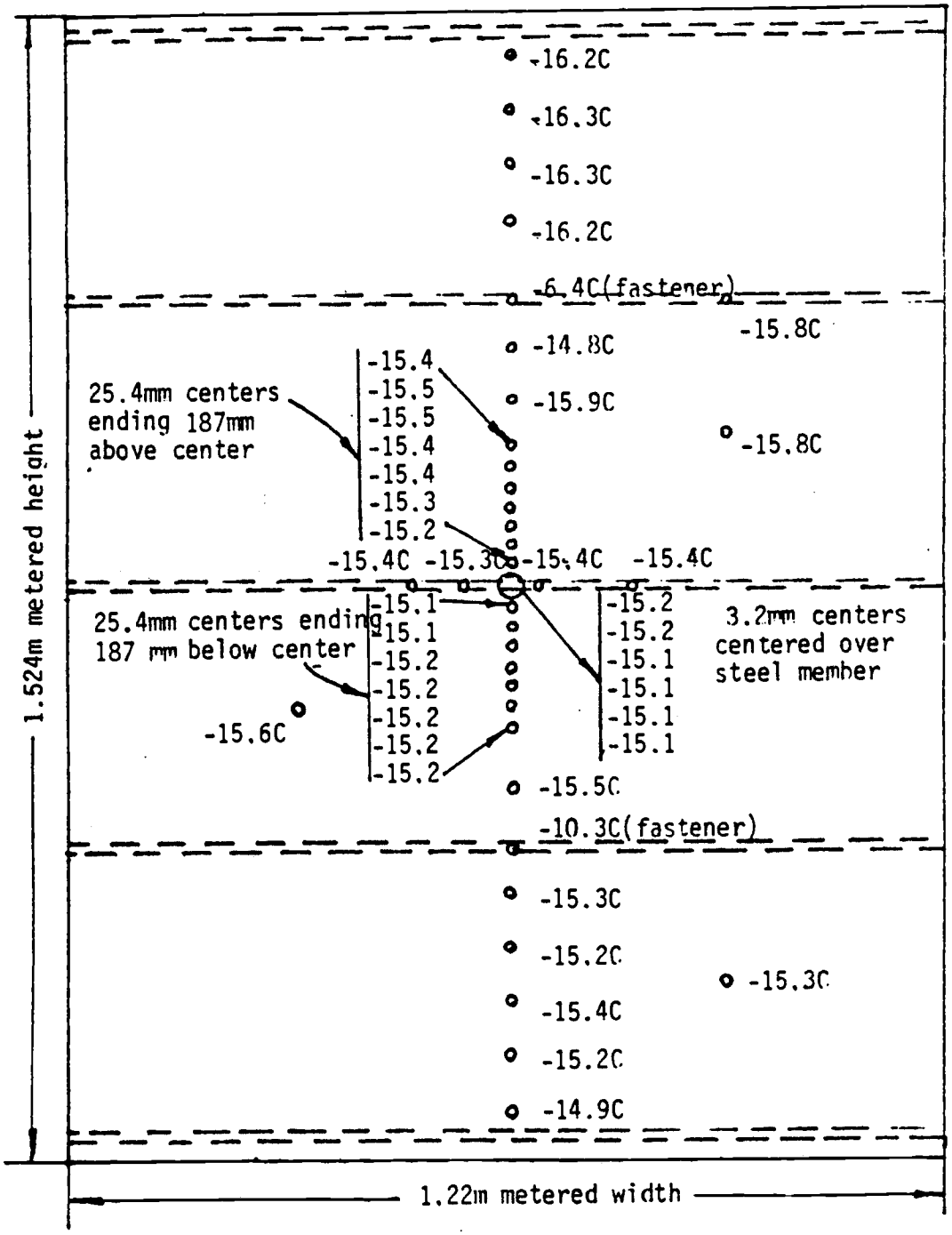

Fig.15
COLD SURFACE TEMPERATURES AND THERMOCOUPLE LOCATION
Panel 6 tested as submitted

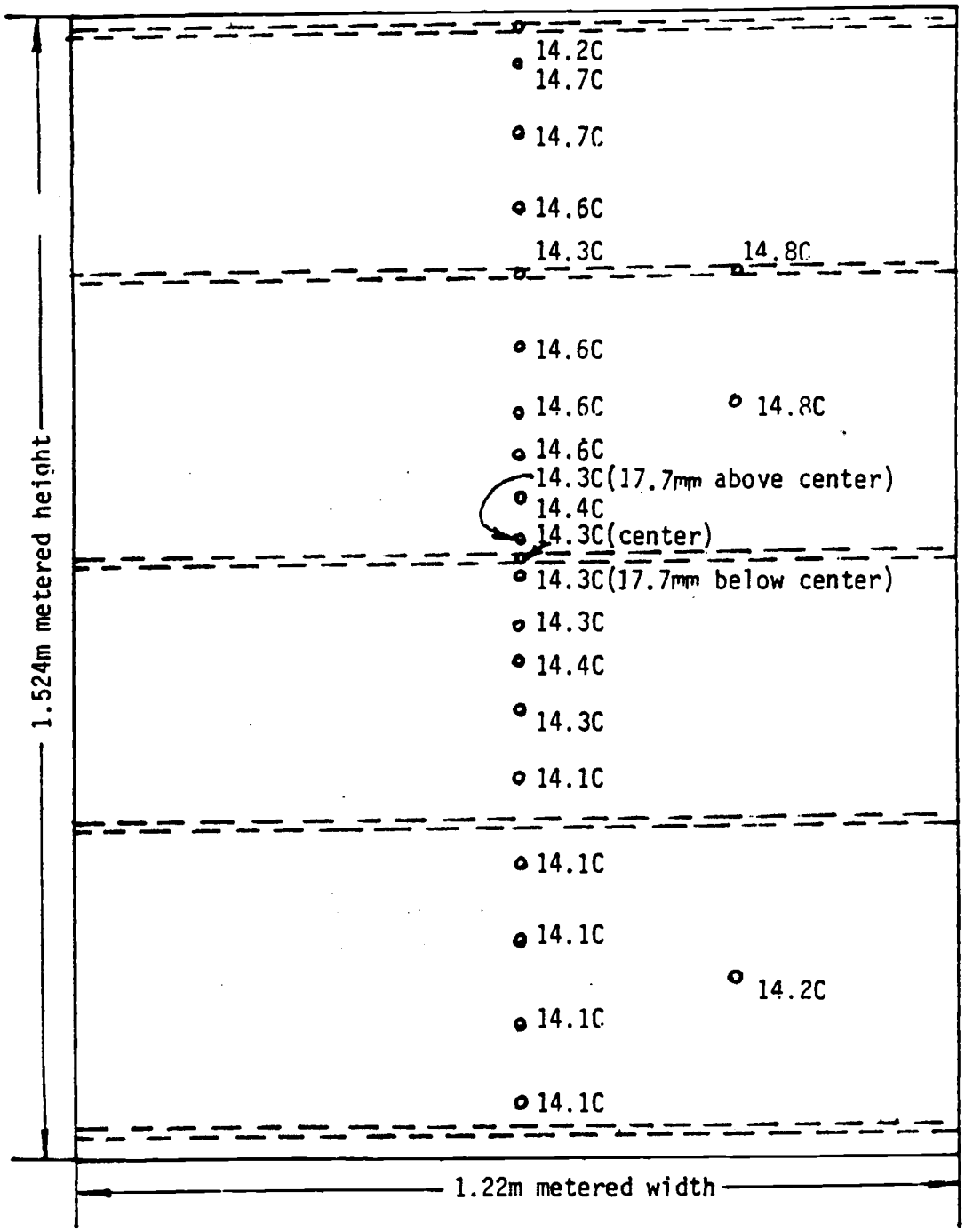

Fig.16
WARM SURFACE TEMPERATURES AND THERMOCOUPLE LOCATIONS
Panel 6 tested as submitted

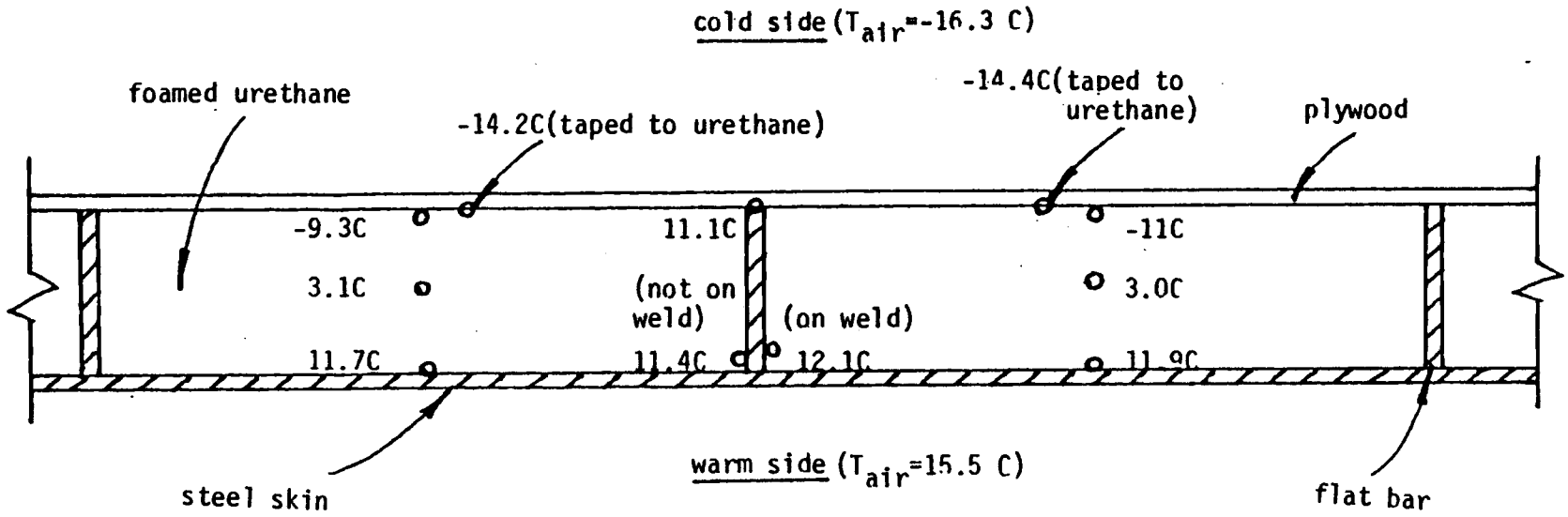

Fig.17
INTERNAL TEMPERATURES AND THERMOCOUPLE LOCATIONS
Panel 7: 50.8mm urethane board removed, foamed urethane left in

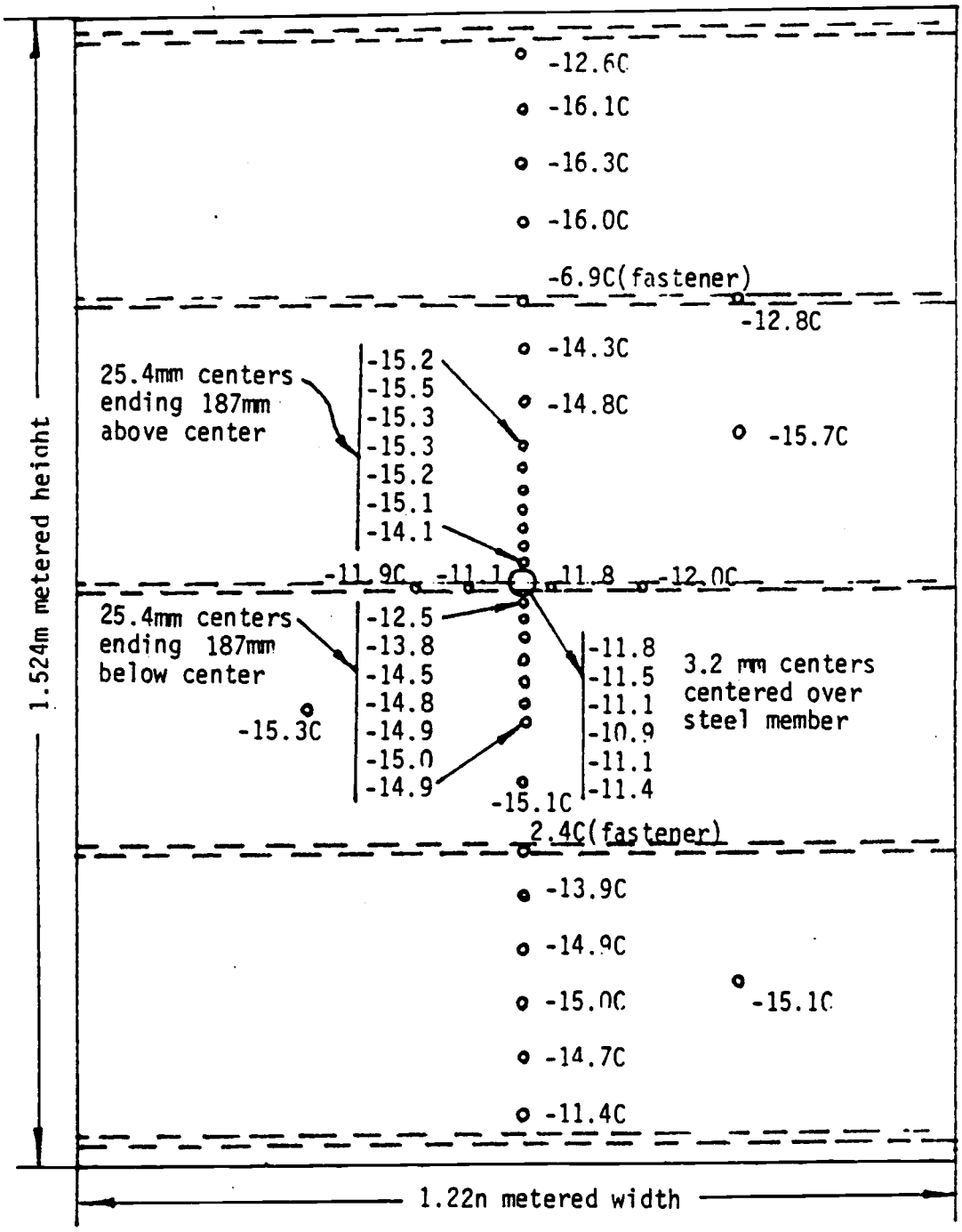

Fig.18
COLD SURFACE TEMPERATURES AND THERMOCOUPLE LOCATIONS
Panel 7: 50.8 mm urethane board removed, foamed urethane left in

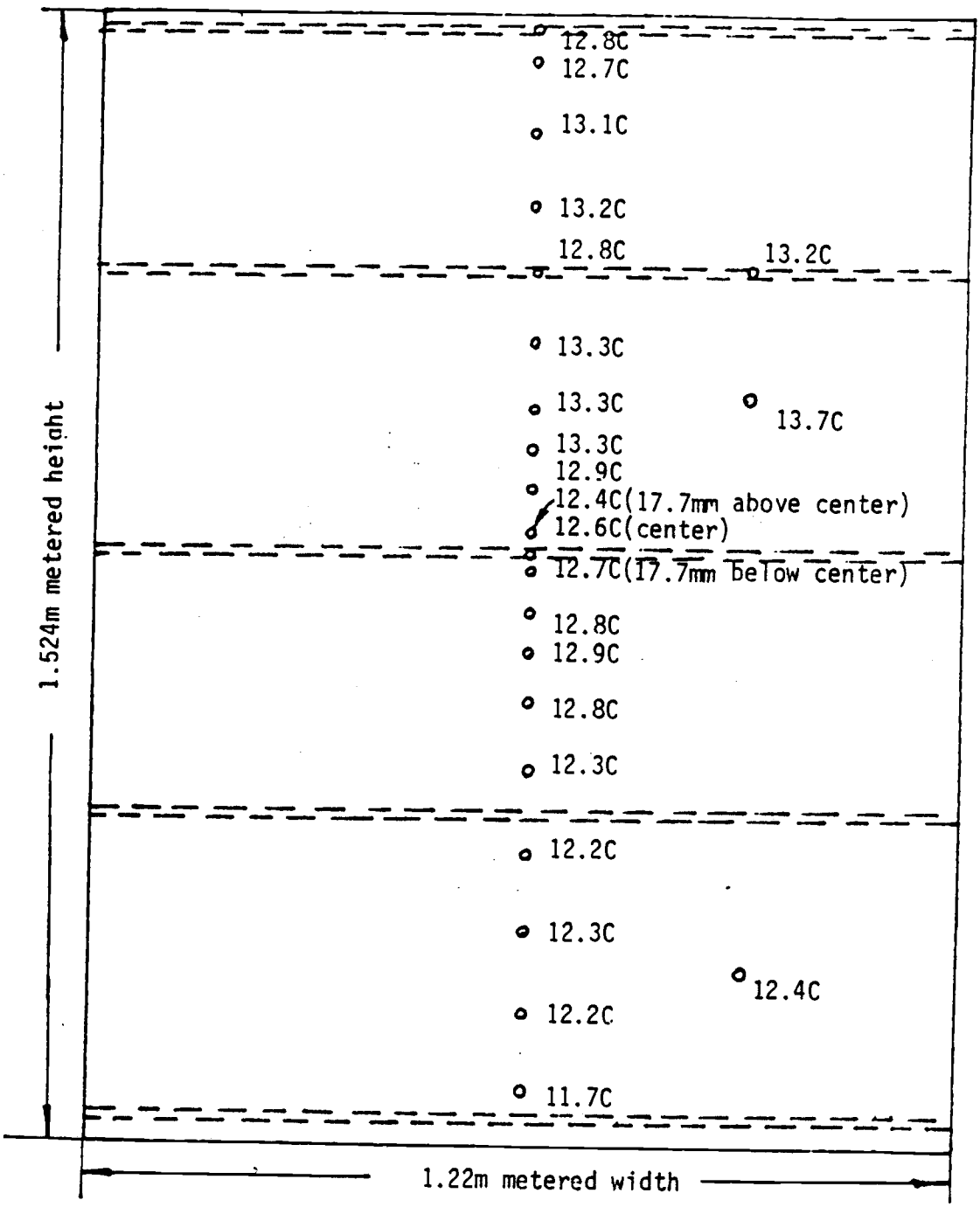

Fig.19
WARM SURFACE TEMPERATURES AND THERMOCOUPLE LOCATIONS
Panel 7: 50.8 mm urethane board removed, foamed urethane left in

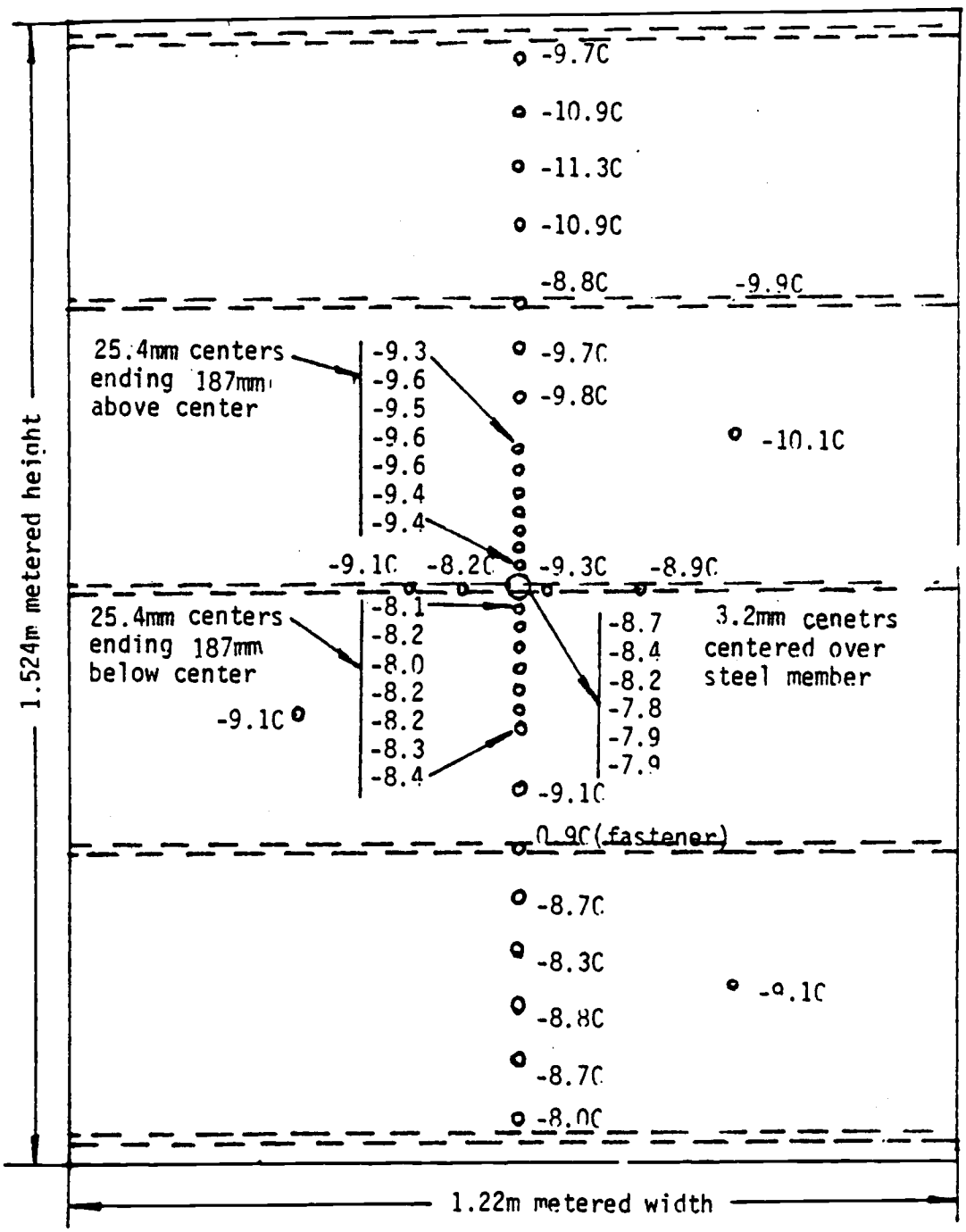

Fig.20
COLD SURFACE TEMPERATURES AND THERMOCOUPLE LOCATIONS
Panel 8: all insulation material removed, plywood sheet installed to panel cold side

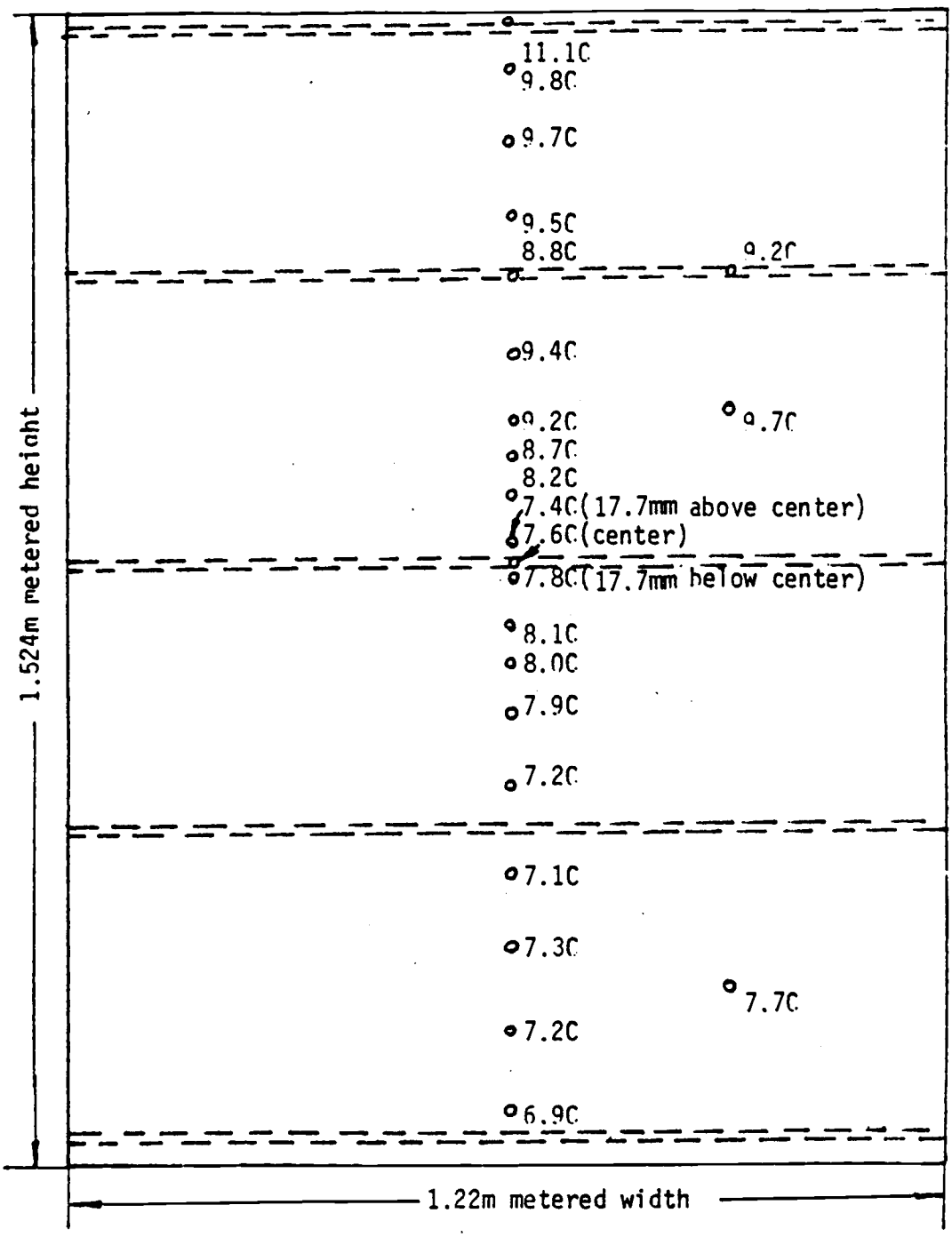

Fig.21
WARM SURFACE TEMPERATURES AND THERMOCOUPLE LOCATIONS
Panel 8: all insulation materials removed,
plywood sheet installed to panel cold side